



School of Chemistry

Synthesis and Analysis of 1:4 Li:N co-doped Diamond Films

Hannah Kitchen

27/04/15

This thesis is submitted in partial fulfilment of the requirements for the Honours degree of MSci at
the University of Bristol

Supervisor: Professor Paul May

Second Assessor: Dr Neil Fox

Third Assessor: Professor Mike Ashfold

Abstract

This study investigated the fabrication of n-type diamond using Li:N co-doping. When nitrogen is used as a dopant it produces a deep donor level. Therefore, it does not act as a suitable semiconductor at room temperature. Theoretical studies suggest that when lithium is used as a dopant and is in interstitial sites in the lattice, it can act as a shallow n-type dopant (a p-type when in substitutional positions). However, lithium atoms cluster together in the lattice and inhibit the electrical properties of the material. It was suggested that a combination of lithium and nitrogen atoms may produce a shallow n-type diamond, since the nitrogen atoms can prevent the lithium atoms from aggregation. The nitrogen atoms also inhibit the lithium atoms from migrating from interstitial to substitutional positions. It was postulated by computer studies and references that a 1:4 ratio of Li:N may produce a shallow donor to create n-type diamond.

To produce the Li:N diamond films, the N-doped diamond was grown first using a HFCVD process with ammonia and nitrogen gas as the source of nitrogen atoms. Subsequently, the lithium precursor, Li_3N solution (in 1% w/v polyoxy in chloroform) was drop-cast onto the N-doped film and the lithium atoms diffused into the film.

After growth of Li:N diamond films, characterisation was performed to evaluate film quality, morphology and dopant concentrations using Raman spectroscopy, SEM and SIMS. Resistance measurements were also recorded to determine if semiconducting diamond had been successfully fabricated.

The Li:N co-doped diamond films were compared to N-doped diamond films and although Raman spectroscopy and SEM images appeared very similar, resistance was greatly reduced using the co-doping process. Furthermore, the I_D/I_G values, providing a $\text{sp}^3:\text{sp}^2$ ratio, were much greater with Li:N co-doping than with N-doping alone.

The ratio of Li:N obtained was 1:6.7, which is similar to the desired ratio of 1:4. The resistance of this sample was 1.8 M Ω which is not low enough for the production of n-type diamond for use as a semiconductor at room temperature. If the ratio is further decreased, theoretically this should result in a lower resistance and potentially n-type diamond.

Acknowledgments

Firstly I would like to thank Dr Muhammad Zamir Othman for the time taken to introduce me to the project and to familiarise me with the new equipment. Also for his general knowledge, patience and support which was invaluable throughout my project.

I would also like to thank my supervisor Professor Paul May, for his insight and general guidance throughout the project and his assistance with the write up, and my second assessor, Dr Neil Fox, for all our meetings where he checked on the progress of my project and my general wellbeing, and for reading my report. For taking the time to read my project I would also like to thank my third assessor Professor Mike Ashfold.

For the help with the machines in the laboratory and for his expertise I would like to thank Dr James Smith, who was always there when needed.

Also thanks to Sarah Halliwell for her assistance with SIMS and for helping me to understand the procedure.

Finally, I would like to thank the entire diamond group for their support and encouragement throughout my project and with any questions that I had.

Contents

Abstract.....	1
Acknowledgments.....	2
1.0 Introduction	5
1.1 History and Properties of Diamond	5
1.2 Doping.....	7
1.2.1 P-type Doping with Boron.....	9
1.2.2 N-type Doping.....	10
1.2.3 Co-Doping.....	15
1.3 p-n Junctions	20
1.4 Applications of Doped Diamond	21
1.4.1 Optics	22
1.4.2 Heat Sink Material.....	23
1.4.3 Light Emitting Diodes	23
1.4.4 Surface Acoustic Wave (SAW).....	23
1.4.5 Cutting Tools	23
2.0 Experimental Techniques.....	24
2.1 Hot Filament Chemical Vapour Deposition (HFCVD)	24
2.1.1 HFCVD Conditions	26
2.1.2 Set up of the HFCVD.....	26
2.2 Nitrogen Doping of the Diamond Film.....	28
2.3 Li ₃ N Addition to N-doped Diamond Films.....	29
2.4 Laser Raman Spectroscopy	30
2.5 Scanning Electron Microscope (SEM)	32
2.6 Resistance Measurements.....	32
2.6.1 Bell Jar Evaporator	32
2.6.2 Oxygen Termination.....	35
2.6.3 Two-point Probe measurement.....	35
2.7 Acid Washing.....	35
2.8 Secondary ion mass spectrometry (SIMS)	36
3.0 Results and Discussion	37
3.1 Determining the optimum amount of NH ₃ gas.....	37
3.2 Determining the optimum amount of N ₂ gas.....	41
3.3 Molybdenum and Silicon Substrates	45

3.4 Comparison to the control.....	49
3.5 Li:N co-doping	53
3.5.1 An N-doped Capping Layer after Lithium Diffusion	57
3.5.2 Decreasing the amount of Nitrogen Atoms	61
3.5.3 Increasing the amount of Lithium Atoms	65
3.5.4 No Capping Layer after Lithium Diffusion	71
3.5.5 Acid Washing.....	73
4.0 Conclusions	77
5.0 Further Work.....	79
5.1 Decreasing the Nitrogen Atoms.....	79
5.2 Different Diffusion Methods.....	79
5.3 Changing the Capping Layer.....	79
5.4 Further Analysis	79
5.5 Resistance Measurements	80
5.6 Oxygen Termination.....	80
6.0 Appendix	81
6.1 Calculation of Li_3N concentration	81
6.2 SEM for Increasing NH_3 Concentration	82
6.3 SEM for Undoped Diamond on a Molybdenum Substrate	83
6.4 Resistance Measurements for Li:N co-doped Diamond	83
6.5 Resistance Measurements with no Capping Layer	83
6.6 Resistance Measurements before and after Acid Washing.....	84
7.0 Bibliography	85

1.0 Introduction

1.1 History and Properties of Diamond

The word diamond originates from the Greek word *adamas*; which means hardest known substance or unbreakable. Diamond, both now and in the past, is in high demand as a gemstone due to its unique characteristics, including its clarity, colour and cut. The earliest records of diamond date back to the 3rd and 4th century in India. India was the only source of diamond until as late as the 1700s when Brazil discovered diamond and in the 1800s, the first diamond mines began in South Africa.

Diamond is a unique material with a broad range of mechanical, chemical and physical properties (**Table 1.1**) therefore it is also a popular material industrially [1–4]. Its exceptional properties make diamond very valuable as it possesses characteristics that are not found in other materials [1].

Table 1.1: Table highlighting the exceptional properties of diamond [1–4].

<u>Properties of Diamond</u>	
Hardest material known ($1 \times 10^4 \text{ kg/mm}^2$)	Chemical resistance
Negative electron affinity	High sound propagation velocity ($17.5 \times 10^3 \text{ km s}^{-1}$)
Highest thermal conductivity known at room temperature ($2000 \text{ W m}^{-1} \text{ K}^{-1}$).	High mechanical strength (90 GPa)
Optical transparency over a broad wavelength range (from UV to IR)	Chemically inert
Low compressibility ($8.3 \times 10^{-13} \text{ m}^2 \text{ N}^{-1}$)	Electron mobility ($2200 \text{ cm}^2 \text{ V}^{-1} \text{ s}^{-1}$)
The lowest thermal expansion coefficient ($1 \times 10^{-6} \text{ K}$)	Hole mobility ($1600 \text{ cm}^2 \text{ V}^{-1} \text{ s}^{-1}$)
Highest bulk modulus ($1.2 \times 10^{12} \text{ N m}^{-2}$)	Very high electric break down field
High electrical resistance with undoped diamond (10^{13} - $10^{16} \text{ } \Omega \text{ cm}$)	
Potential electrical semiconducting properties with n-type diamond	
Electrical semiconducting properties with boron p-type diamond	

Although diamond has many extraordinary properties, there are several drawbacks to this material as diamond is highly expensive and also very rare [2]. It is difficult to utilise diamond's properties due to the strong, short sp^3 covalent bonds that comprise the diamond lattice [2,3]. These covalent bonds consist purely of carbon atoms bonded together in a tetrahedral structure. Natural diamond is scarce, and is located 140-190 km beneath the Earth's mantle. At this depth, there are extremely high pressures of 4.5-6 GPa and temperatures of 1600-2400 K. Magmas beneath the Earth's surface, cause volcanic eruptions and when these occur diamond deep beneath the Earth rises toward the Earth's surface. Once at the surface, the diamond can be extracted. Such conditions highlight why accommodating large amounts of natural diamond is difficult and expensive. Consequently; synthesising diamond in this environment of such extreme temperatures and pressures is a

demanding process. Therefore it would be extremely beneficial to synthesise diamond in a low cost process, so that its properties could be further explored.

Graphite, like diamond, also consists solely of carbon atoms, therefore research into the synthesis of diamond from graphite has been of interest in the past [2]. Graphite does not have tetrahedral bonds like diamond, as each carbon atom is only bonded to three other carbon atoms producing planar sp^2 bonding (**Figure 1.1**). Another difference between the two allotropes is that graphite is composed of different layers with a free electron from each carbon atom delocalised, moving between the layers. This enables it to be a good electrical conductor. Graphite is the most stable allotrope of carbon at ambient temperature and pressure. Therefore, it is difficult to manufacture diamond from graphite, as diamond is the less stable allotrope; so it is an unfavourable process. At room temperature the standard enthalpies between the two forms of carbon are relatively low at 2.9 kJ mol^{-1} [5]. However, there is a large activation energy of $728 \pm 50 \text{ kJ mol}^{-1}$ which prevents the conversion of graphite to diamond [2]. This also means that conditions to produce diamond need to be extreme to overcome this energy barrier. However, an advantage of diamond is that it is metastable, so once diamond is formed, it will not spontaneously convert back to graphite. This feature means that although diamond does not give thermodynamic stability, it does provide kinetic stabilisation. Consequently, the major challenge here is the formation of synthetic diamond.

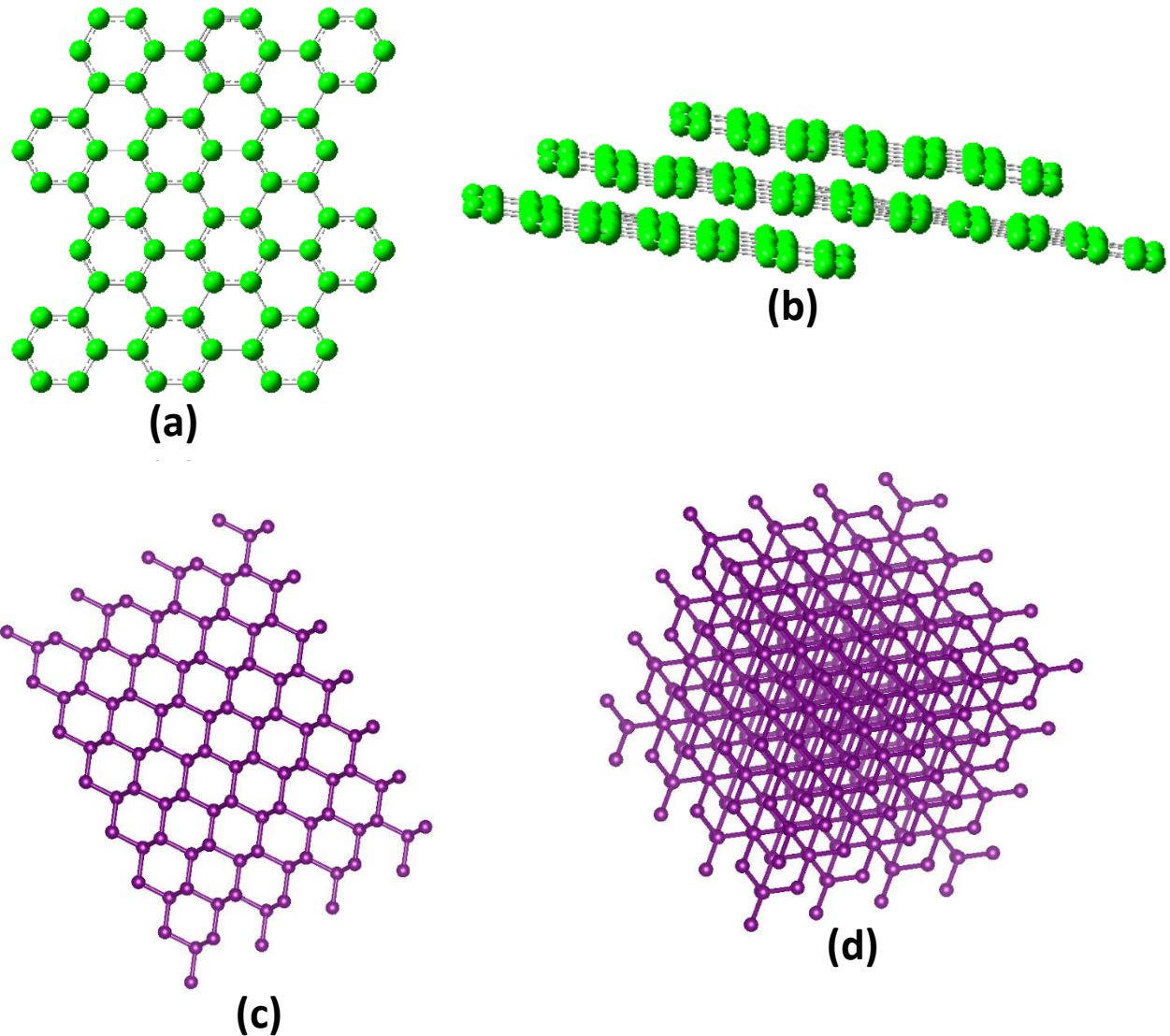


Figure 1.1: Schematic diagram of graphite showing (a) the planer structure and (b) the 3D structure. A schematic of diamond is also shown, again both (c) the planar and (d) the 3D structure are shown.

1.2 Doping

Semiconductors are found in many applications such as transistors, diodes and microprocessor chips. The most generally used semiconductors are either silicon or germanium. However, since silicon can be used at higher temperatures than germanium, it is favoured for more applications. Both these elements are in group 14 of the periodic table, with four valence electrons. Therefore, it would seem appropriate to investigate carbon based materials as potential semiconductors, since carbon also contains four valence electrons.

Diamond is an exceptional insulator due to its wide bandgap of 5.4 eV [6]. However, silicon is also an insulator at room temperature, with a bandgap of 1.1 eV [7], yet once you add dopants to the structure, silicon becomes a semiconductor. Although diamond's bandgap is much larger than

silicon's, it has been suggested that sufficient doping could decrease this bandgap for semiconductive properties to be observed. However, doped diamond is much harder to achieve than doped silicon due to the strongly covalent bonded lattice [8]. If diamond was developed into a semiconductor; it would have unique properties that lower bandgap materials do not possess, for example the application of higher voltages. Semiconducting diamond would provide all the semiconductor properties of silicon; with the addition of a high thermal coefficient, so it could be used in devices at much higher temperatures. Diamond's thermal coefficient is $2000 \text{ W m}^{-1} \text{ K}^{-1}$, therefore diamond can withstand much higher temperatures than silicon which has a thermal coefficient of $149 \text{ W m}^{-1} \text{ K}^{-1}$ [4,9]

Incorporating impurities or defects into the diamond lattice is called doping and it provides additional free carriers into the lattice. These free carriers (either electrons or empty orbitals depending on the type of doping) increase the semiconducting properties of diamond. The concentration of dopant can be controlled; therefore the electrical conductivity can also be controlled. The demand and potential value of diamond is increased as it can develop various properties that are seldom found with natural diamond [10]. Examples include exceptional optoelectronic and electronic properties (see further details in section 1.4).

There are two potential types of doping, p-type and n-type (**Figure 1.2**). It is crucial that both p-type and n-type doping are achieved and produce the appropriate semiconductivity as this will allow diamond to be used in transistors and other electronics. However, diamond's very stable lattice of carbon atoms and hard structure means it can be a challenge to incorporate other atoms into the lattice.

These dopants decrease diamond's large band gap, so it is a more facile process for an electron to be promoted from the diamond valence band to a dopant acceptor hole (p-type doping) or from a dopant donor level to the diamond conduction band (n-type doping). These impurities can either incorporate into the diamond crystals or into the grain boundaries between the crystals.

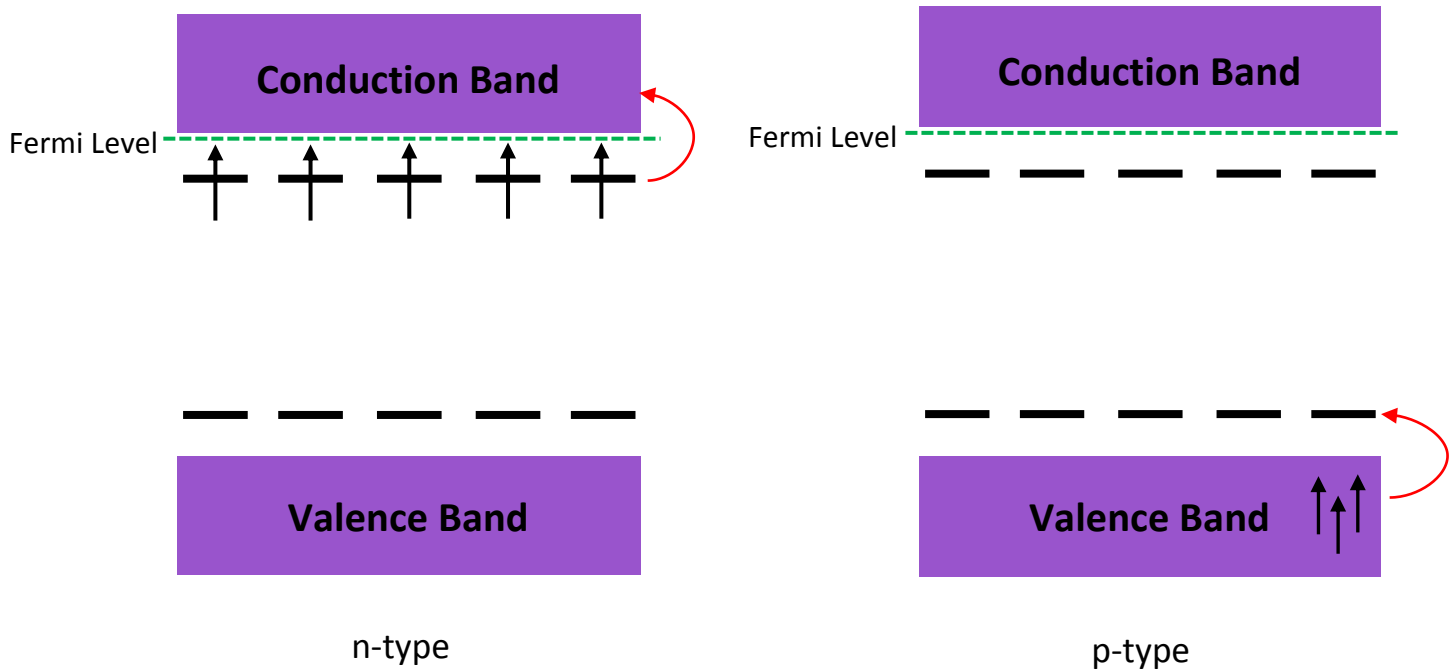


Figure 1.2: Schematic diagram of n-type and p-type doping. The black arrows represent electrons, with the red arrow showing movement of electrons. In n-type doping, the electrons are promoted into the conduction band. In p-type doping, the electrons from the valence band are promoted into empty orbitals (holes).

Atoms can either be deep or shallow defects; this property depends on the state of the impurity once ionised. For instance, when the atom has either donated or accepted an electron (depending on whether it is p-type or n-type) it becomes ionised. For a shallow donor, the excitation energy required to ionise is low. The deeper the impurities in the bandgap; the deeper the donor. For the dopant to be efficiently incorporated, it is essential to have a shallow donor. Therefore, less energy is required to excite an electron from the donor energy level into the conduction band [1]. It is vital to produce doped diamond with a low resistance as this would indicate successful semiconductivity.

1.2.1 P-type Doping with Boron

The most successful and widely used p-type doping is boron since this occurs in nature (type IIb) [1,11]. P-type doping involves introducing an atom with fewer electrons than carbon into the diamond lattice. Therefore, producing empty orbitals (holes) above the valence band which accept electrons. The excitation energy of boron is low at 0.37 eV [11]. The excitation energy is the energy required to promote an electron from the valence band of diamond to the acceptor dopant site. The boron atom is a similar size to the carbon atom at 0.88 Å and 0.77 Å respectively [12,13]. Therefore, it is relatively easy for boron to incorporate into the substitutional sites in the lattice; where it is generally located.

Synthesis of boron doped diamond is relatively simple as it is just a case of addition of boron-containing molecules into the initial reactants. Both CVD (Chemical Vapour Deposition), ion-implantation and HPHT (High Pressure High Temperature) are methods that have produced

successful results in doping with boron [1]. When using HPHT, heavy doping of boron is necessary to produce the required semiconductive properties, yet CVD is the more generally used method [14]. Diborane gas (B_2H_6) is a common source of boron in either microwave plasma or hot filament chemical vapour deposition (MWCVD or HFCVD) reactions. Once doped with boron, diamond can show metallic and superconducting properties [8]. Care must be taken as diborane will spontaneously ignite upon slight contact with water, for example in air. Furthermore, it is an extremely toxic compound, which also means it must be handled carefully.

1.2.2 N-type Doping

N-type doping involves introducing into the diamond lattice an atom with more electrons than carbon. Therefore, since the impurities are electron rich, they will act as donors. The excitation energy is the energy required to promote an electron from the dopant donor level to the conduction band of diamond. N-type doping is a more difficult process than p-type doping for a variety of reasons. For example, the atom may be too large for incorporation, or the donor level produced is too deep. The majority of potential n-type dopants belong to either group 1 or group 15 of the periodic table. Elements in group 1, such as lithium and sodium have been investigated, these must be located on interstitial positions in the diamond lattice to create shallow donors [15]. In group 15, nitrogen, phosphorus and arsenic are potential dopants. These are situated on the substitutional sites in the lattice [16].

Research is still required to determine whether it is possible to achieve semiconductive diamond from n-type doping on a {100} substrate surface, since so far attempts have produced diamond with a resistance that is too high. If n-type semiconductive diamond can be achieved, further investigation of diamond as a product in for example, electronic devices and thermionic emission will be possible. N-type doping, which is a relatively new process, has seen the largest increase in success in the last few decades [1].

1.2.2.1 N-type Doping with Phosphorus

The NIRIM group [17] was the first to produce successful n-type doping. This advance involved the manufacture of phosphorus doped diamond using CVD methods, with PPh_3 as the source of phosphorus [1,18]. Another potential source of phosphorus is PH_3 [19]. Along with CVD methods, phosphorus doped diamond has also been attempted by ion-implantation [1]. However, this phosphorus was incorporated using a {111} surface. N-type doping has not been achieved on {100} surfaces due to the low incorporation of phosphorus [18]. This low incorporation is a result of the larger covalent radii for phosphorus in comparison to carbon at 1.10 Å and 0.77 Å respectively [13,20].

The phosphorus atoms are located in substitutional positions in the diamond lattice and incorporation of phosphorus atoms has shown to increase the growth rate of diamond [19]. However, phosphorus has a relatively deep donor level with an excitation energy of 0.46 eV [21]. This is not shallow enough for a n-type dopant so semiconductive properties are still relatively insufficient. For boron, it was evident that annealing at temperatures of 1700 K improved diamond

conductivity. However, when these conditions were investigated with phosphorus doped diamond, a reduction in conductivity of diamond was observed [1].

1.2.2.2 N-type Doping with Nitrogen

Some success of n-type doping has been found with nitrogen, but resistance remained too high for semiconducting properties of diamond. Nitrogen has been considered a n-type dopant as it has high solubility in diamond and a covalent radii of 0.74 Å which is similar to the carbon atom, 0.77 Å [13]. These features would indicate facile incorporation of nitrogen atoms into the diamond lattice. Furthermore, the formation energy, which is the energy required to incorporate the dopant into diamond is lower for nitrogen than for phosphorus [22].

When diamond is doped with nitrogen atoms there are two potential effects on the diamond lattice. Firstly, type Ia, which consists of nitrogen atoms forming small aggregates in the diamond lattice; or type Ib, where the nitrogen atoms are spread out in substitutional sites. Type Ia is more common in natural diamond, yet in synthetic diamond, type Ib is more generally observed [10]. Therefore, once doped it is more common to observe nitrogen atoms at substitutional sites in the diamond lattice.

When nitrogen gas is added, the nitrogen atoms form HCN by hydrogen abstraction. The hydrogen abstraction enables additional diamond layers to be grown due to more renucleation and the new active sites [23]. However, the ideal concentration of nitrogen must be established as it is crucial to obtain a high quality, continuous film. Jin and Moustakas first suggested that incorporation of nitrogen atoms into the lattice increases the growth rate of diamond and that the Raman spectra shows a more clear diamond peak and a less prominent graphite peak [10,24,25]. Distortion of diamond arises with nitrogen atom incorporation since the N-C bond length is 28% longer than C-C bond [10]. Originally this distortion was thought to be a product of the Jahn-Teller effect yet, this accounts for a C-N bond length that is only 10-14% longer than the C-C bond. The Pauli electrostatic repulsion is more likely to be the reason for this distortion [10].

Research indicates that in substitutional sites nitrogen gives the desired growth rate enhancement and not NH or NH₂ chemisorbing onto the diamond surface [26]. The ratio of C:N is a considerable factor in the determination for the growth rate. If the ratio of C:N is 10:1, growth rates will be much higher than smaller ratios (**Figure 1.3**) [10].

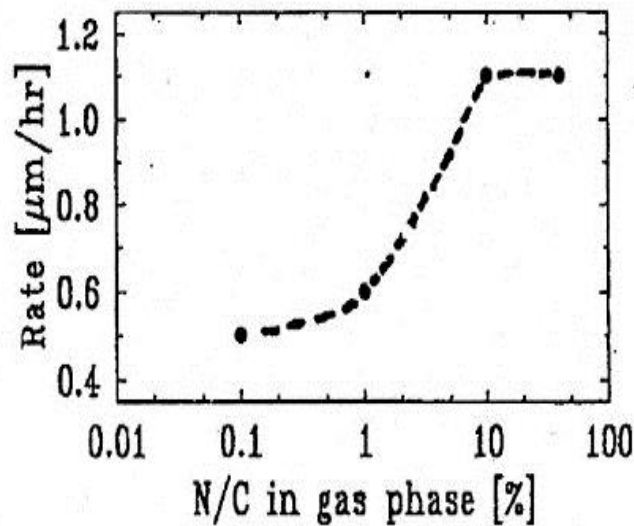


Figure 1.3: Graph showing the growth rate of a diamond film ($\mu\text{m h}^{-1}$) with the ratio of N:C [10].

Nitrogen is a deep donor as the excitation energy is high at 1.62-1.7 eV [21]. This is unsuitable for the production of semiconducting diamond [27,28]. The deep donor level causes a compensation effect and a very high electrical resistance ($\approx 200 \text{ M}\Omega$). This compensation effect results in diamond converting back to its original insulating properties at room temperature [24].

1.2.2.3 N-type Doping with Lithium

Another atom that has been investigated as a potential n-type dopant is lithium. Common sources of lithium for lithium doping include lithium carbonate (Li_2CO_3), lithium oxide (Li_2O), lithium hydride (LiH) and *tert*-butyl lithium. Lithium is a shallow donor with an excitation energy much lower than that for nitrogen at 0.1 eV [29]. However, experimentally the formation energy is high due to the low solubility of lithium in diamond, an issue that the nitrogen atom does not have. Lithium atoms can be incorporated into the diamond lattice using both CVD and HPHT processes. However, these extreme temperatures result in rapid movement of lithium atoms which cluster together to form aggregates in the lattice. Therefore lithium atoms become inactive as the electrons are no longer delocalised [30]. Since the electrons are no longer free to move this results in a high resistance and therefore no semiconductive properties in diamond are observed at room temperature.

The lithium atom has fewer electrons than carbon, so it would be considered a p-type dopant. However, lithium atoms can be located in both interstitial and substitutional sites in the diamond lattice. In interstitial positions lithium acts as a shallow donor (a n-type dopant), but at substitutional positions it acts as a deep acceptor (a p-type dopant) [31]. Therefore, to exploit the shallow donor properties of lithium, it would be advantageous to incorporate lithium atoms at the interstitial sites in the lattice. This would seem plausible since nuclear studies of the radioactive decay of ^8Li indicated that 40% of Li atoms lie on interstitial sites, whereas only 17% lie on substitutional sites [8]. It is unfavourable to have lithium atoms in substitutional positions in the lattice since this would result in both lithium donors and acceptors. Therefore, the donor electrons will have insufficient energy and the semiconductivity is reduced [8,28].

Lithium has a tendency to preferably etch graphite over diamond, which produces a higher diamond to graphite ratio which would be advantageous as it results in a higher quality diamond film [24].

The solubility limit of lithium in the diamond lattice is at $\approx 5 \times 10^{19} \text{ cm}^{-3}$ [24]. At this point, further addition of lithium will no longer have an effect as no more lithium atoms can be incorporated into the lattice. If excess lithium is added, the lithium atoms will react with the gases during the CVD process and a carbide layer will form which prohibits any further diamond formation [24].

1.2.2.4 N-type Doping with Sodium

Doping with sodium atoms has been considered as it has similar properties to lithium. Sodium atoms, like lithium atoms should be shallow donors when incorporated in interstitial positions [15,31]. However, as sodium atoms prefer to sit in substitutional sites, it will not be an effective n-type donor.

1.2.2.5 N-type Doping with Antimony and Arsenic

Antimony and arsenic were both suggested as possible n-type dopants as theoretically they should be shallow donors with excitation energies of 0.3 eV and 0.4 eV respectively [32]. However, when using HFCVD, incorporation of antimony and arsenic atoms proved difficult as they are both relatively large atoms in comparison to carbon. Antimony has a covalent radius of 1.41 Å, and arsenic 1.21 Å, in comparison to carbon atom (0.77 Å) [13,33]. Even at high concentrations there was little incorporation of arsenic and antimony into the diamond lattice. If a MWCVD process was used, this may produce more promising results as there is less of a temperature gradient in comparison to HFCVD. The Raman spectra of an arsenic doped diamond film is shown (**Figure 1.4**) [32].

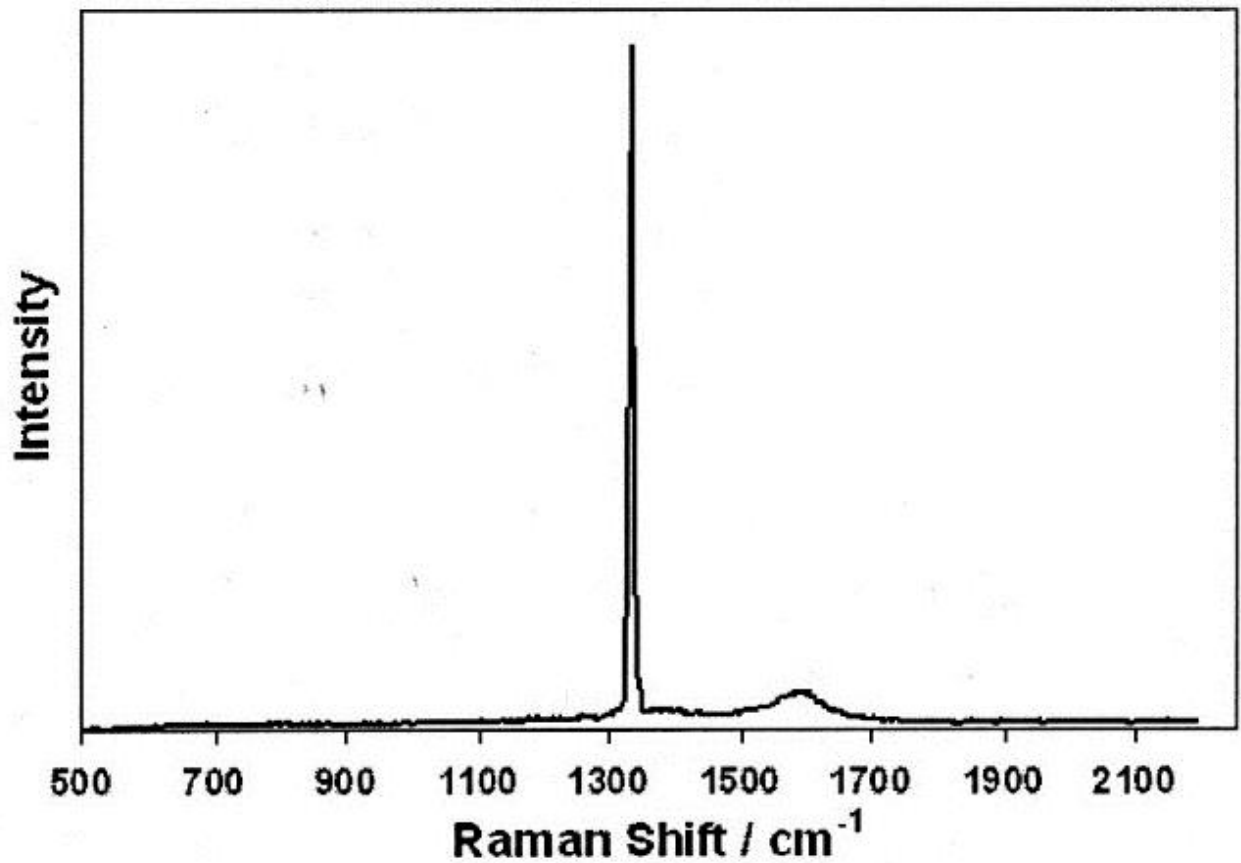


Figure 1.4: Raman spectra (325 nm) of arsenic doped diamond showing the diamond peak at 1332 cm⁻¹ and a slight graphite peak at 1580 cm⁻¹ [32].

A comparison of how impurities can affect the ease of electron transfer in diamond is shown (Figure 1.5) with boron acting as an acceptor (p-type semiconductivity) and phosphorus, nitrogen, arsenic, antimony and lithium acting as donors (n-type semiconductivity).

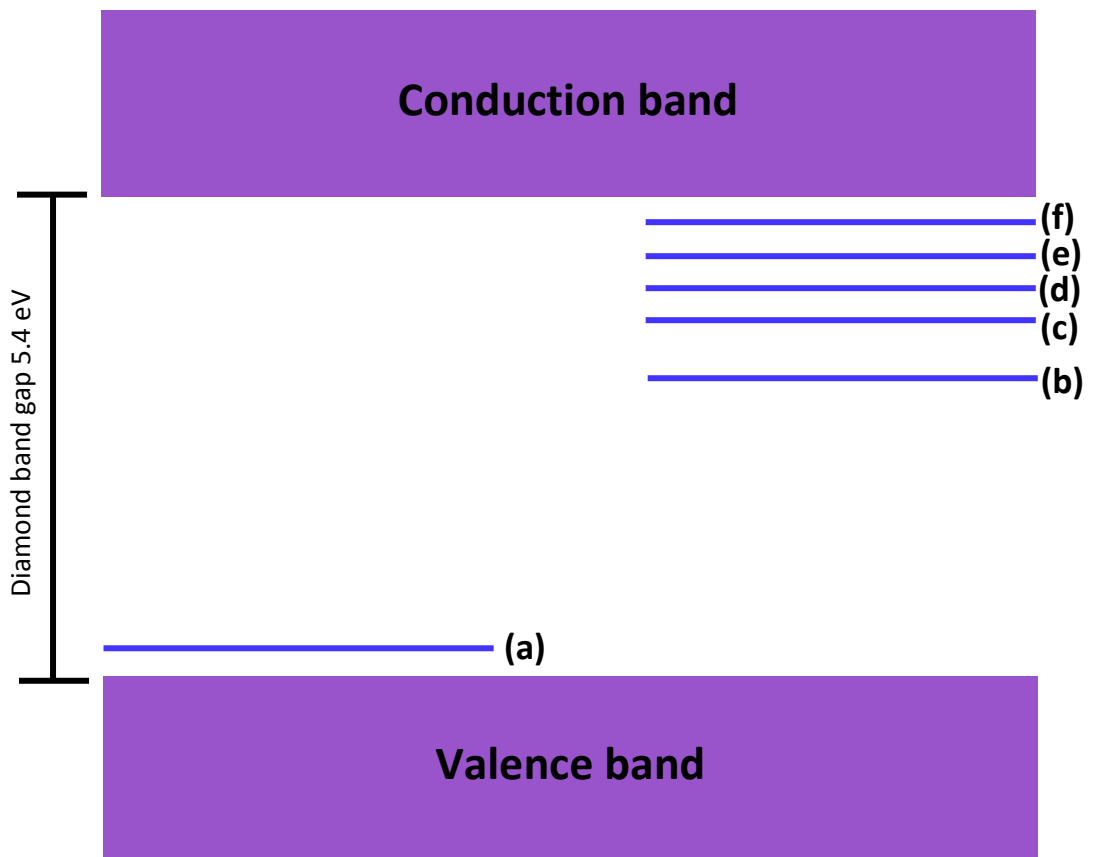


Figure 1.5: An energy level diagram showing different dopant excitation energies in diamond, (a) boron, an acceptor with an excitation energy of 0.37 eV [11] above the valence band, (b) nitrogen, a donor with an excitation energy of 1.62-1.7 eV [21] below the conduction band, (c) phosphorus, a donor with an excitation energy of 0.46 eV [21] below the conduction band, (d) arsenic, a donor with an excitation energy of 0.4 eV [32] below the conduction band, (e) antimony, a donor with an excitation energy of 0.3 eV [32] below the conduction band and (f) lithium, a donor with an excitation energy of 0.1 eV [29] below the conduction band.

1.2.3 Co-Doping

Co-doping involves incorporation of more than one type of impurity into the diamond lattice. This can be accomplished with both n-type and p-type dopants. Although there has been greater interest in n-type co-doping as there have been more limitations with this as opposed to p-type doping.

1.2.3.1 Co-doping with H:B to produce P-type semiconductor.

Hydrogen and boron co-doping was achieved with a pressure of 6 GPa and a temperature between 1560 and 1600 K. In comparison to boron doped diamond, H:B co-doping has a lattice structure that is more compatible to diamond. Due to the incorporation of hydrogen into the bulk of the diamond lattice, the p-type semiconductor was superior to that in boron doping alone. H:B co-doping produced a much higher quality diamond structure with a much larger diamond peak in the Raman data (Figure 1.6) [14].

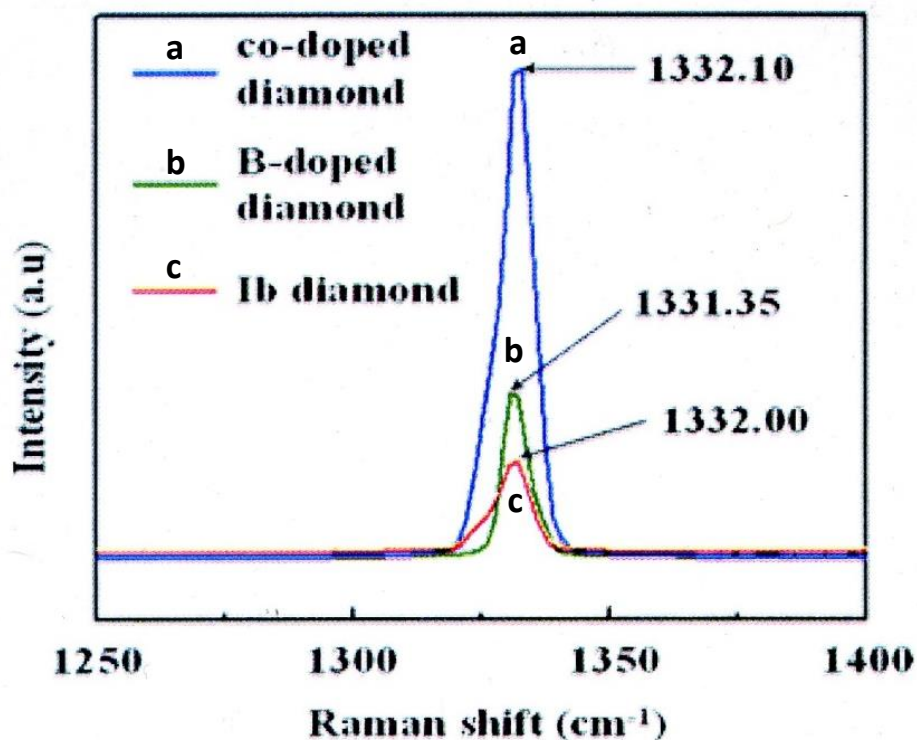


Figure 1.6: Raman spectra of (a) boron and hydrogen co-doped diamond, (b) boron doped diamond and (c) Ib diamond [14].

1.2.3.2 Co-doping with B:S to produce N-type semiconductivity

There has been quite a lot of research into co-doping of diamond with sulphur and boron. Sulphur cannot be introduced into the diamond lattice unless it is co-doped [21]. Firstly, sulphur can be incorporated into the lattice using H₂S gas. With addition of a small concentration of boron; n-type semiconductivity results but, as the boron concentration is increased p-type semiconductivity is observed instead. The majority of sulphur is located near the surface of the diamond and as diamond growth proceeds, the sulphur diffuses into the bulk of the lattice. The boron however was not concentrated at the surface and was spread relatively evenly throughout the lattice. With the addition of heat, the semiconductivity is lost as the activation energy increases from 0.06 – 0.12 eV at room temperature to 1 – 1.5 eV at 400 K [21,34,35].

1.2.3.3 Co-doping with B:N to produce N-type semiconductivity

Boron and nitrogen are another pair of atoms that have been co-doped into diamond-like carbon films. However, although this did increase the semiconductivity of diamond, additional graphitic areas were observed [36].

1.2.3.4 Li:N co-doping

Both lithium and nitrogen can be incorporated into the diamond lattice, yet for different reasons, the desired semiconducting effect has not been achieved (see sections 1.2.2.2. and 1.2.2.3). Therefore, recent research into using a combination of lithium and nitrogen co-doped diamond is still under investigation. Computer models have predicted that atoms with more electrons than lithium, for example nitrogen as it is such a deep donor, can trap and slow the movement of lithium so it can no longer aggregate and cluster together. This means that the electrons remain delocalised and can be transferred through nitrogen into the diamond lattice [37]. It is vital that the diamond lattice is doped with nitrogen atoms before lithium atom incorporation. This ensures that no lithium aggregation can occur [24]. An additional advantage is that it is believed that the nitrogen atoms can prevent the lithium atoms from migrating from interstitial to substitutional sites in the lattice where it would be effective as a p-type dopant [24].

Experiments investigating the effect of over-doping the diamond lattice with nitrogen need to be considered. In order to reduce lithium mobility, it is vital that every lithium atom is adjacent to at least one nitrogen atom [24]. However, if there are too many nitrogen atoms in comparison to lithium, then semiconductivity will not be achieved.

When diamond is co-doped with Li:N, the grain boundaries provide a route for atom migration, yet the atoms move mainly between the grain boundaries and much less so within them [37].

In one study, a 1:1 ratio of Li:N co-doping was suggested with a lithium concentration of $\approx 5 \times 10^{19} \text{ cm}^{-3}$ and a nitrogen concentration of $\approx 3 \times 10^{20} \text{ cm}^{-3}$. Li_3N solution was proposed as the potential dopant for lithium atom incorporation and ammonia gas for the incorporation of nitrogen atoms. However, lithium has one vacant electron and when nitrogen atoms are incorporated into the lattice it has four bonds to carbon, so also has one free electron. Therefore a Li-N bond will form so there will be no free donor electrons [24].

Experiments on Li:N co-doping at a ratio of 1:18 showed that resistance was much lower for Li:N co-doped diamond than for N-doped diamond. At room temperature, a resistance $> 200 \text{ M}\Omega$ was recorded for N-doped diamond, yet for a Li:N co-doped sample with a 1:18 ratio, resistance as low as 10-20 $\text{M}\Omega$ was recorded. This indicates that semiconductive properties of diamond may be feasible. However, this resistance still remains too high for semiconductive properties of diamond. This is believed to be due to both lithium and nitrogen becoming inactive as they are trapped in the sp^2 grain boundaries in the diamond lattice. Alternatively, it has been suggested that if the nitrogen atom concentration is too high, more lithium atoms migrate to substitutional sites and no longer reside in interstitial positions [24]. These results are still promising, and research indicates that a lower concentration of nitrogen atoms may produce the semiconductivity required [24].

The diamond crystals are less smooth with co-doped Li:N diamond in comparison to a N-doped sample (**Figure 1.7**). Incorporating lithium into diamond produces additional nucleation sites [37]. To try to obtain a lower resistance, computer models and other studies suggested a Li:N ratio of 1:4 could produce n-type diamond [38].

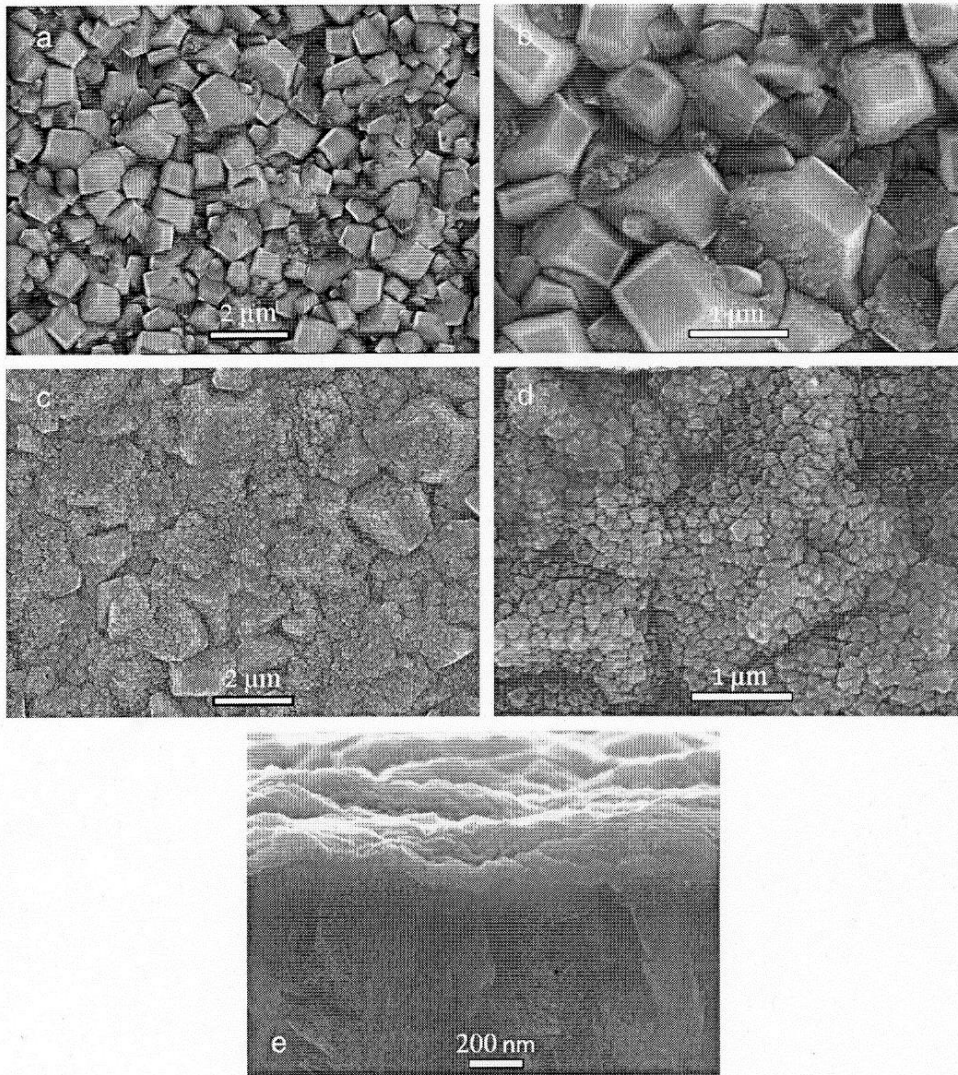


Figure 1.7: SEM micrographs of N-doped MCD (a&b) on a silicon substrate. This can be compared with co-doped Li:N diamond (c&d). Note how these are much less smooth. A thickness of 200 nm was obtained for the Li:N diamond film (e) [37].

With Li:N co-doping, Raman spectra only show graphite and diamond peaks with no additional lithium or nitrogen peaks; so spectra is similar to N-doped and undoped diamond (**Figure 1.8**). Note that the graphite peak is much less prominent with Li:N co-doping, a potential reason for this is the preferential etching of graphite by lithium atoms over diamond [24].

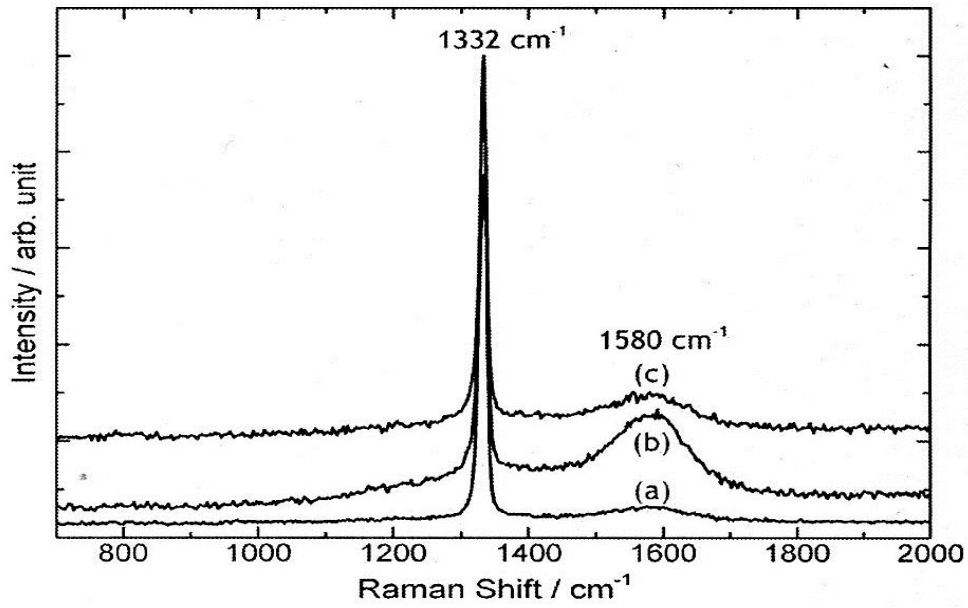


Figure 1.8: Laser Raman spectra (325 nm He-Cd excitation) showing (a) undoped diamond, (b) N-doped diamond and (c) Li:N (1:18) co-doped diamond [37].

Secondary ion mass spectrometry (SIMS) was also performed to obtain information of the concentration of nitrogen and lithium atoms incorporated into the diamond lattice (Figure 1.9).

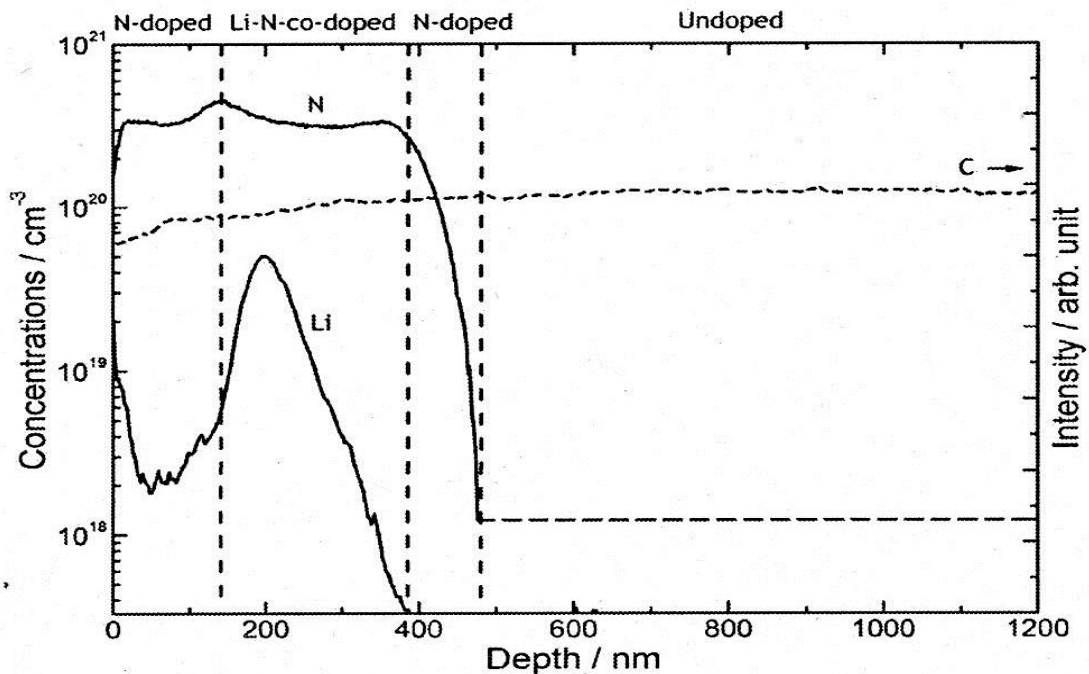


Figure 1.9: SIMS depth profile of co-doped lithium and nitrogen (Li:N, 1:18) when grown on a diamond film in multilayers. The headings above the diagram highlight when in the growing process nitrogen doping and lithium doping occurred [37].

1.3 p-n Junctions

P-n junctions are located at the interface between a p-type and n-type semiconductor (**Figure 1.10**). Hence supporting the argument of why n-type diamond is so crucial to obtain. They are very important in the electronic industry since they are vital for a number of applications including, LEDs, diodes and transistors since with an applied voltage they allow the flow of current in only one direction.

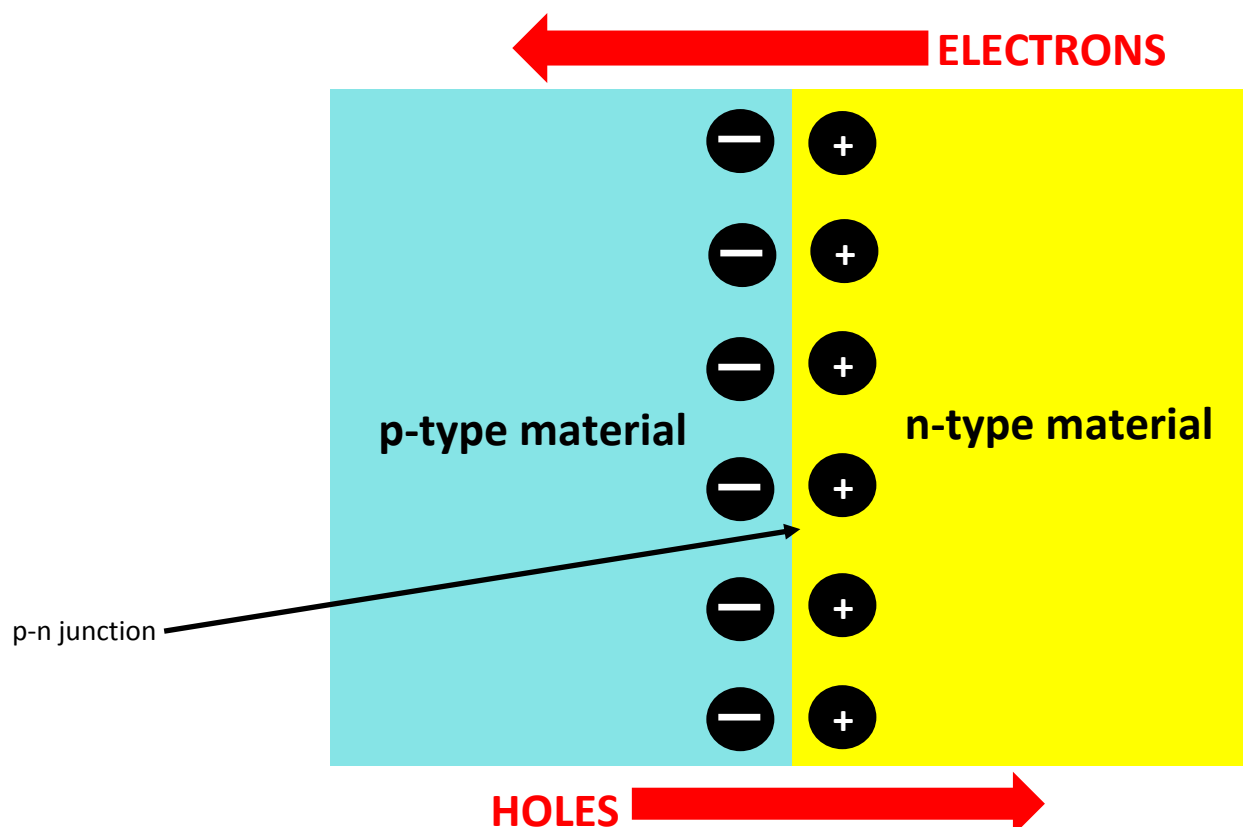


Figure 1.10: Schematic diagram of a p-n junction. The p-n junction is located at the interface between the p-type and n-type material. The n-type material which is electron rich, has a build-up of positive charge at the p-n junction as holes migrate towards it. The p-type material, which is electron deficient, has a build-up of negative charge at the p-n junction where electrons have migrated towards it. Once a voltage is applied, this will allow current to flow in only one direction.

In 1982, natural diamond was used to create a bipolar transistor, since then attempts to synthesize p-n junctions using diamond have increased [39]. P-n junctions are difficult to form using p-type and n-type diamond as a suitable n-type diamond has not yet been synthesized. However, p-n junctions have been created using boron doped diamond (p-type) and phosphorus doped diamond (n-type) and the diode characteristics were promising with this sample [39].

Successful p-n junctions have also been fabricated using boron doped diamond (p-type) and silicon doped cubic boron nitride (c-BN) (n-type) [39]. C-BN is a good choice as it has a similar structure

and similar properties to diamond with the additional advantage that it forms both p- and n-type dopants [39]. A p-n homo junction diode was reported when using HPHT, although CVD may be required to obtain junctions required for the electrical industry [40]. Results highlighted that the diamond film grown on c-BN was of high quality with no graphite peak observed with Raman spectroscopy [39].

A p-n junction has also been synthesised using c-BN alone, with a p-type semiconductor from beryllium doped c-BN and a n-type semiconductor from silicon doped c-BN. The Raman spectrum for this is shown (**Figure 1.11**) [39].

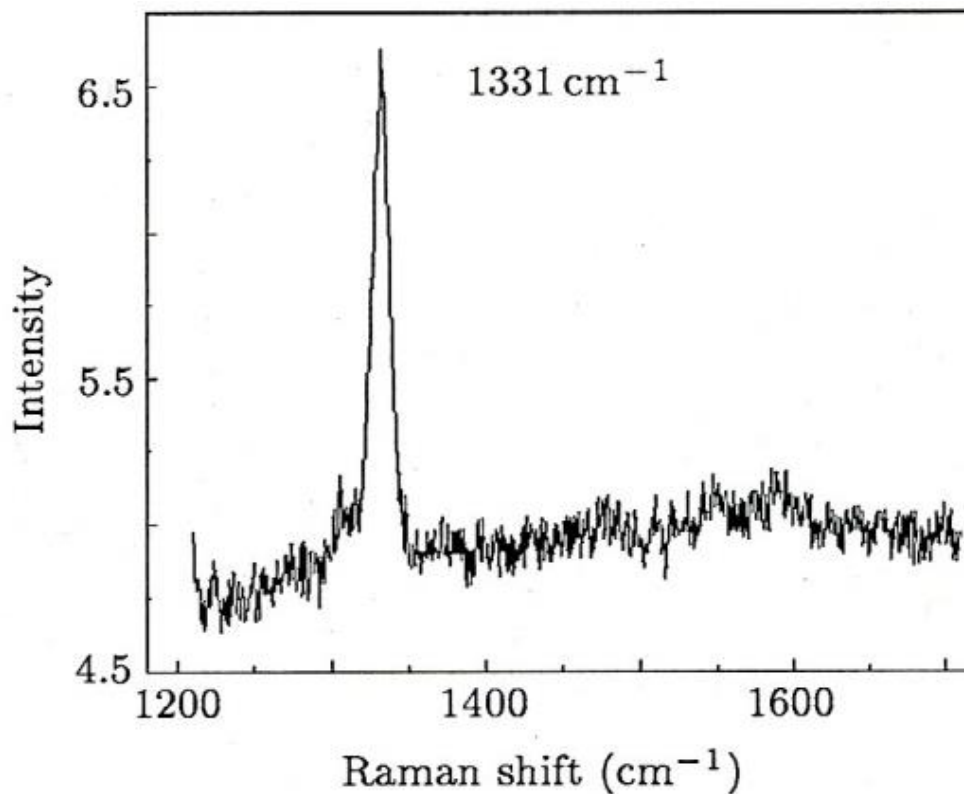


Figure 1.11: Raman spectrum of a diamond film grown on c-BN [39].

1.4 Applications of Doped Diamond

Diamond would be a good semiconductor due to a number of its properties; some of these are shown (**Table 1.2**). For the semiconducting properties of diamond to be utilised, it is important that a high quality film is produced. It is also essential to produce a smooth surface with few residential impurities and low defect density [41].

Table 1.2: Table highlighting the properties of diamond that make it attractive to the semiconducting industry [4,42,43].

Properties of CVD Doped Diamond
High thermal conductivity (2000 W m ⁻¹ K ⁻¹)
High saturation velocity (107 cm s ⁻¹ for holes)
High electron drift velocity
High electric field
High breakdown voltage (10 ⁷ V cm ⁻¹)
High hole mobility (2100 cm ² V ⁻¹ s ⁻¹)
High dielectric strength (10 ⁷ V cm ⁻¹)
Low dielectric constant (5.7 at 300 K at 1-10 kHz)

Properties of diamond have been exploited, for example for Schottky devices, temperatures sensors and pressure sensors with temperatures up to 1000 °C. Conductive diamond could also be used in electrochemistry, and in areas such as electron emission devices, for example, cold cathodes [1]. Another major advance would be to use diamond to activate electronic devices and chips with p-type and n-type doping

The applications of diamond would be greater if both n- and p-type CVD diamond could be synthesised using a cheap and efficient procedure, producing high quality diamond. Not only is diamond essential in the jewellery market, but there are also possibilities for diamond to be used as a heat sink due to its extremely high thermal conductivity. It could also be used in the engineering industry, as an abrasive, and for certain tools as a wear resistant coating [3]. Although the main advantage of CVD diamond is its use as a semiconductor, as noted above, it has many other uses and potential uses in the future.

1.4.1 Optics

The CVD process can produce a freestanding diamond film and this could be useful in an infra-red window. In the wavelength range of 8-12 μm, the IR materials generally used are damaged easily. Therefore, using diamond, the hardest material known, would remove the risk of damage [2].

1.4.2 Heat Sink Material

In electronic and opto-electronic devices, a common problem occurs where the device will overheat and consequently needs to be cooled by a highly conducting material. The heat conductivity of diamond is the largest of any known material at room temperature. Therefore, if diamond could be used in these devices it would increase the efficiency of cooling compared with materials that are already on the market (most commonly copper). Diamond is already used commercially, for example, as submounts for integrated circuits. It has numerous advantages in this field as it has unusual properties for example, it is an electrical insulator [2].

1.4.3 Light Emitting Diodes

For light emitting diodes (LEDs) to be viable, both n-type doping and p-type doping are essential for p-n junction formation (see section 1.3). The acceptors and donors combine to produce photon energy. This is called recombination radiation, a process that exists in natural diamond. Diamond has been used in LEDs and the energies it produces are higher than those already commercially available, for example GaN. Diamond can withstand higher temperatures than those already known, so it is the more superior material (see section 1.1).

1.4.4 Surface Acoustic Wave (SAW)

CVD diamond could be very effective in surface acoustic wave (SAW) filters, which are used in the conversion of mechanical vibrations into radio frequencies. These would be placed on the surface of the filter, CVD diamond films have already been used in this device in mobile phones [2].

1.4.5 Cutting Tools

Due to diamonds profound hardness and its wear resistance, it would be a good cutting tool for a variety of applications. Iron causes diamond to abrade at high temperatures, therefore manufacture of non-ferrous metals, composite materials and plastics are all areas of interest. Research highlights that CVD produces a more superior product than HPHT that can cut faster, has a longer lifetime with a more polished look [2].

2.0 Experimental Techniques

2.1 Hot Filament Chemical Vapour Deposition (HFCVD)

The two most popular CVD processes to grow MCD are MWCVD and HFCVD. A HFCVD system, located in the Diamond Laboratory at the University of Bristol was used for the numerous diamond samples that were grown (**Figure 2.1**). HFCVD is a cheaper process than the MWCVD process which is a much more powerful piece of equipment. HFCVD is also an advantageous technique as the diamond film can be deposited over a large area of substrate [24].

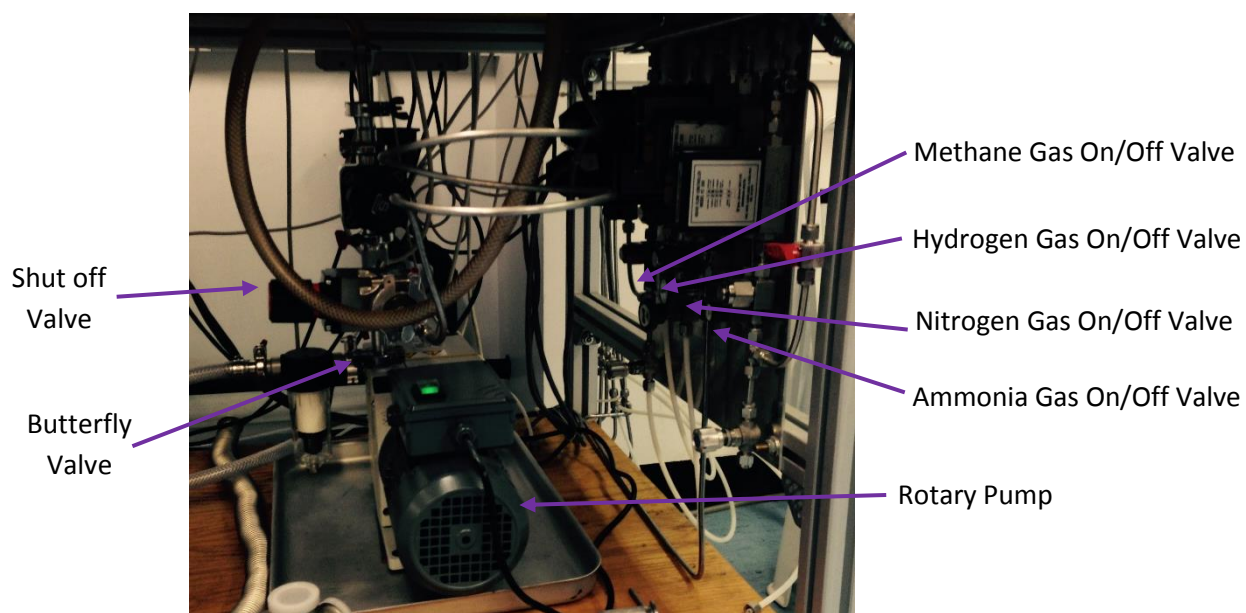
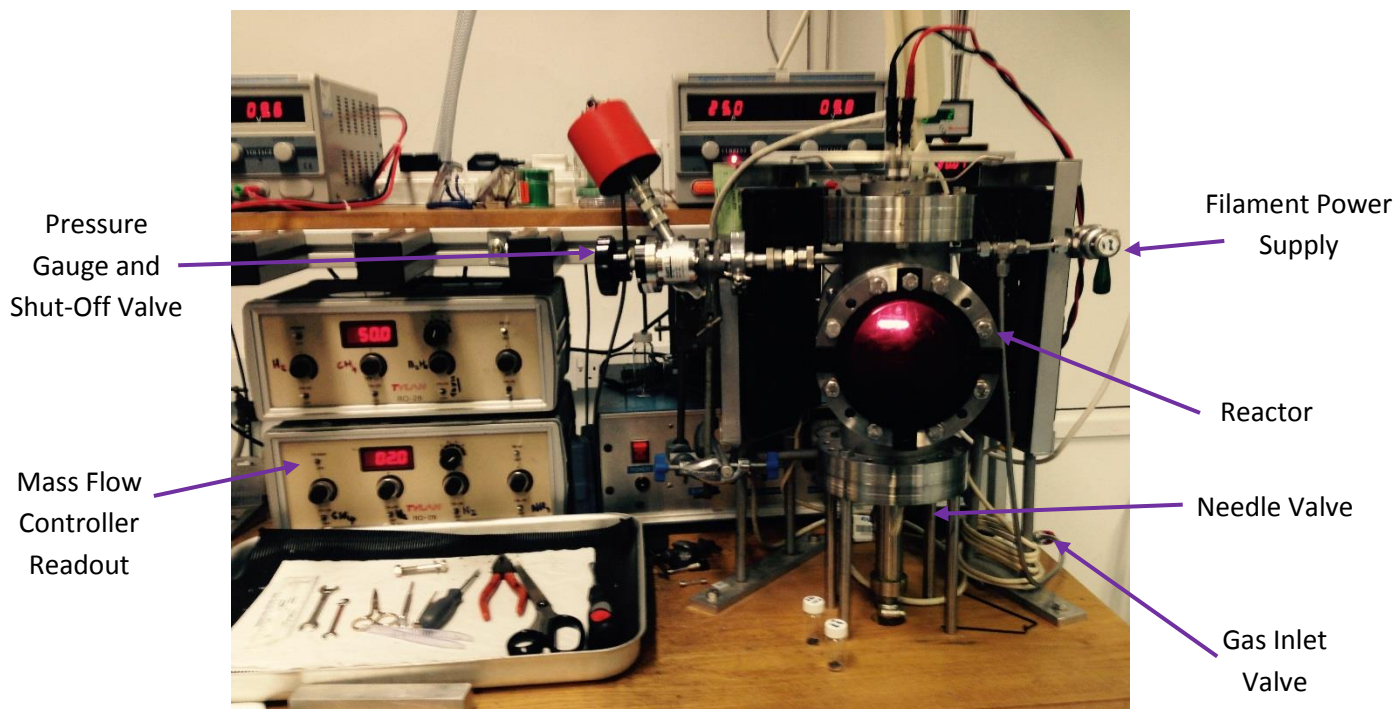


Figure 2.1: Photographs of the Hot Filament reactor used for growth of the diamond films using the CVD process.

2.1.1 HFCVD Conditions

Although filaments such as tantalum or tungsten are popular, a Goodfellow rhenium filament was used in synthesis of the diamond samples. This filament had a purity of 99.97% and a diameter of 0.25 mm. It is a much more expensive filament but is much more durable. The filament was heated to activate the precursor gases for diamond growth. Fabrication of undoped diamond requires CH₄ and H₂ as precursor gases. These gases are mixed in the manifold and entered the reactor where activation occurs. The hot filament elevates temperatures in the reactor and raises energy levels so that radicals can form. From CH₄ gas and H₂ gas, radicals such as H, CH, CH₂ and CH₃ are produced. The reactive radicals proceed to cause high energy reactions as they diffuse towards the substrate surface where the layers of diamond build up. The substrates used in these experiments were either molybdenum or silicon.

When growing diamond onto the molybdenum or silicon substrates many conditions were kept constant (**Table 2.1**).

Table 2.1: Table highlighting the conditions that were kept constant during the CVD process.

Constant Conditions of the HFCVD Reactor
3 parallel rhenium filaments
Filament to substrate distance = 3 mm
Current = 25 A
Pressure = 20 Torr
Self-assembly = Carboxyethylsilanetriol Na Salt 25% in Water and 18 nm Nanodiamond suspension
Mo/Si substrate thickness = 500 μm
Temperature of rhenium filament = 2300-2500 K
Substrate temperature = 1100 K

If N-doped diamond was being synthesised then CH₄, H₂, NH₃ and N₂ were required as precursor gases. N₂ and NH₃ flowed into the reactor in the same manner as CH₄ and H₂ gases. For lithium atom incorporation into the diamond lattice, Li₃N solution was added in a drop-wise fashion, not as part of the precursor gas mixture (see further details in section 2.2 and 2.3).

2.1.2 Set up of the HFCVD

To deposit the diamond, the substrates were placed underneath the rhenium filaments attached to the sample stage (**Figure 2.2**). This was then placed in the stainless steel chamber to be pumped down. To put the chamber under vacuum, a tight seal was secured with three bolts screwed tightly, so that no air could enter the system. The vent was then closed and then the rotary pump (Oerlikon Leybold Vacuum GMBH, D 8 B) was opened along with all other valves (the needle, gas inlet, shut-off and butterfly valves). Lastly, the pressure gauge isolation valve was closed. For the system to be fully pumped down, the pressure had to reduce to < 10⁻² Torr. This took approximately 15 minutes. If

this value was not reached, generally the system was open to air, for example if the bolts were not screwed tightly enough or if the vent was not fully closed.

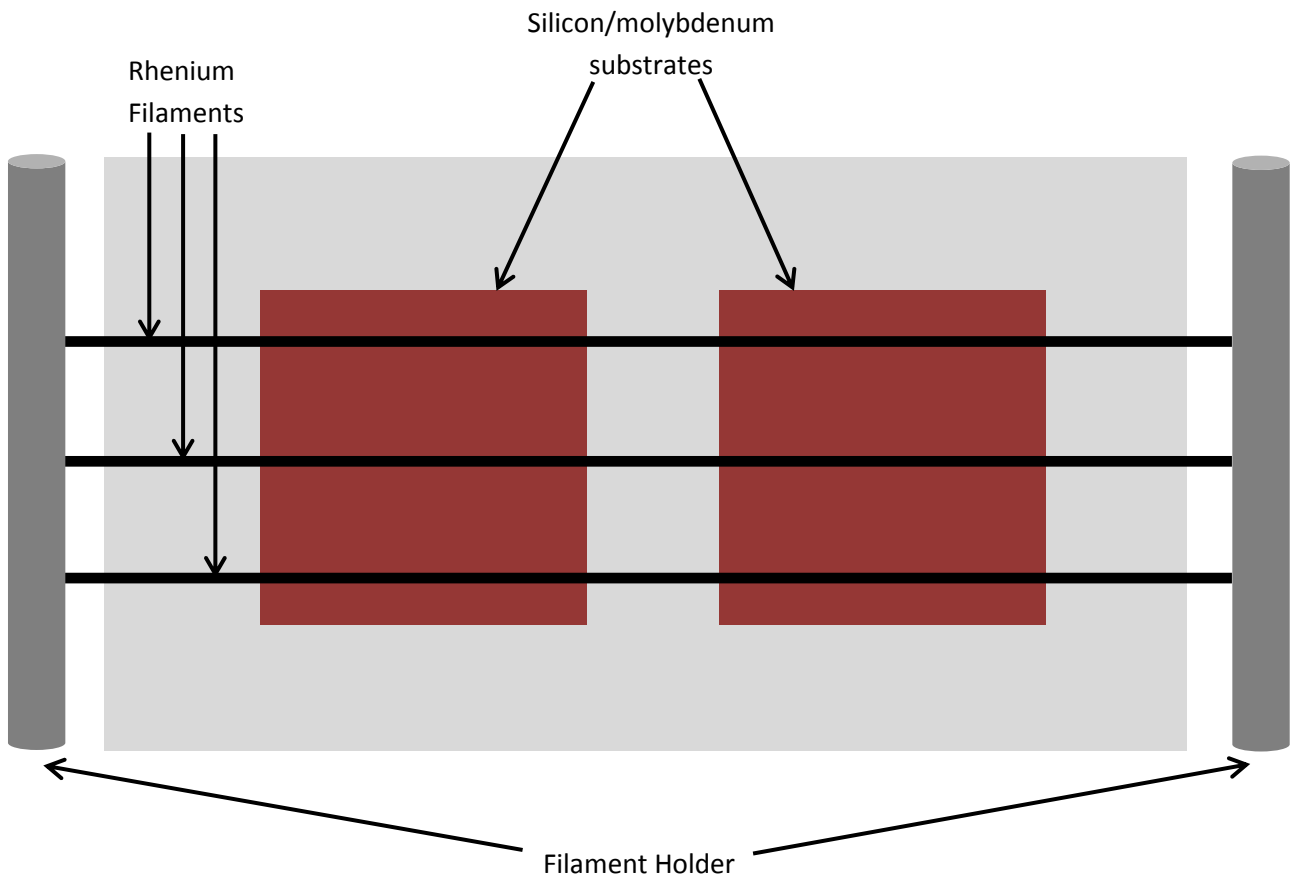


Figure 2.2: Schematic diagram of a top-down view of the sample stage with silicon or molybdenum substrates underneath rhenium filaments.

When a pressure $< 10^{-2}$ Torr was reached, the mass flow controllers (MFCs) were set to the required flow rates (in standard cubic cm per minute, sccm) of the precursor gases. Before heating the filaments, the cooling fans were turned on so that the system did not overheat. The filament power leads were also attached. The MFCs were turned on and the valves permitting gas flow were opened. Once the valves were opened, the gases entered the chamber. This increased the pressure of the system. The rotary pump main valve was then closed, so that pumping only occurred through the small pipe, increasing the pressure inside the chamber further. Finally, the pressure was raised to the optimum value of 20 Torr by closing the needle valve on the small pipe. After the pressure was relatively stable at 20 Torr the filament DC power supply (Digimess, SM3040) was turned on. The power supply controlled the current and the voltage of the system. The current remained at 14 A for 5 minutes to allow the filaments to heat up and was then further increased to 25 A. The current was increased slowly to ensure that the filaments did not break. Once at 25 A the diamond proceeded to grow for a further 3 hours. It was important that the growing conditions were checked regularly. The power and pressure varied, especially in the first 30 minutes of deposition. These

values must remain relatively constant to ensure reliable results. The MFCs were also regularly checked to make certain that the desired flow rate values were being read. This may drop if an inadequate amount of gas was being supplied, for example; if the cylinder had run out.

After 3 hours of growth had been completed, the current was reduced to 20 A. The precursor gas valves were closed and the MFCs were turned off with the exception of the H₂ gas flow. This was so that hydrogen termination could occur. Hydrogen termination is a crucial element of diamond growth. Once the CH₄ gas was turned off no more diamond growth can occur. Therefore there will be dangling bonds on the surface of the diamond film. When growth stops this will form a graphitic layer on the surface if not hydrogen terminated. Since hydrogen is in such high abundance, this will instead form C-H bonds on the surface [2].

After 5 minutes of hydrogen termination, the current was reduced to zero. Again, this was done slowly to ensure that the filament remained intact. The H₂ gas MFC was now turned off and the valve permitting gas flow to the chamber was closed. The rotary pump and the needle valve were then opened to allow the system to pump back to its base pressure.

After a cooling period of approximately 30 minutes, the system was opened up to air to vent the chamber. To do this the pressure gauge isolation valve was closed and all other valves were then closed including the rotary pump. The vent was then opened slowly and the sample was removed from the sample stage.

2.2 Nitrogen Doping of the Diamond Film

For nitrogen atom incorporation, NH₃ gas and N₂ gas were flowed into the reactor along with CH₄ and H₂ gas. To achieve optimum film quality, various percentages for NH₃ and N₂ gas were investigated with respect to H₂ gas, providing different dopant concentrations.

Potential sources of nitrogen include nitrogen gas (N₂), ammonia gas and HMT (hexamethylenetetramine). In HFCVD, ammonia gas has proved more successful than nitrogen gas for nitrogen atom incorporation into the diamond lattice. This is due to the strength of the N-N triple bond in N₂ gas at 945 kJ mol⁻¹. With ammonia gas, the N-H bonds are much weaker at 391 kJ mol⁻¹, so incorporation of the nitrogen atoms is much easier [24]. This is not an issue in MWCVD as it is much more powerful so the higher energy will break apart the N-N triple bonds easily. HMT is advantageous as it produces uniform {100} facets. However, the limitation of HMT is that it is a solid at room temperature, so has to be made into a liquid solution for doping. Furthermore, HMT does not provide sufficient incorporation of nitrogen atoms into the diamond lattice in comparison to ammonia gas.

Both N₂ gas and NH₃ gas were already connected to the MFC. Therefore they were both used for N-doped diamond production. Studies on whether both gases were needed and the optimum amount of each gas are discussed in sections 3.1 and 3.2.

The concentration of CH₄/H₂ was predominantly 0.81%. Occasionally a different quantity was required. Further details are in the section 3.5.2.

Characterisation of the N-doped diamond films were achieved by laser Raman spectroscopy and SEM to examine film quality and morphology.

2.3 Li₃N Addition to N-doped Diamond Films

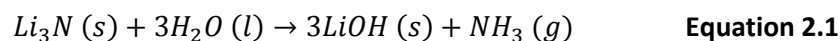
Once N-doped diamond films had been fabricated, the Li₃N solution was added. Li₃N is a solid at room temperature. To form the solution, a suspension of Li₃N powder and chloroform was prepared (in 1% w/v polyoxy in chloroform) with a concentration of Li₃N at 0.49 mol.dm⁻³ (**Figure 2.3**). The particles were evenly distributed with a size of ≈ 1 - 20 μm and an average crystallite separation of 30 μm. Li₃N has a high melting point at 813 °C [44] which ensures it remains in solution at room temperature but evaporates when heated in the reactor.



Figure 2.3: Li₃N solution, prepared by forming a suspension of Li₃N powder and chloroform (1% w/v polyoxy in chloroform).

The N-doped diamond films were grown first to ensure that when Li₃N solution was added, the nitrogen atoms prevented the lithium atoms from clustering together. The Li₃N solution was sonicated for 1 hour before deposition to again ensure that there was no lithium aggregation.

Extreme care was taken with the Li₃N solution as it is extremely flammable upon contact with water and can cause severe burns. Therefore, only a small amount was used to minimise the risk. This reaction produces ammonia and lithium hydroxide (**Equation 2.1**).



Li₃N solution was drop-cast onto the surface of the diamond film using a Gilson pipette. 50 µL of Li₃N solution was added and dried at a time and then another 50 µL was added and dried until the required volume was obtained. The Li₃N was added in such small portions to ensure it did not spill and remained on the film. This was also done to minimise risk. After the final addition had dried the samples were placed back underneath the rhenium filaments in the sample stage. This was then placed into the chamber to be pumped down (section 2.12) and ready for diffusion of lithium atoms into the diamond lattice. Although much the same, there were slight differences in the growth procedure.

Firstly the filaments were heated up slowly for 5 minutes at 14 A with *only* H₂ gas switched on. Very quickly, white fumes were observed indicating that Li₃N was reacting with hydrogen radicals to form LiH. When these fumes disappeared, the Li₃N was melting and lithium atoms started diffusing into the diamond lattice. This took place after approximately 15 minutes. The current was then increased slowly to 25 A to allow further lithium diffusion for 1 hour. Subsequently, there was an addition of 0.81% CH₄/H₂, still at 25 A, for a further 5 minutes. This permits further diamond growth which produces a diamond capping layer over the newly diffused lithium atoms [24]. Finally, the diamond surface was hydrogen terminated under normal conditions used for deposition, with a reduced current of 20 A for 5 minutes. The reactor was then cooled and vented (section 2.2.1).

Characterisation of the Li:N co-doped films was achieved using laser Raman spectroscopy and SEM to examine film quality and morphology. SIMS was also used when required to obtain the lithium (Li⁺) and nitrogen (CN⁻) concentrations in the lattice.

Similar to nitrogen atom incorporation, there were other possibilities that could have been used for the lithium containing compound. Ideally, the lithium compound would be in the gaseous phase, as this could then be added to the MFCs. Therefore it could enter the reactor through a valve, in the same manner as H₂, CH₄, N₂ and NH₃ gases. Organo-lithium compounds were the most promising compounds but could not be used due to their explosive reactivity. Therefore, a solid lithium containing compound was required that did not have such explosive reactivity. It was also important that it did not react with the other precursor gases inside the reactor. Lithium salts such as LiCl, and lithium oxides were both discarded due to unwanted reactions that might damage the vacuum pump and the filament respectively. Lithium carbide was also a candidate, yet its melting point at 550 °C [24], is lower than that of Li₃N at 813 °C [44]. Therefore, Li₃N solution would evaporate slower due to the higher melting point and more was available for diffusion.

2.4 Laser Raman Spectroscopy

Raman spectroscopy is a light scattering technique where monochromatic light is absorbed by the diamond sample. This technique is non-destructive, which is a great advantage since it did not damage the diamond samples, which meant that further analysis could be performed. The UV laser provides energy to the sample resulting in lattice vibrations. Scattered light is then detected and the shift in frequency coincides with vibrational energy levels of the material being analysed. If the emitted light is at a lower vibrational energy than the incident light a Stoke shift will be produced. If the emitted light is at a higher vibrational energy, these are anti-Stokes shifts [45].

Both Rayleigh and Raman scattering occur in Raman spectroscopy. Rayleigh scattering is much more frequent than Raman and is at a much higher intensity in the resulting spectrum. Rayleigh scattering is elastic and involves no overall net transfer of energy. Raman scattering is inelastic and involves a transfer of energy. Therefore the Rayleigh scattering is generally filtered out so the Raman scattering can be observed and analysed [45].

The laser Raman spectrometer (Renishaw 2000) located in the Chemistry department in the University of Bristol (**Figure 2.4**) was used to analyse the film quality of the diamond sample.



Figure 2.4: The laser Raman Spectrometer Renishaw 2000, located in the Chemistry department in the University of Bristol.

UV excitation was used with a Helium:Cadmium (He:Cd) laser (325 nm). The UV laser was selected as it has a higher sensitivity to sp^3 carbon. Green and IR excitation are also possible with, Green, Ar^+ (514 nm), and IR, diode laser (785 nm). These techniques are more sensitive to sp^2 carbon, therefore were not used in this study [24].

The centre of the spectrum was normalised at 1332 cm^{-1} for the diamond peak and the graphite peak was observed at 1580 cm^{-1} . The samples were run for 30 minutes by an exposure time of 60 seconds with 30 accumulations. Cosmic ray removal was applied as Raman is a very sensitive technique which can potentially pick up cosmic rays if these are not removed. The scan type was set to static.

Analysis of the diamond film quality was achieved by studying the diamond to graphite ratio. This is a measure of the intensity of the diamond peak in the Raman spectra with respect to the intensity of the graphite peak (**Equation 2.2**). Ideally this value should be as high as possible meaning a higher proportion of sp³ diamond features in the lattice with a lower proportion of sp² graphite at grain boundaries.

$$\frac{I_D}{I_G} = \frac{\text{Intensity of Diamond Peak}}{\text{Intensity of Graphite Peak}} \quad \text{Equation 2.2}$$

What has been referred to as the ‘graphite’ peak may not be completely from graphite. It may be increased by diamond sp² carbon; which are areas where diamond cannot form all its 4 bonds so is actually sp² diamond and not sp³ diamond.

2.5 Scanning Electron Microscope (SEM)

The scanning electron microscope (SEM) (JEOL JSM 6330F) is located in the Interface Analysis Centre (IAC), Physics department, University of Bristol. This was used in conjunction with the Raman spectroscopy to examine film morphology. An optimal diamond film produced uniform {100} square diamond facets with a large crystal size and few graphite areas.

The conditions for the SEM are given in **Table 2.2**.

Table 2.2: The conditions used in this study to obtain SEM images from the SEM (JEOL JSM 6330F) in the IAC, Physics department, University of Bristol.

External Voltage	10 kV
Current	12 μA
Working Distance	7-8 mm

2.6 Resistance Measurements

After the samples were grown and analysed, resistance was measured to see how the different doping concentrations affected conductivity.

2.6.1 Bell Jar Evaporator

In order to measure the resistance of the diamond samples, the sample required metal contacts. To obtain the metal contacts, silver particles were evaporated onto the diamond samples using a bell jar evaporator (Edwards Coating System E306A) (**Figure 2.5**). This is located in the Diamond Laboratory at the University of Bristol. Silver was the chosen metal as it has a very low resistivity of $1.58 \times 10^{-8} \Omega \cdot \text{m}$ [46]. This can be compared to diamond which at room temperature has a resistivity of $1 \times 10^{14} \Omega \cdot \text{m}$ [2]. Therefore, silver would have no effect on the resistance measurements of diamond. Furthermore, silver is easy to deposit, it is not easily oxidised in air and is a relatively cheap metal.



Figure 2.5: The ball jar evaporator, located in the Diamond laboratory, University of Bristol with the thickness monitor and the Edwards Pirani 1001 pressure monitor on top of the bell jar.

Firstly a tungsten filament was positioned inside the bell jar in between 2 powered posts. It was vital that there was a strong connection here so that the current could flow. Since this study required silver contacts, a silver wire was attached to the tungsten filament. The diamond samples were then placed inside the bell jar approximately 10 cm beneath the tungsten filament. Silicon masks with two $1 \times 1 \text{ mm}^2$ square holes cut out on opposite corners were placed on top of the diamond samples (**Figure 2.6**). These two holes ensured that only two square contacts of silver were evaporated onto the diamond samples. It was important that the evaporated silver made perfect squares on the diamond film as this would provide a good contact. If contacts were not square, inconsistent resistance results would be obtained. The bell jar was then sprayed with Bell Bright, a protective coating, which allowed easier cleaning of silver after evaporation.

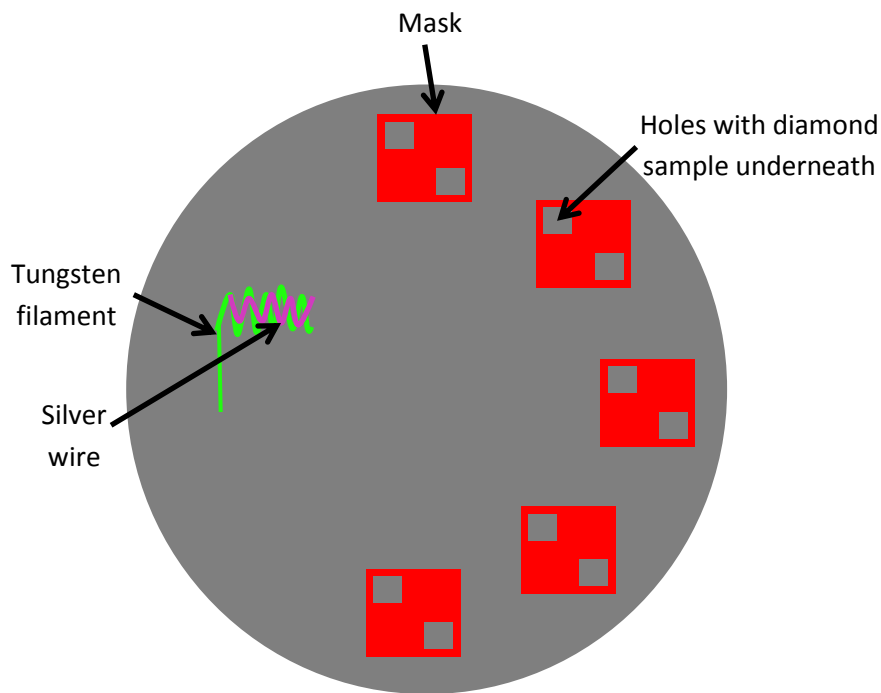


Figure 2.6: Schematic and photograph of the inside the bell jar evaporator showing the masks with $1 \times 1 \text{ mm}^2$ holes with the diamond sample underneath. The tungsten filament and silver wire can also be viewed.

The bell jar was then evacuated. Once under vacuum there was a delay for approximately 15 minutes while the pressure reduced to $< 10^{-2}$ Torr. Once this pressure was reached it was important

to check that the silver wire was still in place and that the masks were still over the diamond samples since vibrations may have caused movement. If the masks moved, perfect squares would not be obtained and if the silver wire was not attached to the tungsten filament, evaporation of silver would not occur. The pressure was then further reduced to 2×10^{-5} Torr, this could take any period of time over 2 hours.

Once at this low pressure, the current was increased slowly to heat the tungsten filament and therefore the silver wire. A thickness monitor (Agar quartz crystal resonator) displayed the thickness of silver contact. The current continued to be increased slowly to approximately 10-15 A when silver evaporation began and the value on the thickness monitor started to increase. A slow steady increase in thickness was required as this ensured an even layer of silver. Once 50 nm of silver had been deposited, the current was slowly reduced to 0 A, the system was cooled and pumped down.

After cooling, the system was opened to air. The seal of the bell jar had to be broken for sample removal.

2.6.2 Oxygen Termination

After growth, the diamond films had been hydrogen terminated (see section 2.1.2). This results in surface conductivity that would affect the resistance measurement. Therefore, before resistance measurements could be taken the samples were oxygen terminated as this provides an insulating layer that removes surface conductivity. To do this the samples underwent ozone plasma treatment using the UVO Cleaner (42A-220) for 30 minutes [24].

2.6.3 Two-point Probe measurement

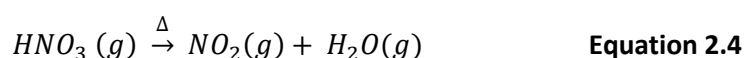
After oxygen termination, the resistance was measured with a Fluke 289 True RMS Multimeter and a two-point probe. This was the fundamental step of this study, to identify if diamond samples with low resistance had been achieved. Care was taken with the point probes as the silver contacts could easily be scratched off which would remove the necessary ohmic contact.

2.7 Acid Washing

Semiconducting diamond films have the potential to be used as acid sensors [47]. Therefore once the Li:N co-doped diamond films had been grown they were tested in a strong acidic solution. Resistance of the diamond films were measured before and after this acid wash to evaluate how resistant the co-doped films were to the acid.

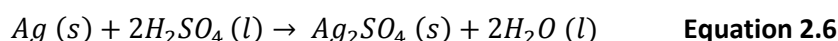
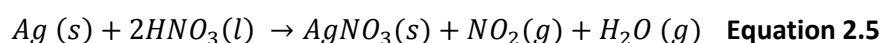
This process used very concentrated H_2SO_4 , therefore gloves, lab coats and eye protection were worn at all times.

Firstly a round bottom flask (RBF) was washed with a small portion of the acid. This ensured that there was no water in the flask as this would have produced a highly exothermic reaction. Once washed, 100 mL of 95% w/v H₂SO₄ was added and the diamond samples were placed in the flask along with 6.5 g KNO₃. The contents were then refluxed at 180 °C for 20 minutes until the colour of the solution changed from colourless to dark brown. The H₂SO₄ and KNO₃ reacted to produce HNO₃ (**Equation 2.3**). With heat the HNO₃ produced gaseous NO₂ which was observed by dark orange fumes (**Equation 2.4**). Remaining under reflux, the heat was then maintained at 180 °C and the solution was left for a further 30 minutes. When the reaction had completed, the heat was turned off and the solution was left to cool.



After cooling, the acid was removed into the appropriate container. The diamond samples were then washed thoroughly to ensure that all the acid was removed and dried.

The silver contacts that been evaporated onto the diamond films for resistance measurements were removed during the acid wash. This was a result of the reaction of silver with HNO₃ and H₂SO₄ producing silver nitrate and silver sulphate respectively (**Equation 2.5 and Equation 2.6**). Therefore, additional silver contacts had to be evaporated onto the sample after the acid wash (see section 2.6) for further resistance measurements.



2.8 Secondary ion mass spectrometry (SIMS)

Secondary ion mass spectrometry (SIMS) located in the Interface Analysis Centre, Physics department, University of Bristol, provides information on the concentration of lithium and nitrogen atoms in the diamond films.

15 nm of silver was evaporated onto the Li:N co-doped diamond sample (section 2.6.1) before any SIMS measurement. This was to produce a conducting layer onto the surface of the film to ensure there was no charging effect. The SIMS was calibrated [24] before use for lithium and nitrogen so that the absolute concentration could be determined. The incident beam used was Ga⁺ ions and the secondary ions detected were Li⁺ for lithium and CN⁻ for nitrogen. Also detected was C⁺ which was used as a baseline for which Li⁺ and CN⁻ could be calibrated.

3.0 Results and Discussion

3.1 Determining the optimum amount of NH₃ gas

Firstly, it was important to determine the optimum concentration of NH₃ and N₂ gas before lithium could be incorporated into the diamond lattice. This enabled the optimum N-doped diamond film to be fabricated. The amount of NH₃ gas was determined first. A range of concentrations of NH₃ gas were evaluated and no N₂ gas was added into the reactor to ensure it did not affect the results.

The amount of CH₄ gas was kept constant at 0.81% with respect to H₂ gas. The percentages of NH₃/H₂ assessed ranged from 0.09% to 0.38%.

The N-doped diamond samples grown looked very similar to undoped diamond with a grey film being produced. Both Raman spectroscopy and SEM imaging were analysed to evaluate the optimum NH₃ concentration.

Analysis of the Raman data (**Figure 3.1**) highlights that the graphite peak at 1580 cm⁻¹ appears to be least prominent for the lower concentrations of NH₃ gas. 0.09% and 0.13% NH₃/H₂ have smaller graphite peaks than those observed from 0.17% to 0.24% NH₃/H₂. However, the higher concentrations of NH₃/H₂ from 0.27% to 0.38% appear to have a slightly reduced graphite peak than the intermediate concentrations. This could indicate that if concentrations were increased further, the graphite peaks may become even less prominent than that seen at the lowest concentrations.

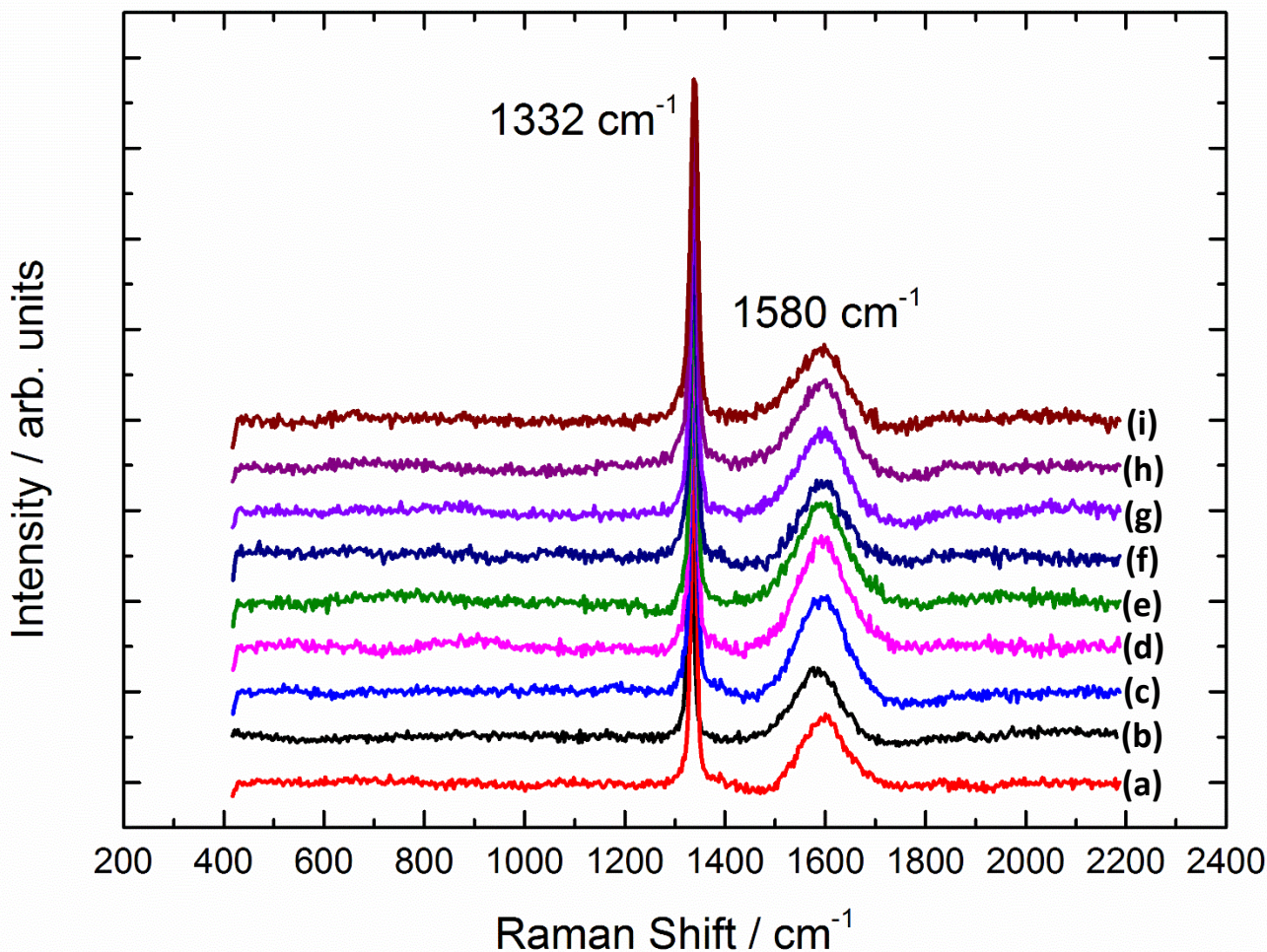


Figure 3.1: Raman spectra using UV, He:Cd 325 nm showing the diamond peak (1332 cm^{-1}) and the graphite peak (1580 cm^{-1}) highlighting how the proportion of graphite changes as the NH_3 concentration is increased. CH_4/H_2 was kept constant at 0.81% and no N_2 gas was used to ensure this did not affect results. All samples were grown on molybdenum substrates with (a) 0.09% NH_3/H_2 , (b) 0.13% NH_3/H_2 , (c) 0.17% NH_3/H_2 , (d) 0.20% NH_3/H_2 , (e) 0.24% NH_3/H_2 , (f) 0.27% NH_3/H_2 , (g) 0.31% NH_3/H_2 , (h) 0.34% NH_3/H_2 and (i) 0.38% NH_3/H_2 .

I_D/I_G values (see section 2.4) were then calculated so the proportion of diamond to graphite could be analysed (Figure 3.2). The higher the ratio of $I_D:I_G$ gives evidence that there is higher ratio of sp^3 carbon (diamond) in the lattice compared to sp^2 carbon (graphite). It is apparent that the graphitic content in the diamond film increases as the amount of NH_3/H_2 is increased up to approximately 0.20%. The I_D/I_G values decrease from 5.52 (0.09% NH_3/H_2) to 2.89 (0.20% NH_3/H_2). This agrees with what was evident in the Raman data where the graphite peak increased for these values. It would be expected that 0.24% NH_3/H_2 would follow this trend, but the I_D/I_G values begin to increase from this point. This results in a higher diamond to graphite ratio. This increase was expected from values from 0.27% to be consistent with the Raman data. The increase from 4.33 (0.27% NH_3/H_2) to 4.53 (0.38% NH_3/H_2) was predicted from the Raman data. What is clear from the I_D/I_G values at these higher concentrations is that the ratio does not reduce to the values seen with 0.09% and 0.13% NH_3/H_2 . As 0.13% NH_3/H_2 has a high I_D/I_G at 5.39 and the least prominent graphite peak in the Raman data is it the optimum concentration so far.

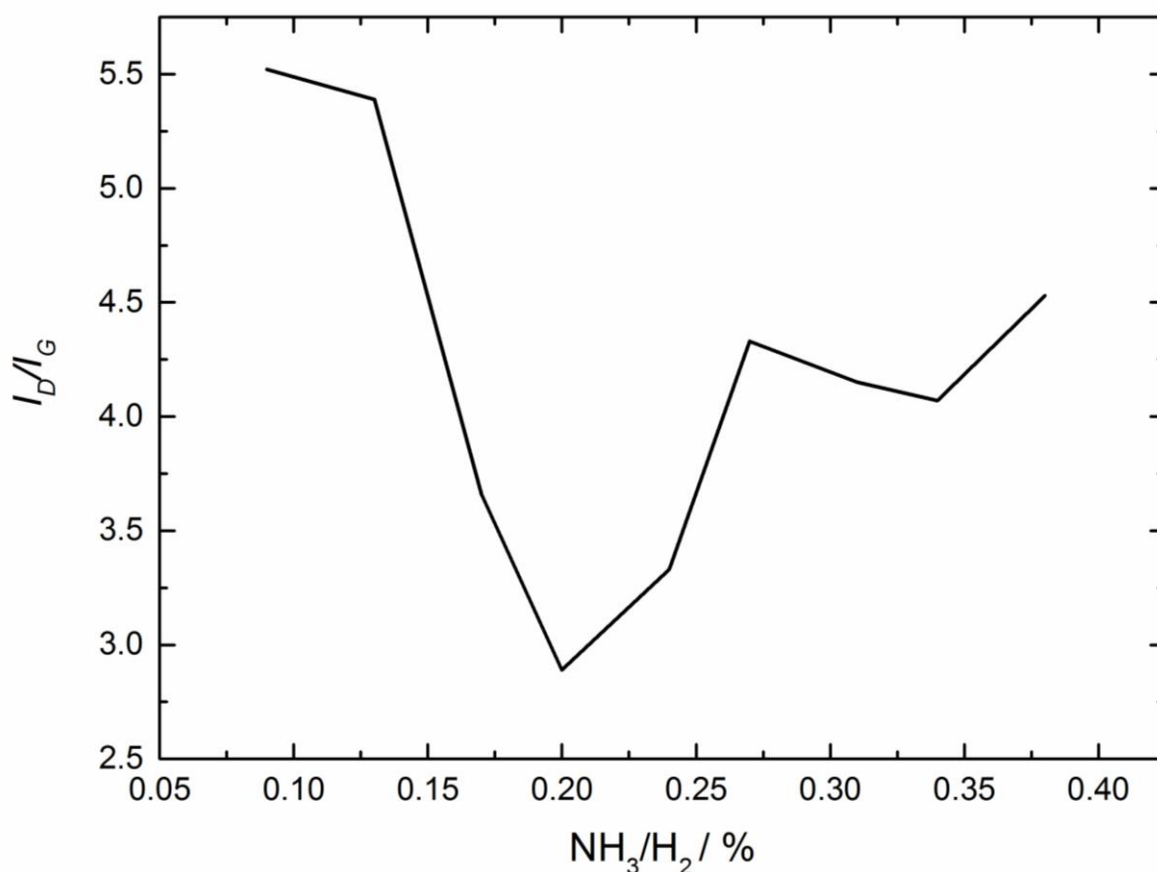
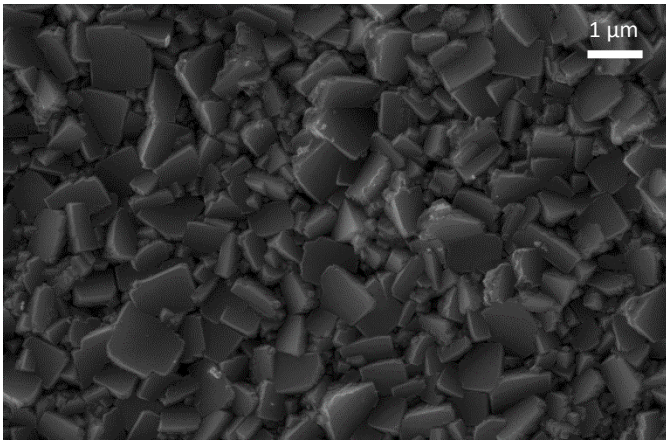
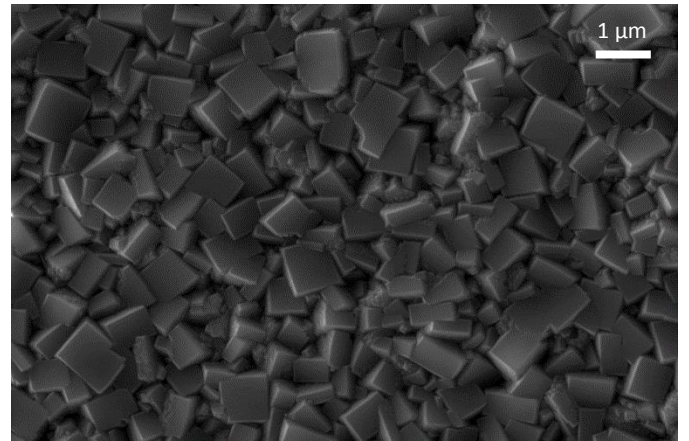


Figure 3.2: The I_D/I_G data as the concentration of NH_3/H_2 gas increases. CH_4/H_2 was kept constant at 0.81% and no N_2 gas was used.

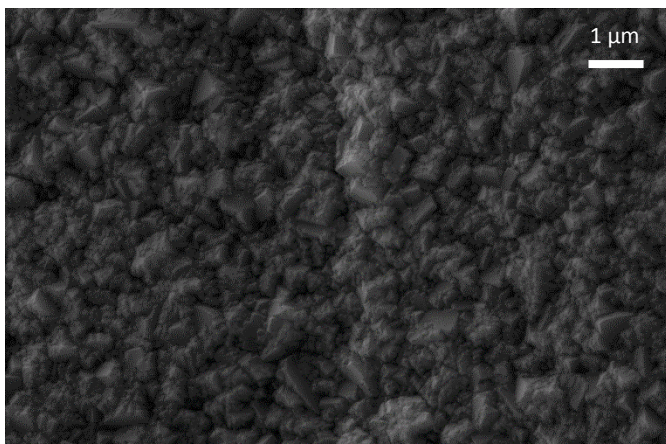
SEM images were produced (**Figure 3.3**) for increasing concentrations of NH_3/H_2 . These images illustrate that 0.09% and 0.13% NH_3/H_2 have a more crystalline film morphology than higher concentrations. The graphite content is higher with 0.09% NH_3/H_2 which is in agreement with the Raman data. The crystal sizes for both concentrations are relatively similar at $\approx 1 \mu\text{m}$, although, there appears to be a slightly higher proportion of larger crystals for 0.09% NH_3/H_2 . Looking at the overall film morphology, 0.13% NH_3/H_2 is a more faceted film with better defined $\{100\}$ square facets. As the quantity of NH_3/H_2 is increased to 0.17% and 0.20%, the graphitic areas increase dramatically. The morphology is much less crystalline with no complete $\{100\}$ square facets observed. With further increases to 0.24% and 0.27% NH_3/H_2 the film morphology is slightly better and some diamond crystals have started to form, but still no complete $\{100\}$ square facets are observed. Furthermore, the amount of graphitic areas remains high. As the concentration of NH_3/H_2 is further increased to 0.31%, 0.34% and 0.38%, the quality of the diamond film increases slightly with $\{100\}$ square facets observed. However, these are much smaller as crystal size was reduced to $\approx 0.5 \mu\text{m}$.



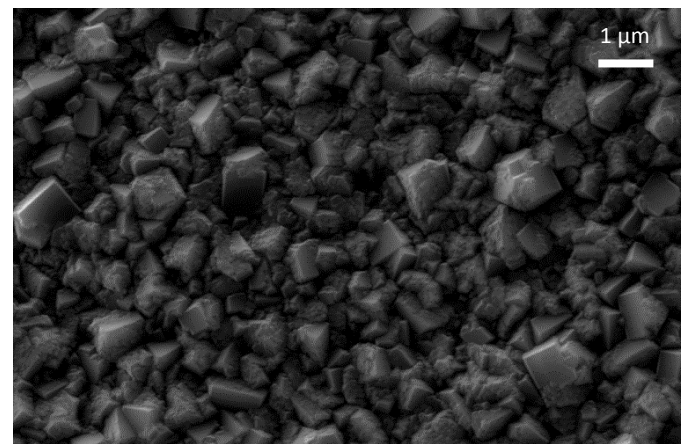
(a)



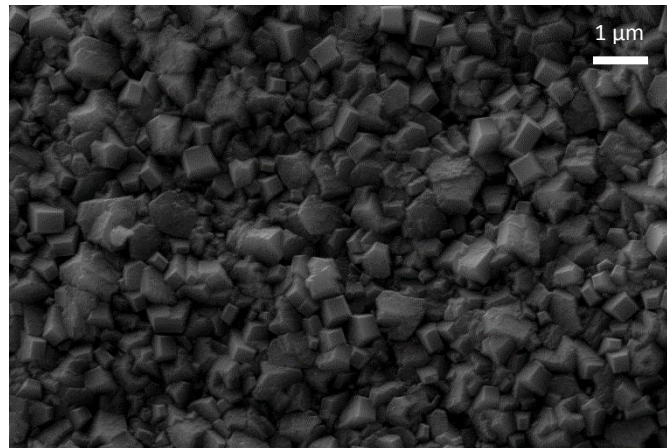
(b)



(c)



(d)



(e)

Figure 3.3: SEM images showing the morphology of N-doped diamond samples on molybdenum substrates. CH_4/H_2 was constant at 0.81%. No N_2 gas was used. The amount of NH_3/H_2 was (a) 0.093%, (b) 0.13%, (c) 0.20%, (d) 0.27% and (e) 0.38%

Taking Raman data, I_D/I_G values and SEM images all into account, it is apparent that lower amounts of NH_3 gas give a better morphology with a lower proportion of graphite with respect to diamond.

Although films for 0.09% and 0.13% NH_3/H_2 are relatively similar, the data shows 0.13% NH_3/H_2 to be the most promising. Therefore, this percentage was used for the remainder of the experiments. However, using 0.09% NH_3/H_2 is likely to have produced similar results.

3.2 Determining the optimum amount of N_2 gas

Since the optimum percentage of NH_3 gas had been concluded, the optimum amount of N_2 gas that gave a high quality diamond film needed to be determined. A high quality film consisted of a morphology with square {100} facets with a low proportion of graphitic areas. When using the HFCVD process, not the MWCVD process, NH_3 gas dictates the incorporation of nitrogen atoms into the diamond lattice, not N_2 gas. This is because of the strong N-N triple bond in N_2 [24] (see section 2.2). Therefore, only the film quality and morphology was analysed in this section.

The amount of CH_4 and NH_3 gas were kept constant at 0.81% and 0.13% respectively with respect to H_2 flow. The quantity of N_2/H_2 was varied from 0% to 0.40%.

A grey film was produced when N-doped diamond samples were grown with nitrogen gas which looked very similar to both undoped diamond films and N-doped diamond films grown with NH_3 gas only (Figure 3.4).

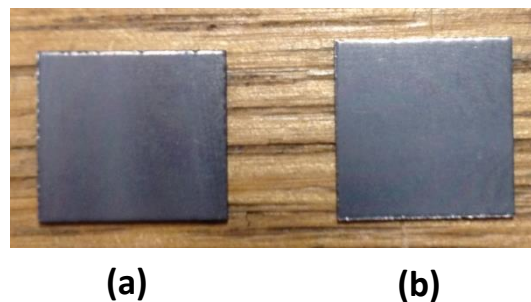


Figure 3.4: N-doped diamond films with (a) NH_3 gas only and (b) NH_3 and N_2 gas.

The Raman data (Figure 3.5) highlights that 0.23% N_2/H_2 appears to have the lowest graphite peak at 1580 cm^{-1} . The graphite peak increases from 0% to 0.16% N_2/H_2 and then drops at 0.23% N_2/H_2 . The fact that 0% N_2/H_2 and 0.23% N_2/H_2 have less prominent graphite peaks than 0.16% needs to be considered. An explanation for this may be that N-doped diamond can be grown to a high quality using ammonia alone and no nitrogen gas. When you first add nitrogen gas the film quality decreases, however the film quality then begins to increase at a slightly higher concentration (i.e. at 0.23% N_2/H_2). At concentrations above 0.23%, the graphite peak appears to increase with increasing N_2/H_2 concentration. These more prominent graphite peaks indicate that there is a high proportion of sp^2 carbon at grain boundaries. This data highlights that above 0.23% N_2/H_2 , the concentration is too high and the film quality is reduced.

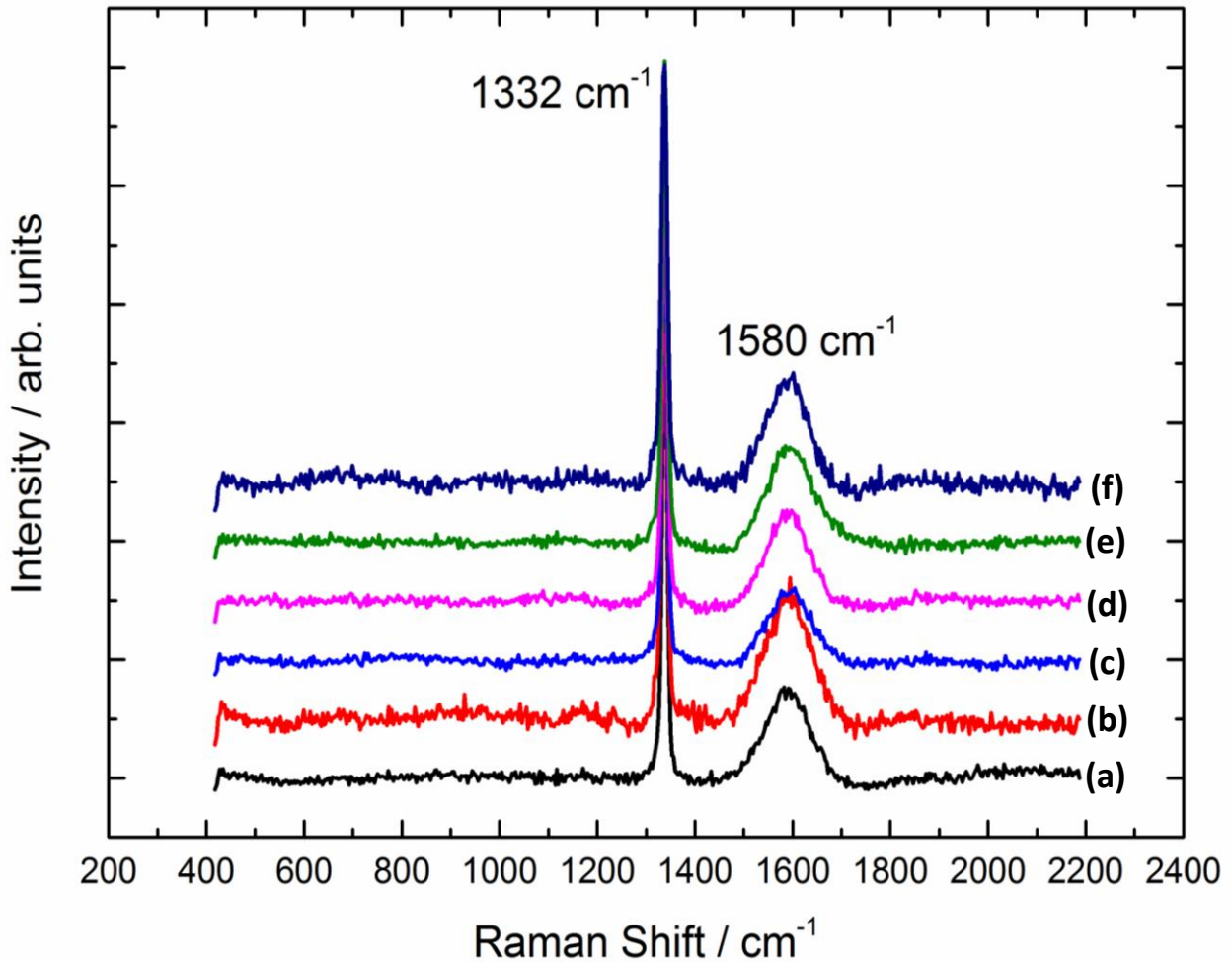


Figure 3.5: Raman spectra using UV, He:Cd 325 nm showing the diamond peak (1332 cm^{-1}) and the graphite peak (1580 cm^{-1}) comparing N-doped diamond samples with different N_2 gas concentrations. The CH_4/H_2 was constant at 0.81% and the NH_3/H_2 was 0.13% for all samples on molybdenum substrates with (a) 0% N_2/H_2 , (b) 0.16% N_2/H_2 , (c) 0.23% N_2/H_2 , (d) 0.28% N_2/H_2 , (e) 0.33% N_2/H_2 and (f) 0.40% N_2/H_2 .

The $\text{sp}^3:\text{sp}^2$ ratio was studied (**Figure 3.6**) and is relatively consistent with the Raman data. The 0.23% N_2/H_2 sample gave the highest I_D/I_G value at 6.92. This agrees with the low graphite peak observed in the Raman data. The value of I_D/I_G for 0% N_2/H_2 is also relatively high at 5.39. This gives further evidence that although the addition of N_2 does decrease the graphite peak, no N_2 gas also appears to produce a highly crystalline diamond film. As expected from the Raman data, the I_D/I_G value drops significantly to 2.99 at 0.16% N_2/H_2 . Concentrations from 0.28% N_2/H_2 and above are also in agreement with the Raman data due to the decrease in the I_D/I_G values from 5.32 (0.28% N_2/H_2) to 2.48 (0.40% N_2/H_2). Although, it is interesting the extent to which the I_D/I_G value drops from 5.12 at 0.33% N_2/H_2 to 2.48 at 0.40% N_2/H_2 , since in the Raman data the graphite peak does not appear to reduce that significantly. This implies that the diamond peak at 0.40% N_2/H_2 is also decreasing resulting in a lower I_D/I_G value.

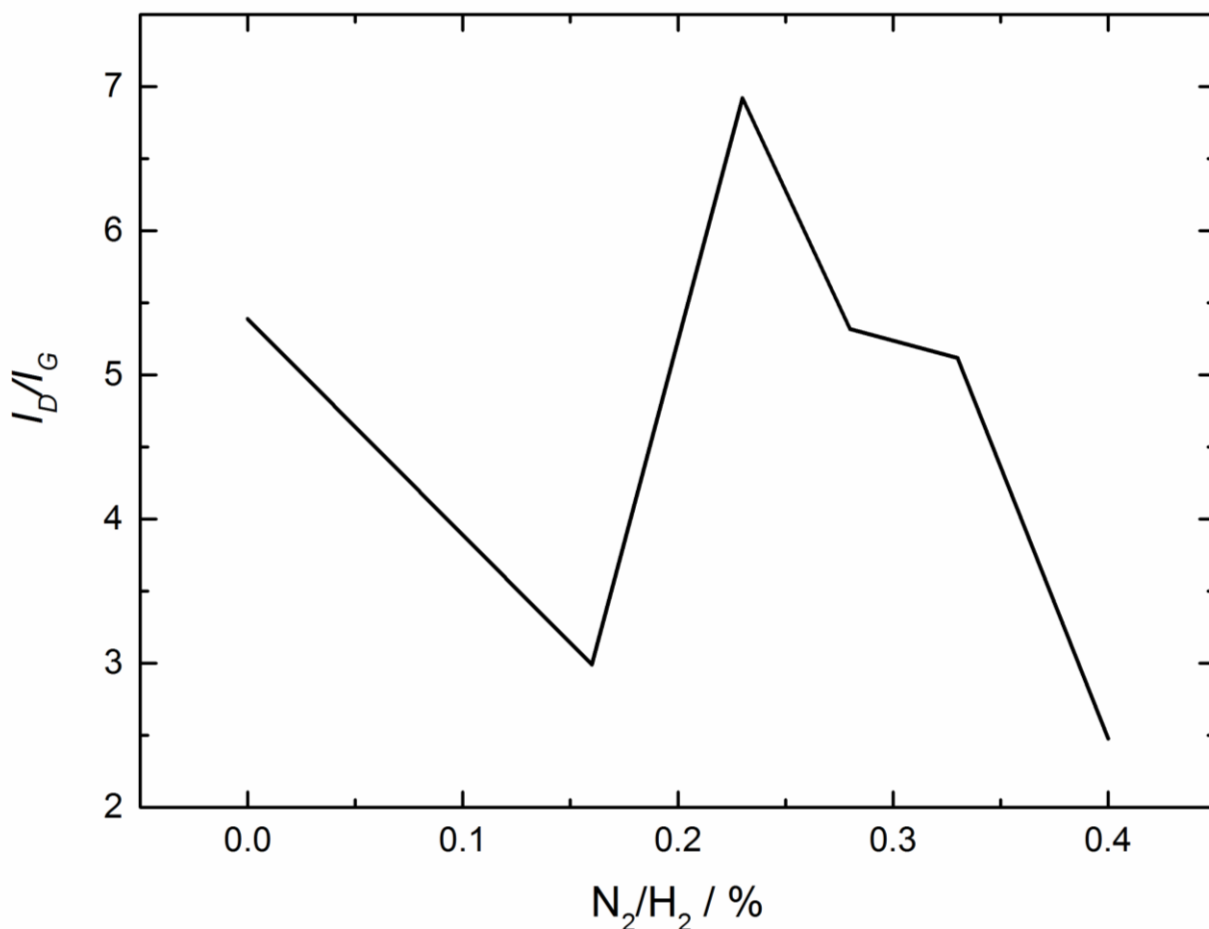
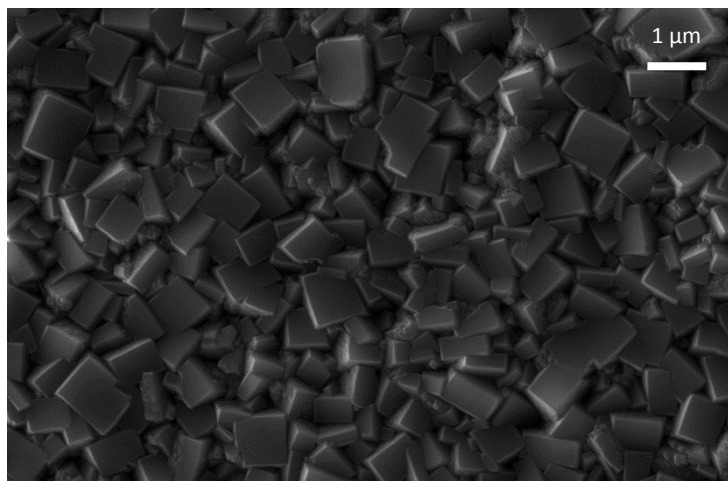
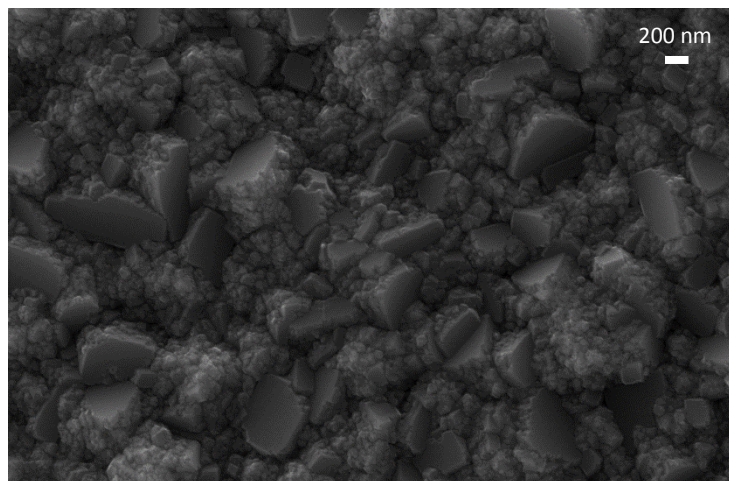


Figure 3.6: The I_D/I_G data as the concentration of N_2 gas increases. CH_4/H_2 and NH_3/H_2 were kept constant at 0.81% and 0.13% respectively.

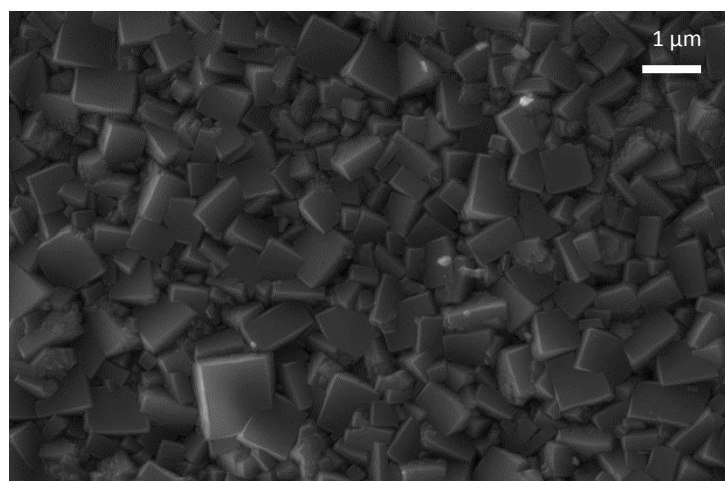
The SEM images (**Figure 3.7**) demonstrate that 0.28% N_2/H_2 gave the most uniform {100} facets with a low number of graphitic areas. This is interesting since it was expected, from Raman data and I_D/I_G values that this would have more graphitic areas than 0.23% N_2/H_2 . Although upon close inspection, both images have a low proportion of graphitic areas, yet the crystals for 0.28% N_2/H_2 have very sharp edges highlighting good crystalline regions. However, for both 0.23% and 0% N_2/H_2 the film morphology is also highly faceted. The crystal size of these three percentages was $\approx 1 \mu m$. As the amount of N_2/H_2 was increased to 0.33% there is a slight decrease in the film quality. There are more graphitic areas and a lower quality of {100} facets. However, some $1 \mu m$ diamond crystals are still observed. In agreement with the Raman data and I_D/I_G values, with 0.16% and 0.40% N_2/H_2 the film morphology decreases significantly. No full {100} facets are observed since they are obscured by the large increase in graphite areas. Furthermore, the scale of the images has been reduced to nanometres also highlighting the decreased crystal size. Since the SEM and Raman data both showed similar results for 0.16% and 0.40% N_2/H_2 , this indicates that there is a balance of the concentration of N_2 gas. If the quantity is too high or too low, the film quality is significantly decreased.



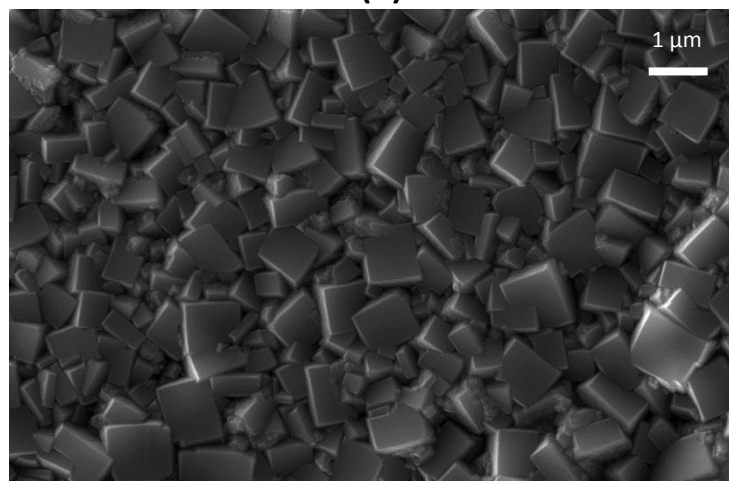
(a)



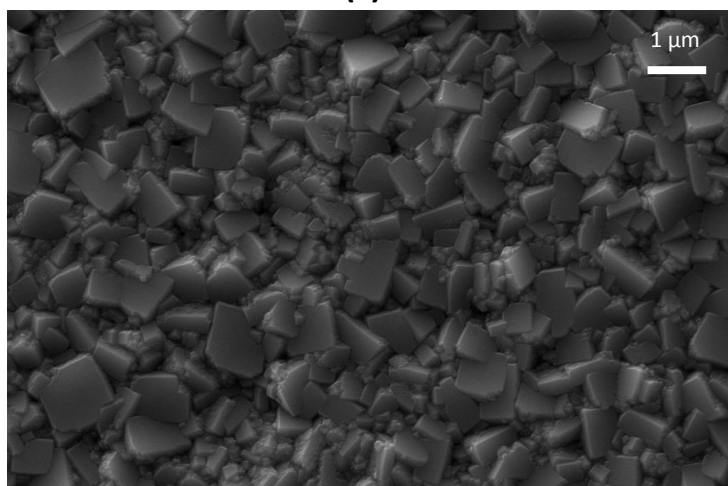
(b)



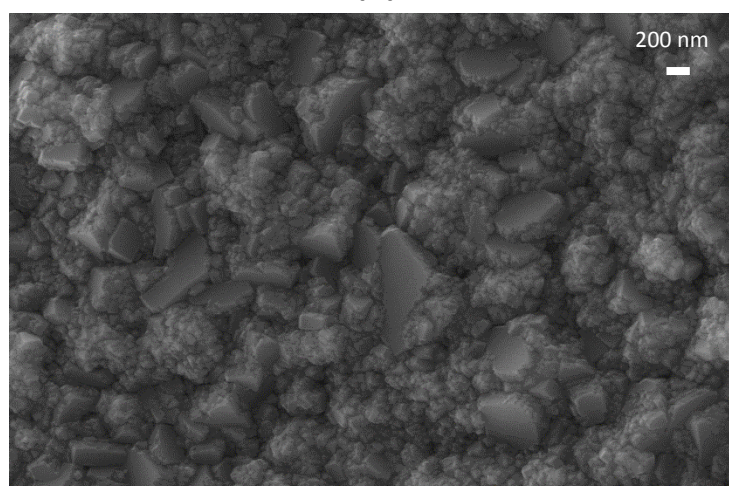
(c)



(d)



(e)



(f)

Figure 3.7: SEM images showing the morphology of N-doped diamond films on molybdenum substrates. The percentages of CH₄ and NH₃ were 0.81% CH₄/H₂, and 0.13% NH₃/H₂. The N₂/H₂ was (a) 0%, (b) 0.16%, (c) 0.23%, (d) 0.28%, (e) 0.33% and (f) 0.40%.

Taking both Raman data, I_D/I_G values and SEM data into account, 0%, 0.23% and 0.28% N_2/H_2 give the most promising results. 0% N_2/H_2 has been excluded as it has been suggested that the addition of nitrogen gas increases the growth rate of diamond films. This is due to the increased amount of HCN produced, leading to more H abstraction and a faster growth rate [48]. Therefore in future sections in this study 0.23% and 0.28% N_2/H_2 were evaluated with 0.13% NH_3/H_2 .

3.3 Molybdenum and Silicon Substrates

In the previous studies molybdenum substrates were evaluated. However, since both molybdenum and silicon substrates were available, a comparison of these was completed. This allowed determination of the optimum substrate for N-doped diamond growth. Although quite infrequent, delamination of the diamond film was observed on some molybdenum substrates (**Figure 3.8**). This was due to the internal stress produced when the substrate and diamond cool down after growth. This occurred only on molybdenum substrates and not on silicon substrates. This is because of the similar thermal expansion coefficient between silicon and diamond at 298 K, at $2.56 \times 10^{-6} K^{-1}$ [49] and $1.1 \times 10^{-6} K^{-1}$ [2] respectively. Molybdenum has a slightly higher thermal expansion coefficient at $4.8 \times 10^{-6} K^{-1}$ at 298 K [50] which results in occasional delamination.

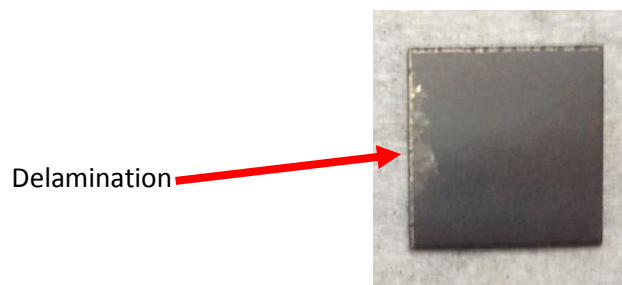


Figure 3.8: Photograph of a N-doped diamond film grown on a molybdenum substrate with delamination. This was caused because the thermal expansion coefficient of molybdenum is different to that of diamond.

Conditions for N-doped diamond growth on different substrates were CH_4/H_2 at 0.81%, NH_3/H_2 at 0.13% and N_2/H_2 at 0.23% or 0.28%.

The Raman data (**Figure 3.9**) for the N-doped samples demonstrates that for 0.23% N_2/H_2 the graphite peak seems relatively constant at $1580 cm^{-1}$ for both silicon and molybdenum substrates. For 0.28% N_2/H_2 , the graphite peak appears to reduce very slightly when a silicon substrate is used.

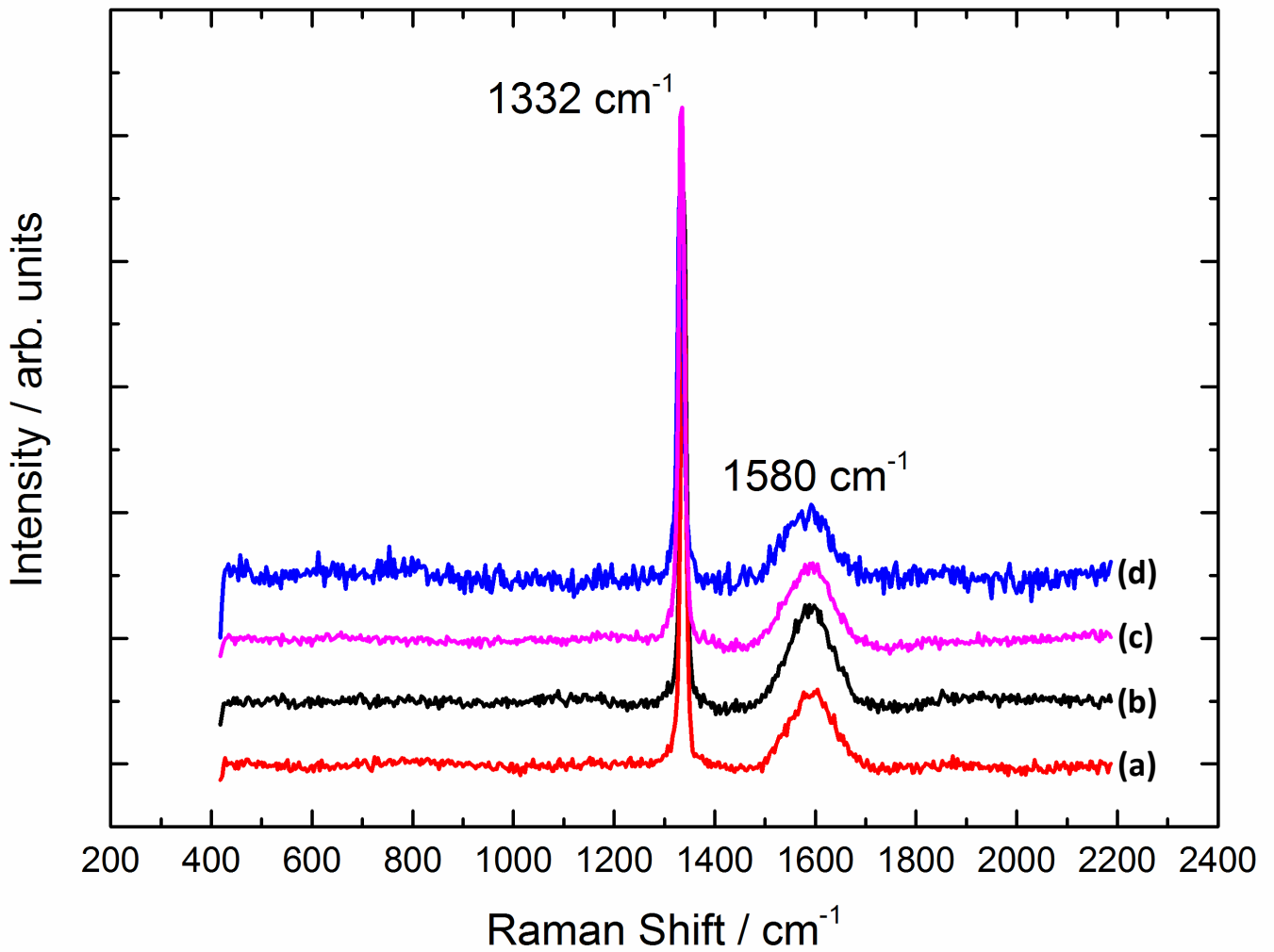


Figure 3.9: Raman spectra using UV, He:Cd 325 nm showing the diamond peak (1332 cm^{-1}) and the graphite peak (1580 cm^{-1}) comparing N-doped diamond samples on molybdenum and silicon substrates. The CH_4/H_2 was constant at 0.81% and the NH_3/H_2 was 0.13% for all samples with (a) 0.23% N_2/H_2 on a molybdenum substrate, (b) 0.28% N_2/H_2 on a molybdenum substrate, (c) 0.23% N_2/H_2 on a silicon substrate and (d) 0.28% N_2/H_2 on a silicon substrate.

The I_D/I_G values were compared (Figure 3.10) and are in the range of 5.3-7, this demonstrates that there is little difference between molybdenum and silicon substrates in terms of sp^3 to sp^2 ratio. This agrees with the Raman data, where the graphite peak difference was negligible for the different substrates.

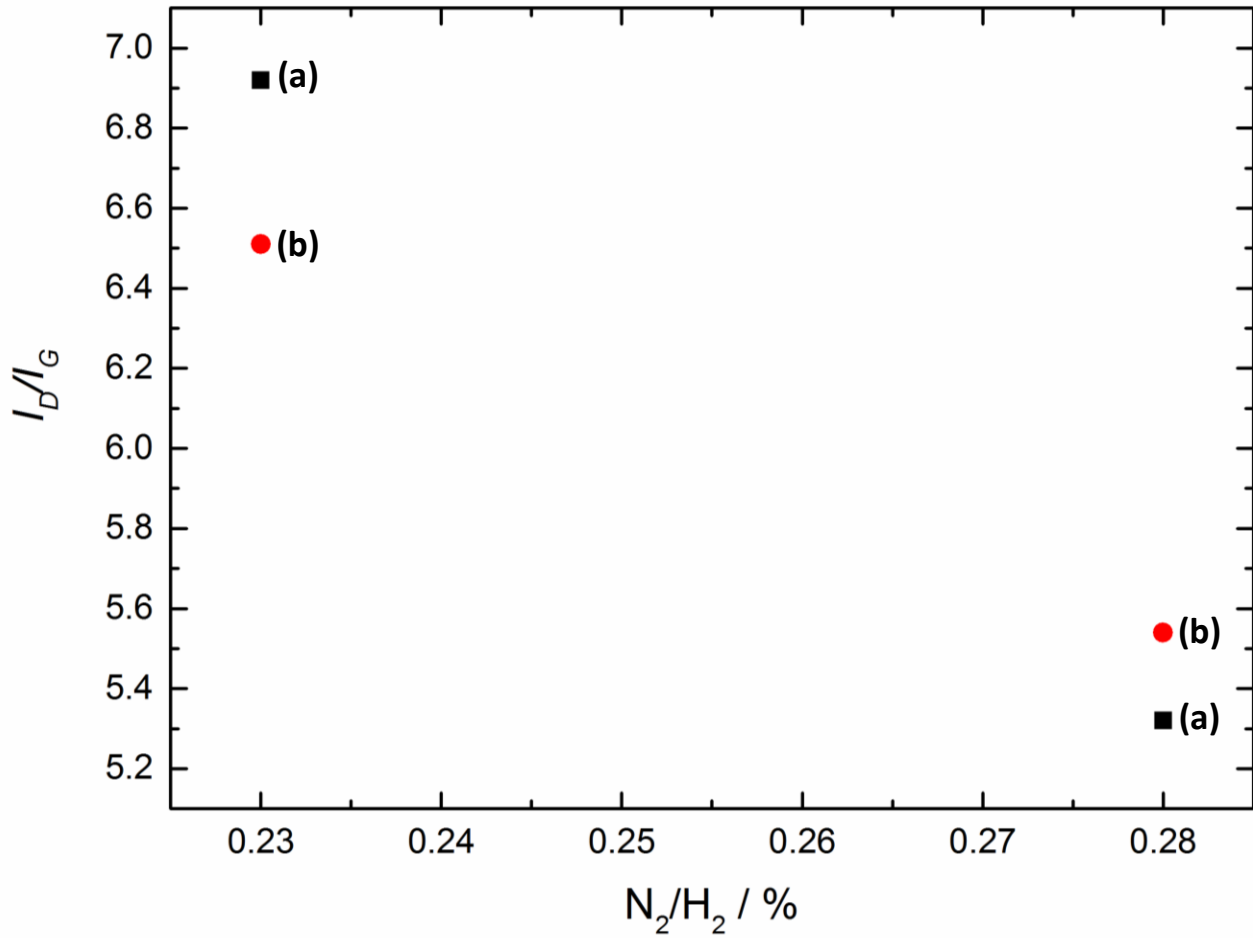
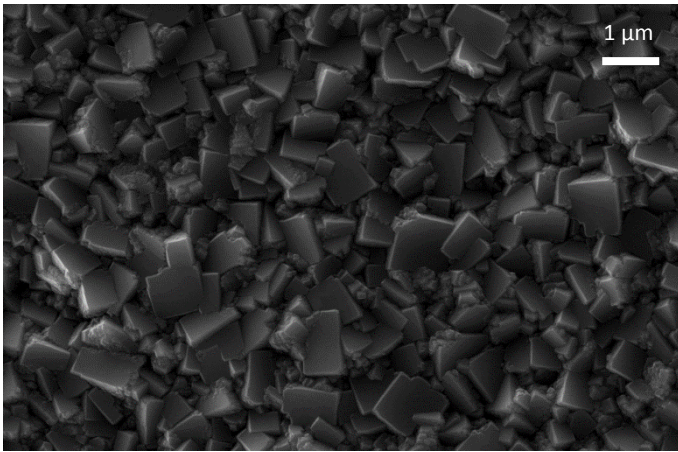
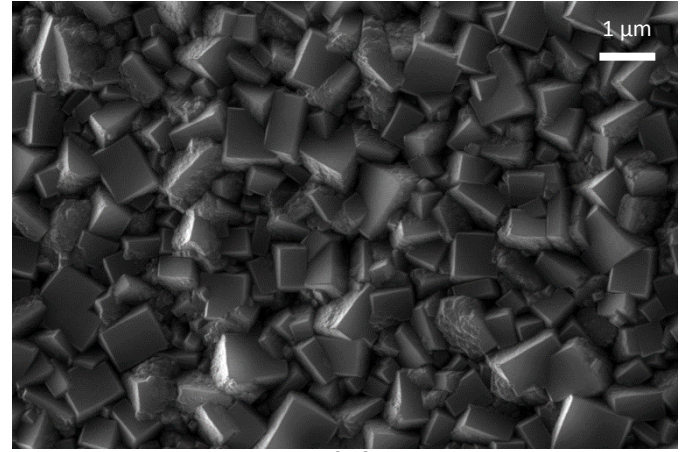


Figure 3.10: I_D/I_G data for nitrogen-doped diamond samples with, (a) a silicon substrate and (b) a molybdenum substrate.

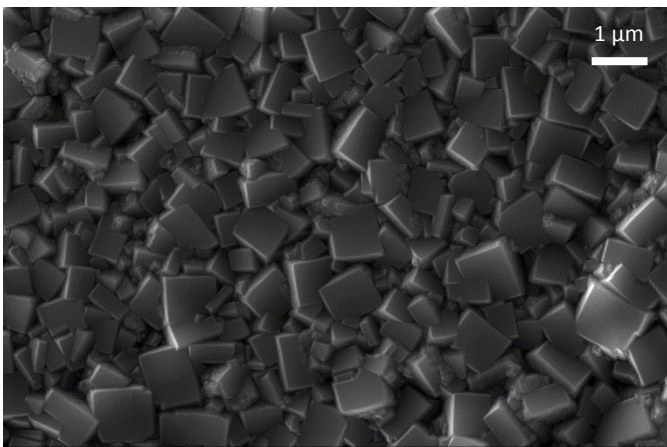
Unsurprisingly, molybdenum and silicon substrates both give similar SEM images (Figure 3.11). All samples show a uniform morphology with {100} square facets and a good crystal size.



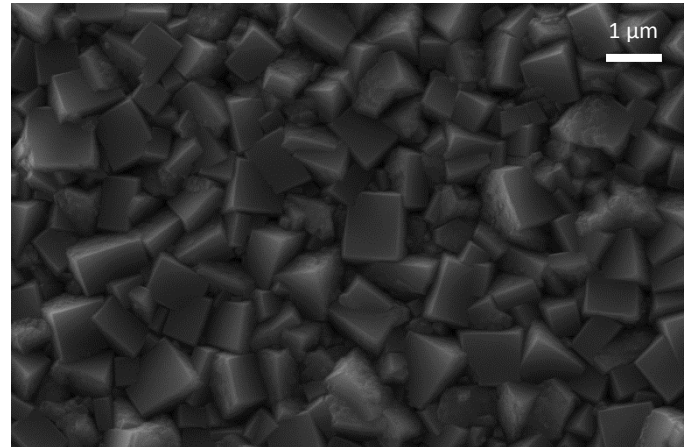
(a)



(b)



(c)



(d)

Figure 3.11: SEM images showing the morphology of N-doped diamond samples on molybdenum and silicon substrates. The amount of CH_4/H_2 was constant at 0.81% and the NH_3/H_2 concentration was also constant at 0.13%. The N_2/H_2 quantities were (a) 0.23% on a molybdenum substrate, (b) 0.23% on a silicon substrate, (c) 0.28% on a molybdenum substrate and (d) 0.28% on a silicon substrate.

Resistance measurements (**Table 3.1**) were also studied to observe any differences highlighted when using different substrates. These were only recorded for the 0.28% N_2/H_2 sample. It was evident that resistance of the diamond sample on a molybdenum substrate is much lower at 52-58 M Ω than the silicon substrate at 180-210 M Ω . Theoretically, the resistance should be the same on both substrates when the same conditions have been used for diamond growth. Initially it may be believed that the molybdenum substrate would be more ideal as a low resistance is required for n-type diamond. However, the resistance must be a result of the diamond sample and not the substrate. The resistivity of the substrate must affect the result; otherwise results would have been similar for both substrates. The lower resistance observed with the molybdenum substrate is due to the lower resistivity of molybdenum at $5.57 \times 10^{-9} \Omega\cdot\text{m}$ at 298 K [51]. The silicon substrates were purchased from Silicon Prime Wafers with an n-type silicon property. These had a resistivity of $1\text{-}10 \times 10^{-2} \Omega\cdot\text{m}$

at 298 K which is much higher than the resistivity of molybdenum. It is evident that the resistivity of molybdenum is much lower than diamond, $1 \times 10^{14} \Omega \cdot \text{m}$ at 298 K [2]. Therefore, this decreases the total resistance of the sample. Even though silicon also has a lower resistivity compared to diamond, the difference is much less significant. Furthermore, values for resistance for the silicon substrate agree with literature at $\approx 200 \text{ M}\Omega$ [24], whereas with molybdenum; values are much too low.

Table 3.1: Resistance measurements for molybdenum and silicon substrates.

Substrate	Resistance / $\text{M}\Omega$
Molybdenum	52-58
Silicon	180-210

Overall, silicon was chosen as the substrate for N-doped diamond growth. Although the film quality was much the same, resistance and delamination were less affected when using silicon as the substrate for diamond growth.

3.4 Comparison to the control

To examine how effective nitrogen doping was, the N-doped samples were compared to undoped diamond samples (control samples). The control used CH_4 gas *only* at 0.81% with respect to H_2 flow. The N-doped samples used the same CH_4 content at 0.81% CH_4/H_2 with NH_3/H_2 at 0.13% and N_2/H_2 at 0.23% or 0.28%. Diamond-on-silicon substrates were analysed since in the previous section (section 3.3) this was determined to be the optimum substrate.

The Raman data (**Figure 3.12**) reveals that the control has a much lower graphite peak than the N-doped samples. This can be explained since incorporating nitrogen atoms into the diamond lattice increases the number of grain boundaries [52]. This only occurs if a high proportion of nitrogen is incorporated. The undoped diamond will also have grain boundaries but these appear to be reduced in comparison to the N-doped diamond. Therefore, resulting in a very low, almost negligible sp^2 graphite peak.

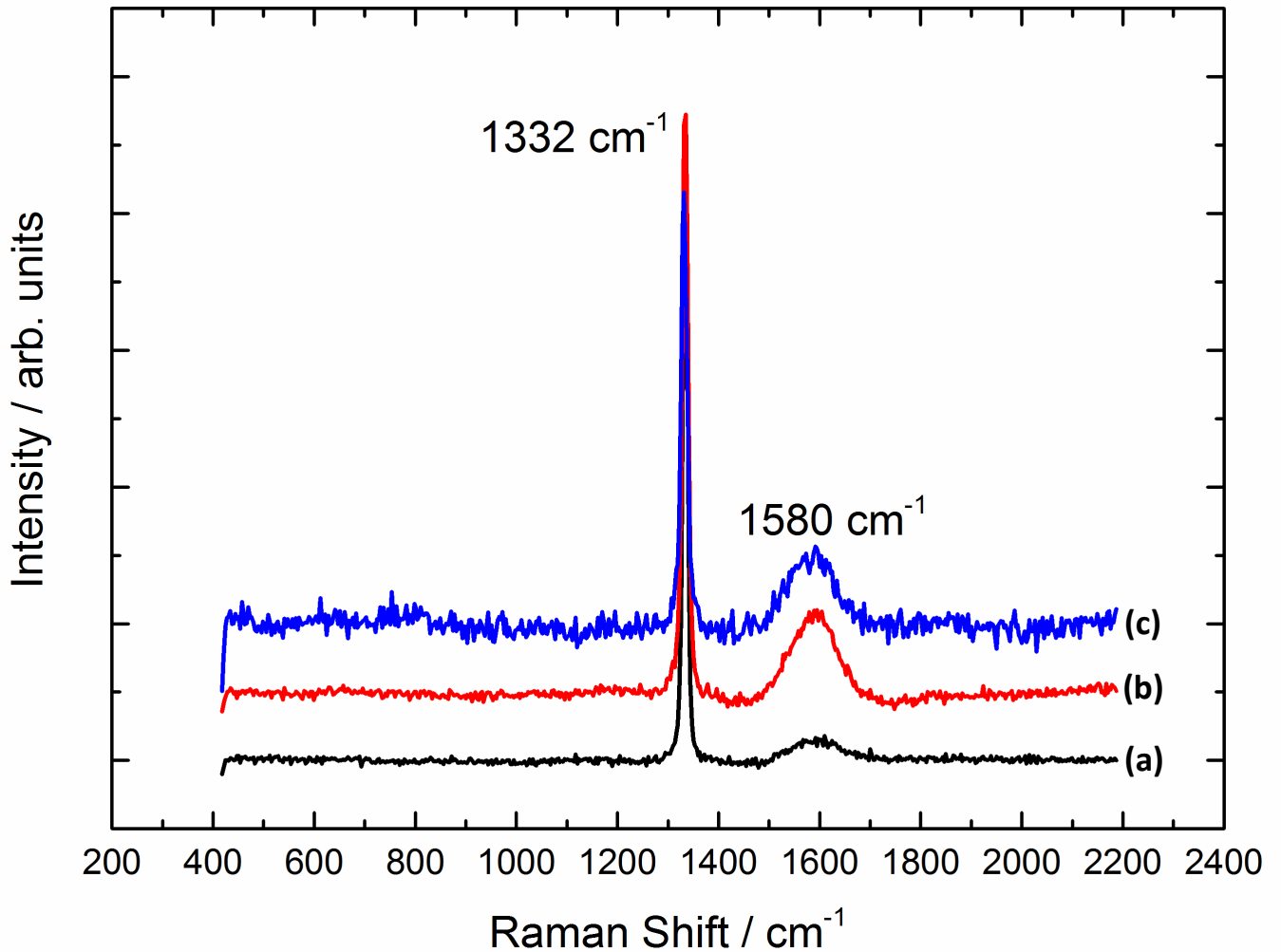


Figure 3.12: Raman spectra using UV, He:Cd 325 nm showing the diamond peak (1332 cm^{-1}) and the graphite peak (1580 cm^{-1}) comparing N-doped to undoped diamond on silicon substrates. CH_4/H_2 at 0.81% for all samples and (a) 0% N_2/H_2 and 0% NH_3/H_2 (undoped), (b) 0.23% N_2/H_2 and 0.13% NH_3/H_2 and (c) 0.28% N_2/H_2 and 0.13% NH_3/H_2 .

The I_D/I_G data (Figure 3.13) is consistent with the Raman data, highlighting a very large I_D/I_G value for the control (0% N_2/H_2) at 31.7. This is approximately 5 to 6 times greater than that of N-doped diamond samples and is consistent with the minimal graphite peak for the control seen in the Raman data. Although a high I_D/I_G value is desired, undoped diamond will not produce n-type diamond.

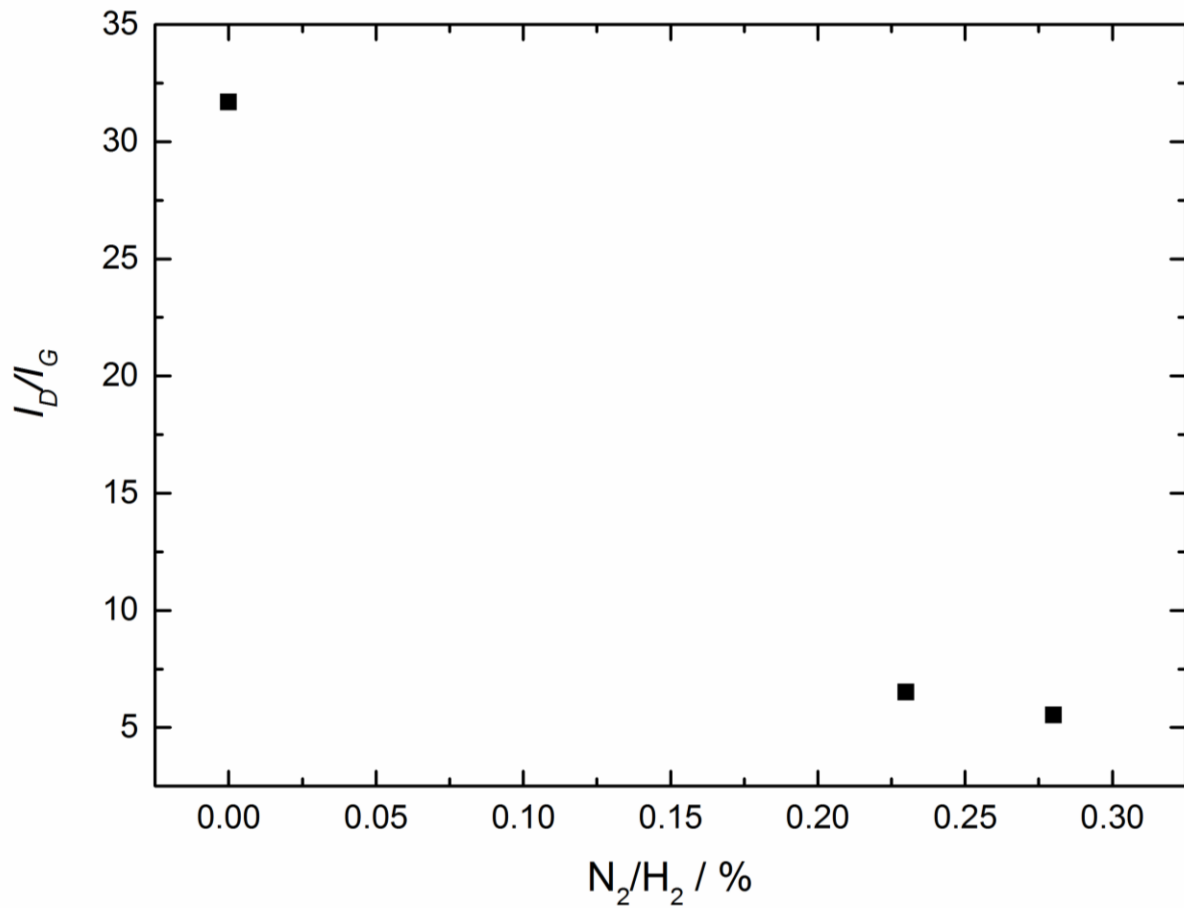


Figure 3.13: I_D/I_G data for N-doped diamond in comparison to the control (undoped diamond).

The SEM images (**Figure 3.14**) highlighted a highly different morphology for the control in comparison to N-doped films as it does not produce {100} square facets but random facets. This evidence verifies why nitrogen atom incorporation is necessary to produce the film quality required.

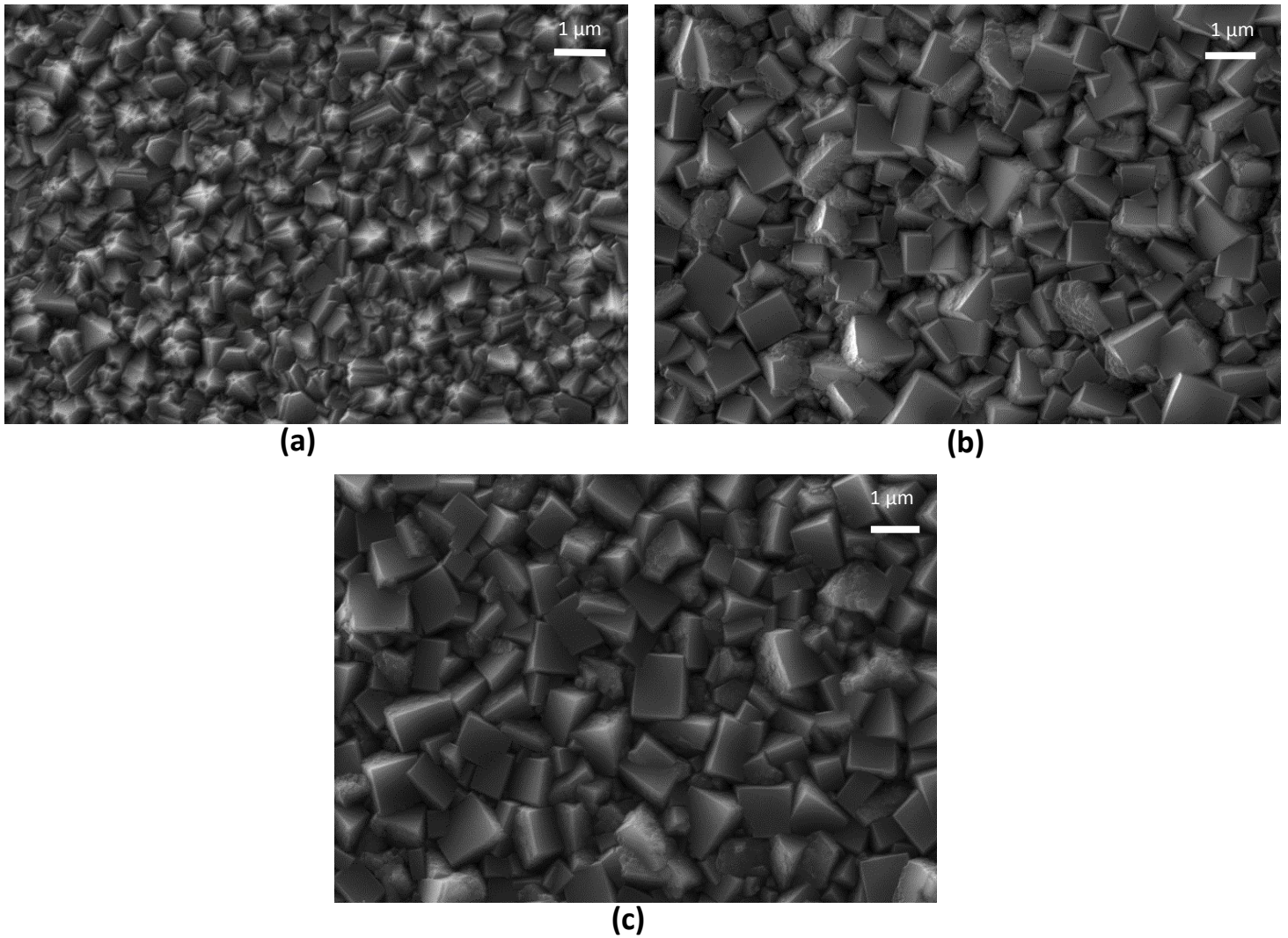


Figure 3.14: SEM images comparing N-doped and undoped diamond samples on silicon substrates. The amount of CH₄/H₂ was constant at 0.81% for both the undoped and N-doped samples. The NH₃/H₂ for the N-doped samples was 0.13%. The N₂/H₂ and quantities were (a) 0% (control), (b) 0.23% and (c) 0.28%.

Resistance measurements were recorded (**Table 3.2**) and highlight that the undoped diamond had a lower resistance to N-doped diamond. This is because the undoped diamond can form dangling bonds or holes at grain boundaries. The undoped diamond is acting like p-type diamond through the dangling bonds, holes or other impurities. The dangling bonds on the surface of the film can produce holes in the bulk. Therefore, this will produce a lower resistance, since conduction can occur via the grain boundaries [52,53]. When a small amount of nitrogen is added to the film, they can bond to these defects, passivating them, thus the resistance increases hugely. With further additions of nitrogen, n-type doping will begin to appear.

Table 3.2: Resistance measurements for undoped and N-doped diamond films.

Conditions of the Sample	Resistance / M Ω
Undoped	70-90
N-doped with 0.23% N ₂ /H ₂	154-156
N-doped with 0.28% N ₂ /H ₂	180-210

3.5 Li:N co-doping

As stated in the experimental section (section 2.3), Li₃N solution was the lithium containing precursor used for diffusion of lithium atoms into the diamond lattice.

The N-doped diamond film had been successfully prepared with the standard CH₄ gas at 0.81% and NH₃ gas at 0.13% with respect to H₂ flow. Since 0.23% and 0.28% N₂/H₂ gave the most encouraging film qualities determined by analysis of SEM and Raman data (see further details in section 3.2), both these samples were subsequently lithium doped. To produce Li:N co-doped diamond, there was an addition of 100 μ L Li₃N solution. The samples were grown on silicon substrates and were compared to N-doped diamond samples, also grown on silicon substrates. The Li:N co-doped films are a darker grey than the N-doped films.

Analysis of the Raman spectra (**Figure 3.15**) highlighted that the graphite peaks at 1580 cm⁻¹ do not show a significant decrease with addition of Li₃N solution. For 0.28% N₂/H₂ the graphite peak appears the same with and without lithium atom incorporation. However, close inspection of the 0.23% N₂/H₂ graphite peak does show a slight reduction with lithium atom incorporation. It was postulated that the graphite peak would become much less prominent with Li₃N addition as it has been suggested that lithium preferentially etches graphite over diamond [24]. However, the data here do not concur with this.

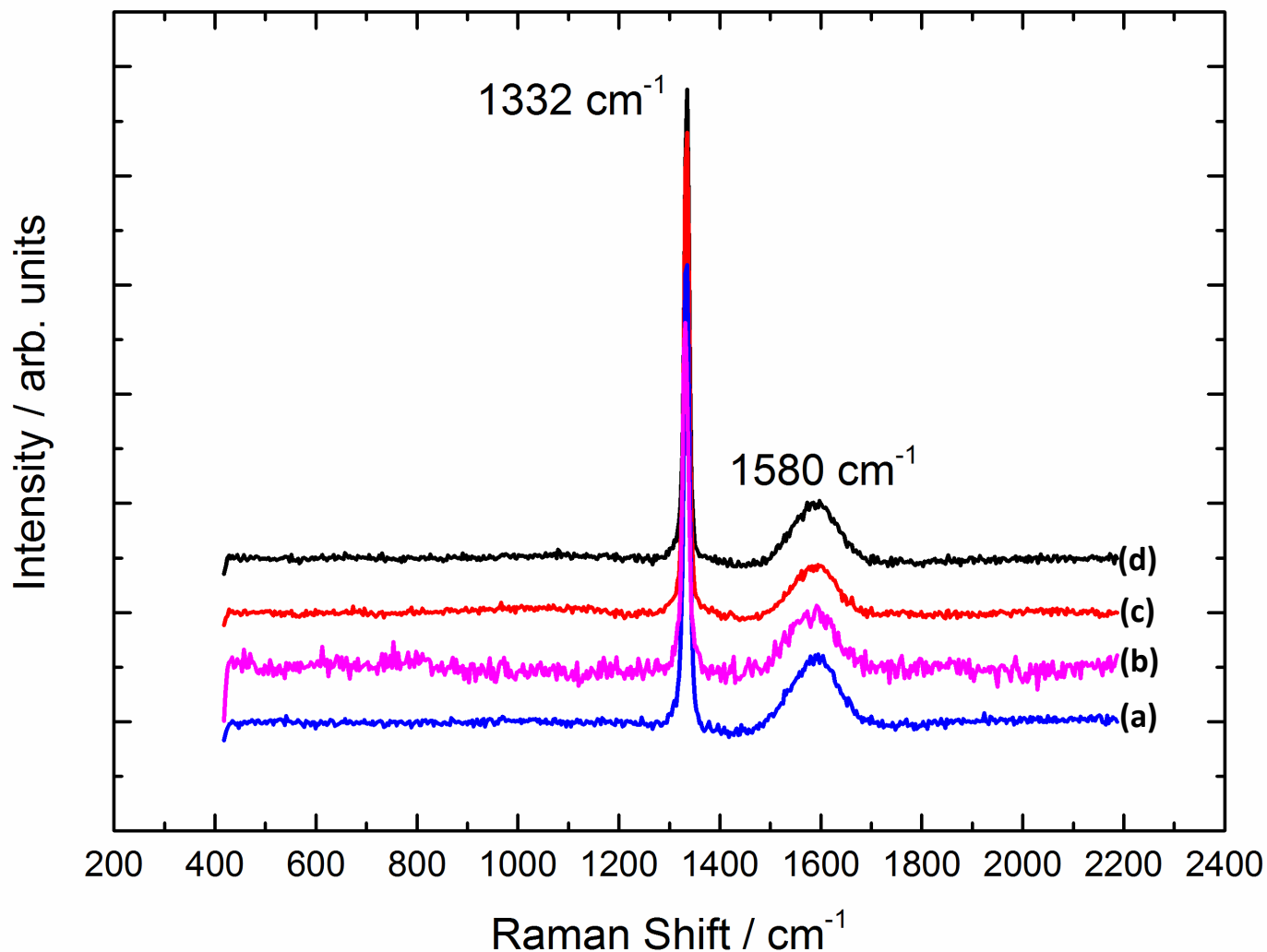


Figure 3.15: Raman spectra using UV, He:Cd 325 nm showing the diamond peak (1332 cm^{-1}) and the graphite peak (1580 cm^{-1}) showing the difference between N-doped and Li:N co-doped diamond films. The CH_4/H_2 was kept constant at 0.81%, NH_3/H_2 was also constant at 0.13%, (a) N-doped film with 0.23% N_2/H_2 , (b) N-doped film with 0.28% N_2/H_2 , (c) Li:N co-doped film with 0.23% N_2/H_2 and (d) Li:N co-doped film with 0.28% N_2/H_2 .

However it is clearer when analysing the I_D/I_G data (Figure 3.16) that there is preferential etching of graphite by the lithium atoms. Li:N co-doped diamond films increase the I_D/I_G values by approximately 1.5 times in comparison to N-doped diamond films. The increased I_D/I_G values could be a result of a more prominent diamond peak for Li:N films at 1332 cm^{-1} . The I_D/I_G values are similar for Li:N co-doped diamond for both 0.23% and 0.28% N_2/H_2 , therefore, both samples were used for further studies. However, since the 0.23 N_2/H_2 sample has a higher I_D/I_G , this is the most promising film so far.

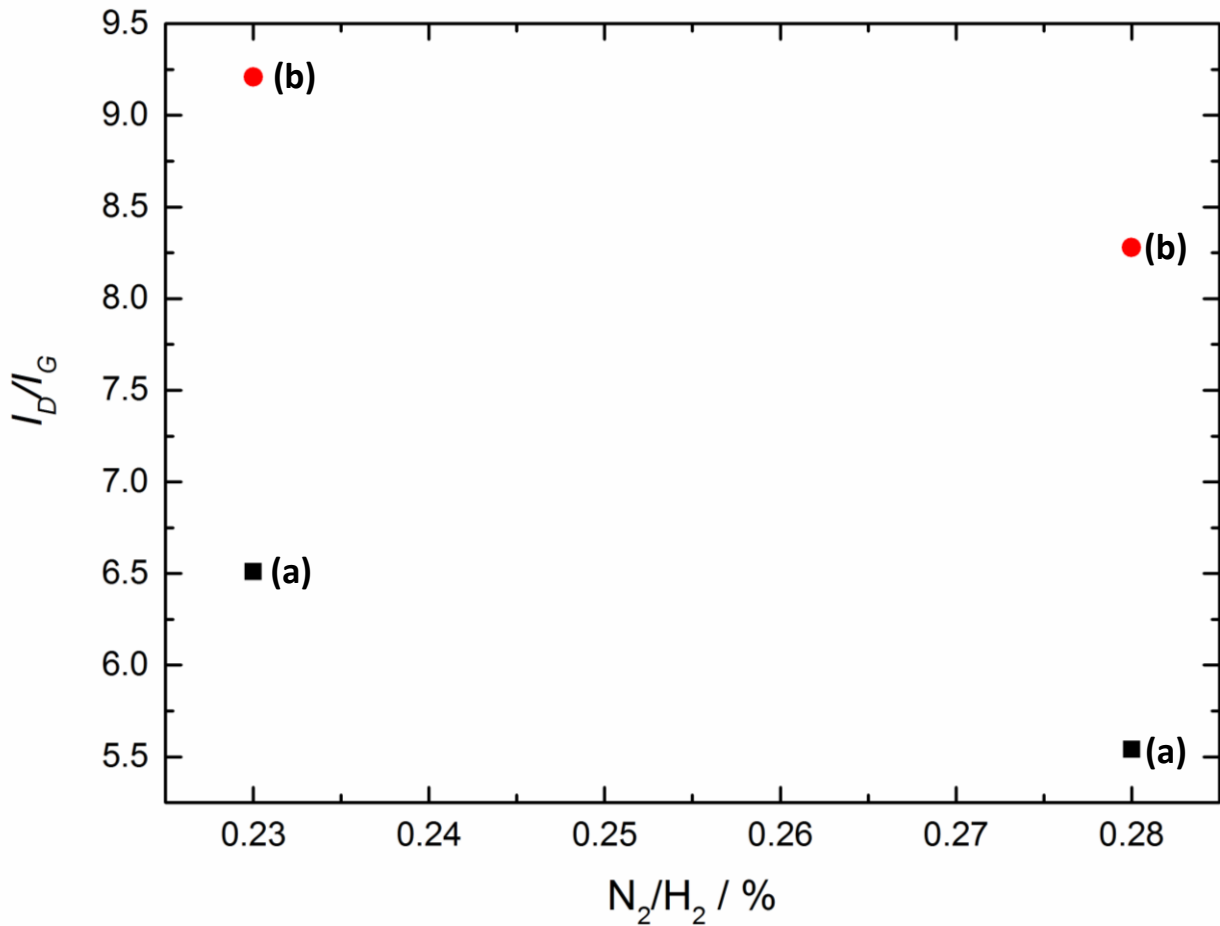


Figure 3.16: I_D/I_G data for (a) N-doped and (b) Li:N co-doped diamond films with 0.23% or 0.28% N_2/H_2 .

Interpreting the SEM images (**Figure 3.17**) of the 0.23% N_2/H_2 diamond sample demonstrates that similar morphologies are evident with and without lithium atom incorporation. With both images, {100} square facets are observed with a good crystal size. The film morphology has not drastically changed with lithium atom incorporation, yet it could be speculated that there are slightly more {100} facets with the Li:N sample. This would explain the higher I_D/I_G values calculated. In contrast, the SEM images for the 0.28% N_2/H_2 diamond samples with and without Li_3N are very different. The graphite areas seem to increase with lithium atom incorporation. Furthermore, the crystal size has decreased and only a few crystals are larger than 0.5 μm . In all other samples, the crystal size is approaching 1 μm . This image highlights that although for the Li:N co-doped sample there may be more diamond regions than in the N-doped sample, (evident from the I_D/I_G values), the film quality has greatly decreased. It is evident that although there is still an abundant amount of {100} square facets for the lithium incorporated sample, these facets can no longer grow as large due to the abundant graphite areas in the film. This demonstrates that too much N_2 gas can decrease the film morphology significantly.

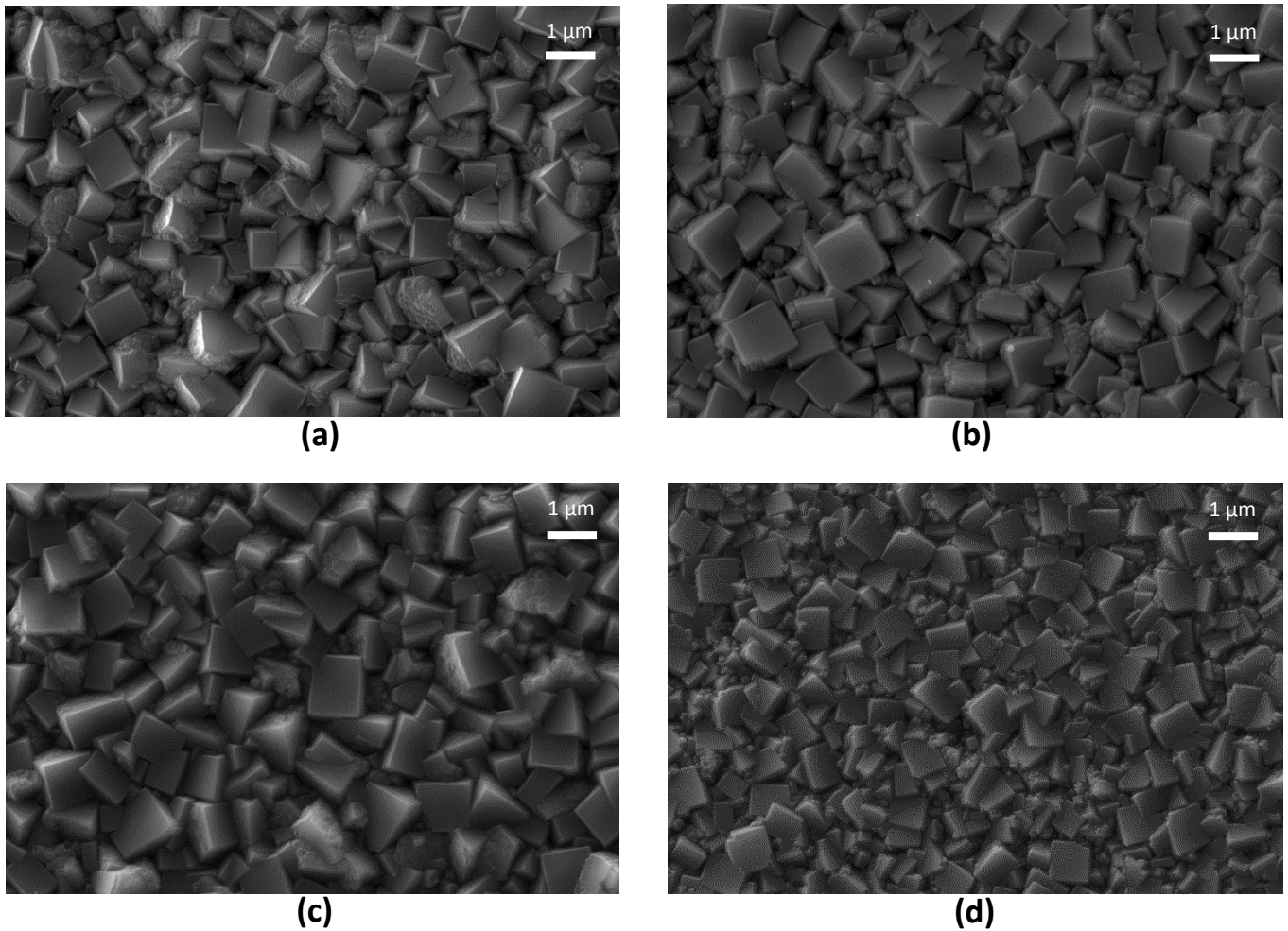


Figure 3.17: SEM images showing the morphology of N-doped and co-doped Li:N diamond samples (with 100 μL Li_3N solution) on silicon substrates. All images have 0.81% CH_4/H_2 and 0.13% NH_3/H_2 , (a) N-doped diamond with 0.23% N_2/H_2 (b) Li:N co-doped diamond with 0.23% N_2/H_2 (c) N-doped diamond with 0.28% N_2/H_2 and (d) Li:N co-doped diamond 0.28% N_2/H_2 .

Raman spectroscopy, SEM images and I_D/I_G values indicate that the Li:N co-doped diamond with 0.23% N_2/H_2 is the most promising. However, the resistance of both 0.23% and 0.28% N_2/H_2 were studied. The general aim of this project is to achieve a Li:N ratio of 1:4 which should have a low resistance. The resistance of the Li:N diamond should be lower than the N-doped sample since the sample is increasing in semiconductivity. This is because with N-doping alone, the nitrogen atoms are deep donors so semiconductivity does not occur at room temperature. At elevated temperatures the semiconducting properties increase as there is more energy available for the excitation of electrons from the donor level to the conduction band of diamond (see section 1.2.2).

When measuring resistance, a two point probe was placed on the two silver contents which had previously been evaporated onto the diamond samples (see section 2.6). The probes were placed at different areas of the silver contacts so that a range of resistances were obtained (**Table 3.3**).

These results show that for the 0.23% N_2/H_2 Li:N co-doped sample the resistance is greatly reduced. The N-doped sample is as high at 154-156 M Ω which then decreases to 7-16 M Ω for the Li:N sample.

This is highly promising, highlighting that the incorporation of lithium atoms is increasing semiconductive properties.

Unfortunately the same decrease is not observed for the 0.28% N₂/H₂ samples. The Li:N diamond sample decreases in resistance from 180-210 MΩ for the N-doped sample to 125-130 MΩ for the co-doped sample. This demonstrates that although the SEM images are not particularly promising for this Li:N co-doped sample, the lithium atom incorporation is still reducing the resistance of the sample.

It should be noted that resistance was extremely variable for all samples and that an average was taken to provide values seen in **Table 3.3**. Therefore, it would be beneficial to study the 0.28% N₂/H₂ sample in more detail since less repeats were done for this sample.

Table 3.3: Resistance measurements for N-doped and Li:N co-doped diamond films.

N-doped or Li:N co-doped diamond	Resistance/ MΩ
0.23% - Li:N co-doped diamond	7-16
0.23% - N-doped diamond	154-156
0.28% - Li:N co-doped diamond	125-130
0.28% - N-doped diamond	180-210

To summarise, the data analysed (Raman data, I_D/I_G values, SEM images, resistance) show that the Li:N samples increase the semiconductivity at room temperature. Since the Li:N sample with 0.23% N₂/H₂ produced more promising results, these conditions were used for further studies.

To obtain a 1:4 Li:N co-doped diamond sample, it was believed that a resistance of ≤ 1 MΩ was required. Therefore further research was undertaken to reduce the resistance of the films and hence the ratio of Li:N.

3.5.1 An N-doped Capping Layer after Lithium Diffusion

The resistance of the Li:N co-doped samples studied so far are too high to produce the 1:4 ratio required. One idea to try to lower the resistance was to change the capping layer after lithium diffusion into the diamond lattice. If the undoped capping layer was changed to a N-doped capping layer, this should theoretically reduce the resistance (**Figure 3.18**). The undoped capping layer should have a high resistance as it is insulating diamond whereas the N-doped capping layer should reduce the resistance of the film. This capping layer was grown for two minutes instead of the five minutes as previously used in section 2.3.

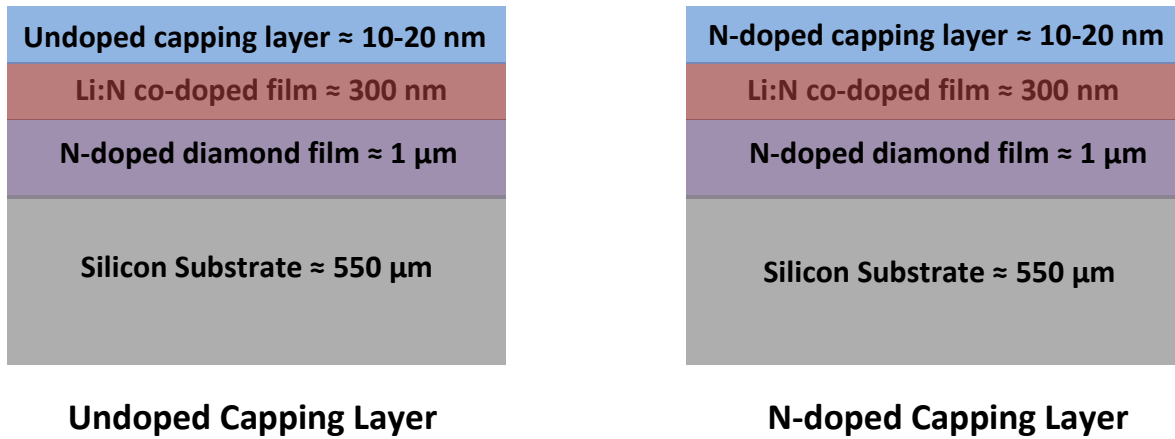


Figure 3.18: Schematic showing the undoped and N-doped capping layer that should theoretically reduce resistance.

The Raman data (**Figure 3.19**) shows that the N-doped capping layer appears to have a slightly more prominent graphite peak than the undoped capping layer. This is consistent with the lower graphite peak observed for undoped diamond in comparison to N-doped diamond in section 3.4. However, since it is only the capping layer that has been altered, a drastic change in the graphite peak was not expected.

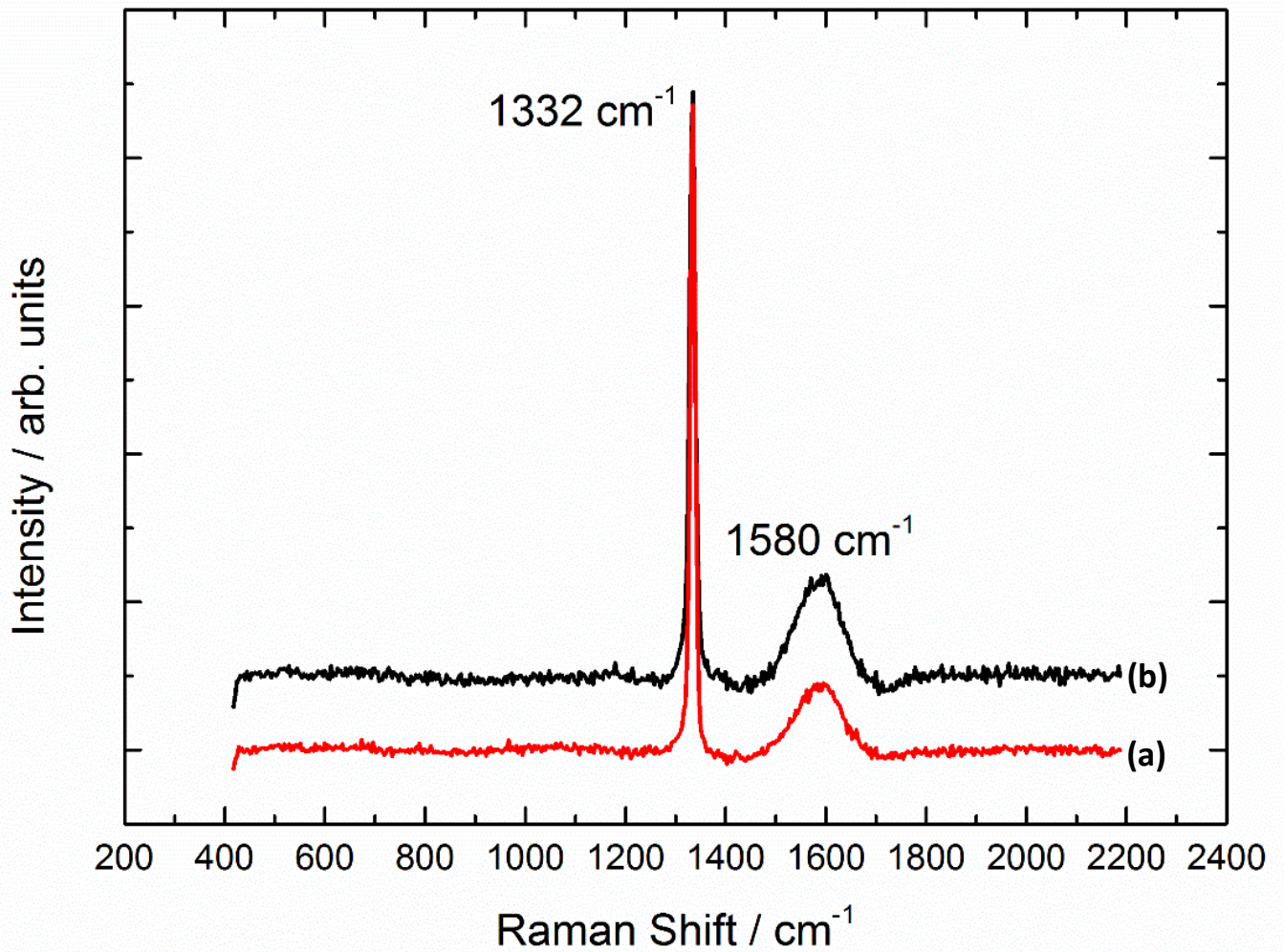


Figure 3.19: Raman spectra using UV, He:Cd 325 nm showing the diamond peak (1332 cm^{-1}) and the graphite peak (1580 cm^{-1}) of Li:N co-doped diamond samples. Constant amounts of NH_3/H_2 at 0.13% and N_2/H_2 at 0.23% were used but with different capping layers after lithium diffusion (a) undoped capping layer (b) N-doped capping layer.

Upon inspection of the I_D/I_G data (Figure 3.20) it is evident that the N-doped capping layer reduces the film quality by nearly double. It reduces from 9.21 with an undoped capping layer to 5.00 with a N-doped capping layer.

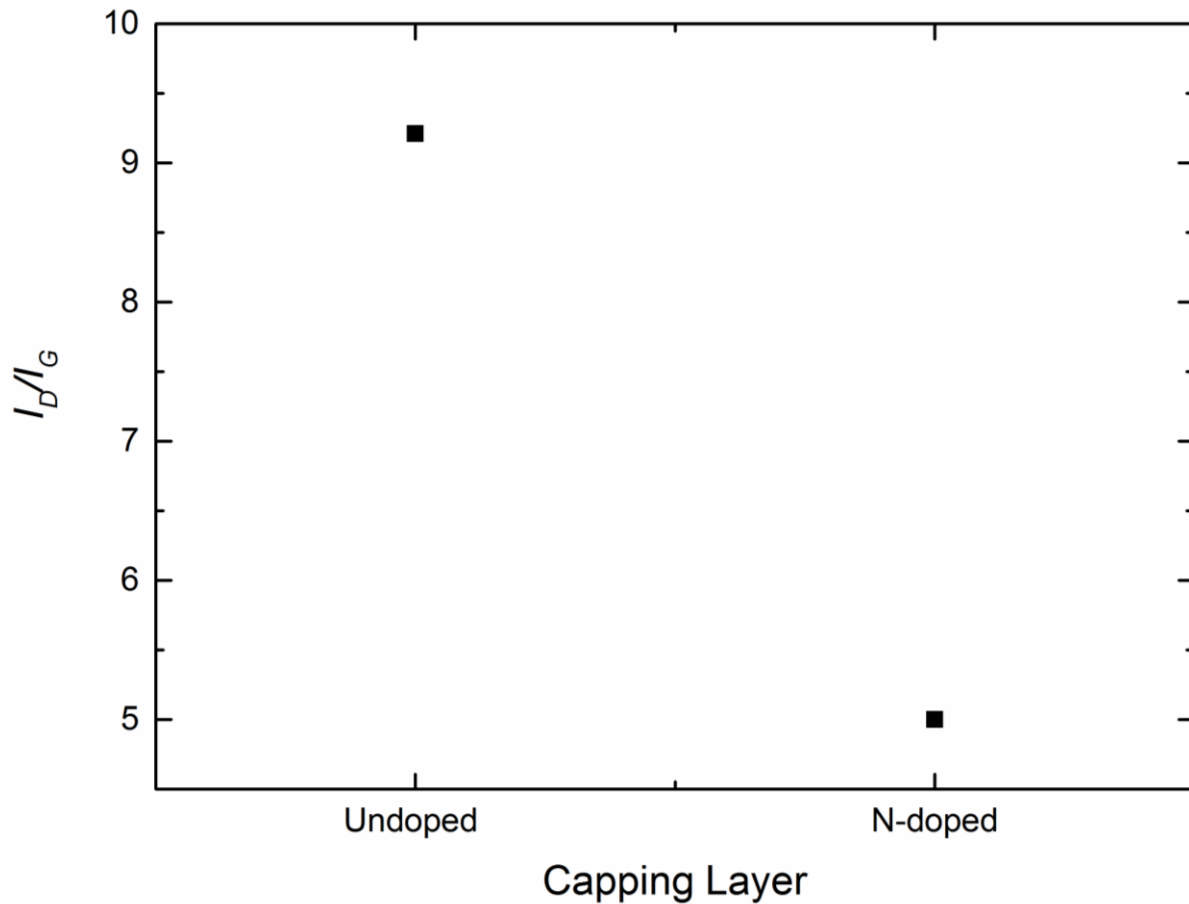


Figure 3.20: I_D/I_G data for the undoped and N-doped capping layers.

Resistance of these samples were then studied (**Table 3.4**). The N-doped capping layer increases the resistance from 7-16 M Ω for the undoped capping layer to 197-200 M Ω for the N-doped capping layer. Theoretically, it was suspected that the N-doped layer would reduce the resistance of the film. A reason for the increase in the resistance could be that since the sample was only N-doped for two minutes with a relatively low concentration of nitrogen (0.23% N₂/H₂ and 0.13% NH₃/H₂) this passivated p-type defects. It could be postulated that the resistance may be unchanged as it is being measured throughout the bulk of the film and therefore changing the capping layer has no effect. Yet since the resistance increases, this could be due to inconsistency with the resistance measurements. Therefore more samples need to be measured to confirm these behaviours. Otherwise, this result cannot yet be explained.

Table 3.4: Resistance measurements for the Li:N diamond films with different capping layers.

Capping Layer	Resistance / M Ω
Undoped	7-16
N-doped	197-200

Since the resistance did not decrease, no further analysis was done on this sample (SIMS, SEM). Further Li:N diamond films were grown with the original undoped capping layer.

3.5.2 Decreasing the amount of Nitrogen Atoms

Previously, Li:N co-doping has been achieved with a 1:18 ratio [37]. The aim of this project was to produce a 1:4 ratio of Li:N. To achieve this, either the amount of lithium drop cast onto the diamond sample could be increased, or the amount of nitrogen atoms could be decreased. This was attempted first in this study.

To try to decrease the amount of nitrogen atoms in the diamond lattice, a higher concentration of CH₄ gas was used. It was postulated that this would result in a higher ratio of CH₄:NH₃.

Note, this study used ratios for CH₄ and NH₃ gas, and N₂ gas was not used. This was because it is the nitrogen atoms from NH₃ gas that are incorporated into the diamond lattice. N₂ gas is responsible for the film morphology. Therefore, the N₂/H₂ was kept constant at 0.23%.

In previous studies, standard amounts of CH₄/H₂ at 0.81% and NH₃/H₂ at 0.13% gave a ratio of 6:1 for CH₄:NH₃. Therefore, to decrease the nitrogen atom incorporation, a ratio of CH₄:NH₃ of 10:1 and 15:1 were synthesized. This was done by increasing the percentage of CH₄/H₂ to 1.29% and 1.94% respectively. All results were compared using silicon as the substrate.

As the amount of CH₄ is increased, it is evident from the Raman data that the graphite peak at 1580 cm⁻¹ becomes much more prominent (**Figure 3.21**). It has been suggested that as the methane concentration increases, the sp² graphite areas also increase, yet it was not known the concentration that this would occur. The increase in methane gas used in this study significantly decreased the film quality. This high graphite peak could imply that using the higher methane concentration has produced NCD [54].

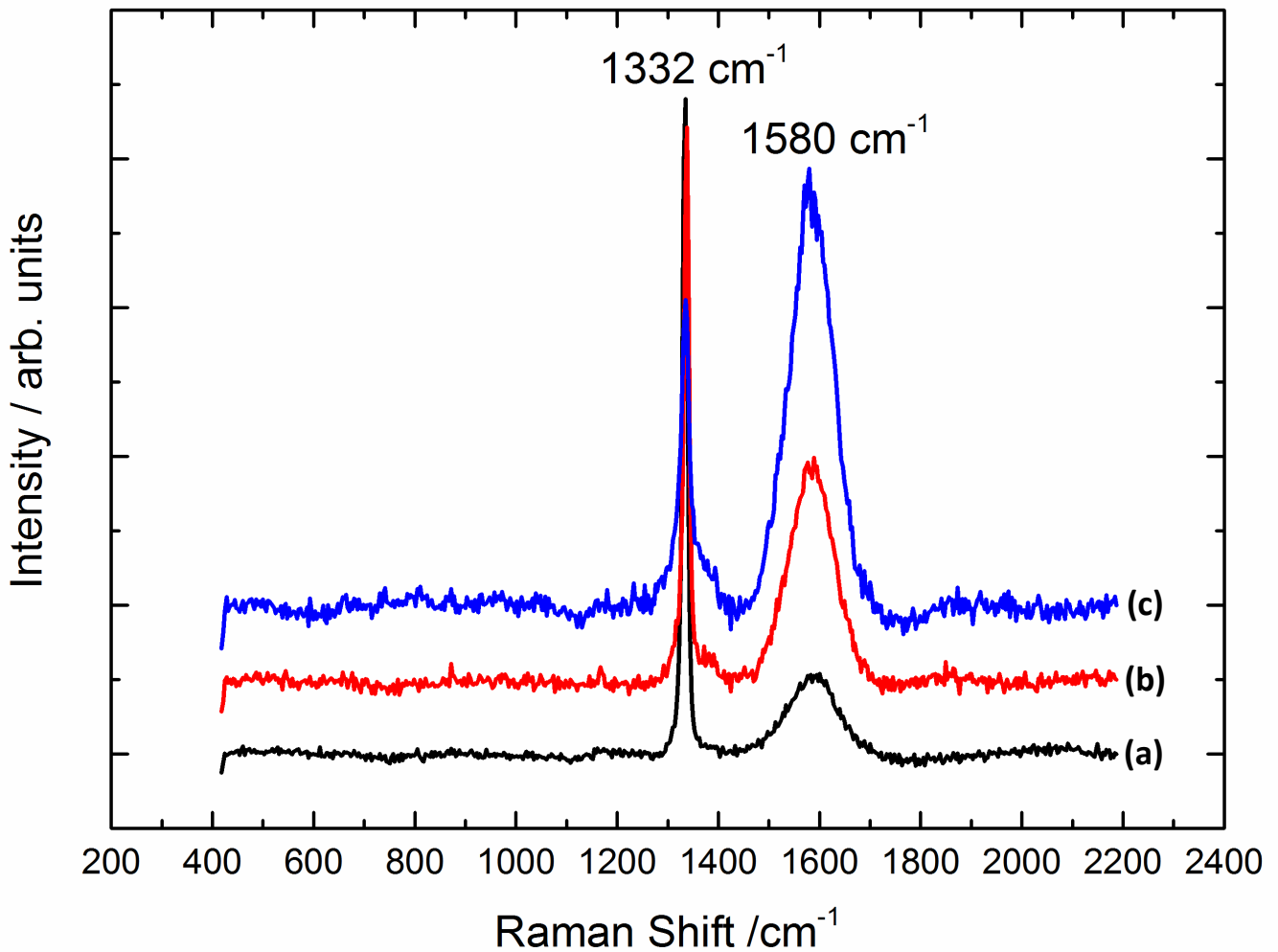


Figure 3.21: Raman spectra using UV, He:Cd 325 nm showing the diamond peak (1332 cm⁻¹) and the graphite peak (1580 cm⁻¹) of N-doped diamond samples. Constant amounts of NH₃/H₂ at 0.13% and N₂/H₂ at 0.23% were used with increasing amounts of CH₄ gas, (a) CH₄/H₂ at 0.81%, (b) CH₄/H₂ at 1.29% and (c) CH₄/H₂ at 1.94%.

The ratio of sp³:sp² was also measured using the I_D/I_G data (**Figure 3.22**) obtained from the Raman spectroscopy. This confirms, along with the Raman data, that as the CH₄ concentration is increased, there is a much lower proportion of sp³ carbons in the lattice compared to sp² graphitic carbon. At a ratio of 6:1 CH₄:NH₃ the I_D/I_G value is 9.05, this decreases greatly to 2.54 at 10:1 and then even further to 0.70 at 15:1.

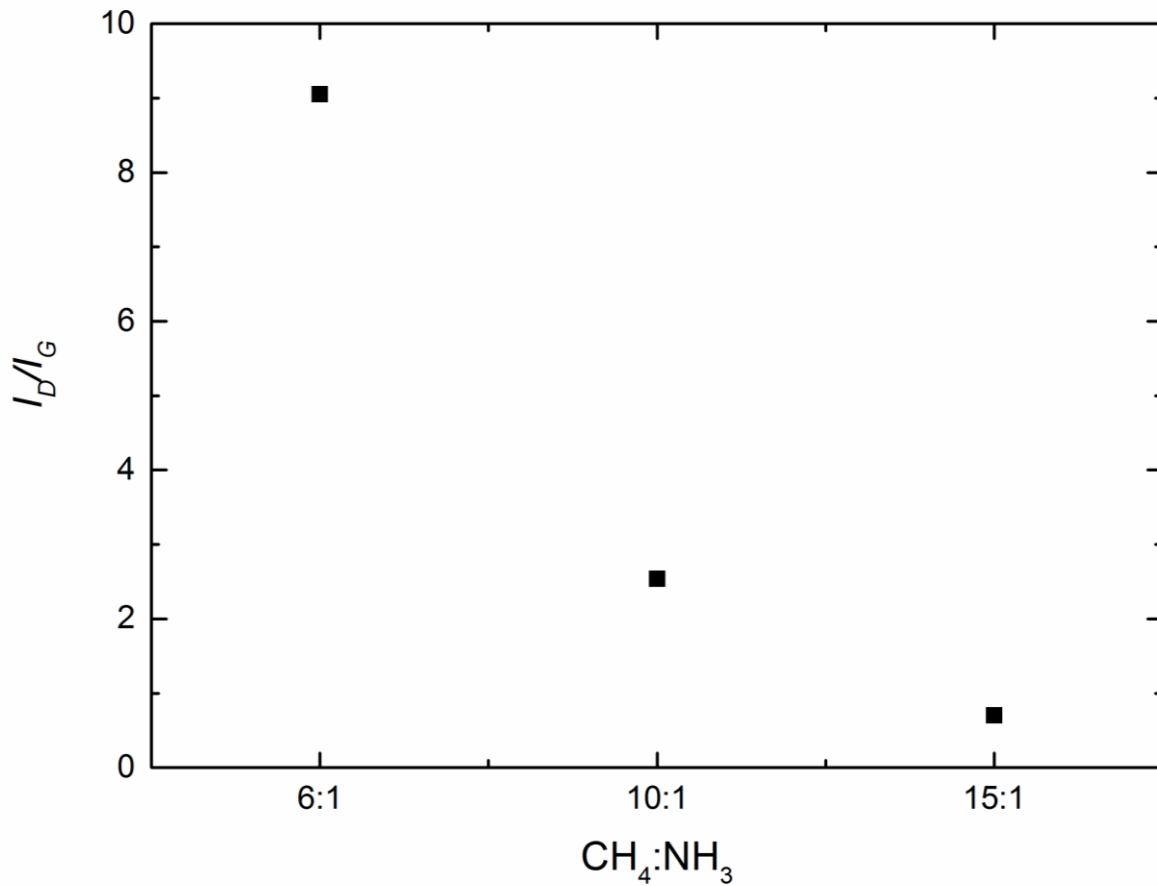


Figure 3.22: I_D/I_G data for the increasing methane concentration with respect to ammonia gas.

The increase in graphite areas was clarified when the SEM images were analysed (**Figure 3.23**). When the methane concentration is increased, a cauliflower structure is observed confirming that the diamond lattice has become nanocrystalline diamond (NCD) as opposed to microcrystalline (MCD). This was an outcome that was predicted but it was not certain at which concentration of CH₄ gas this would occur. NCD has a higher degree of sp² carbon, therefore explaining the prominent graphite peak observed in the Raman data and the low I_D/I_G values [54].

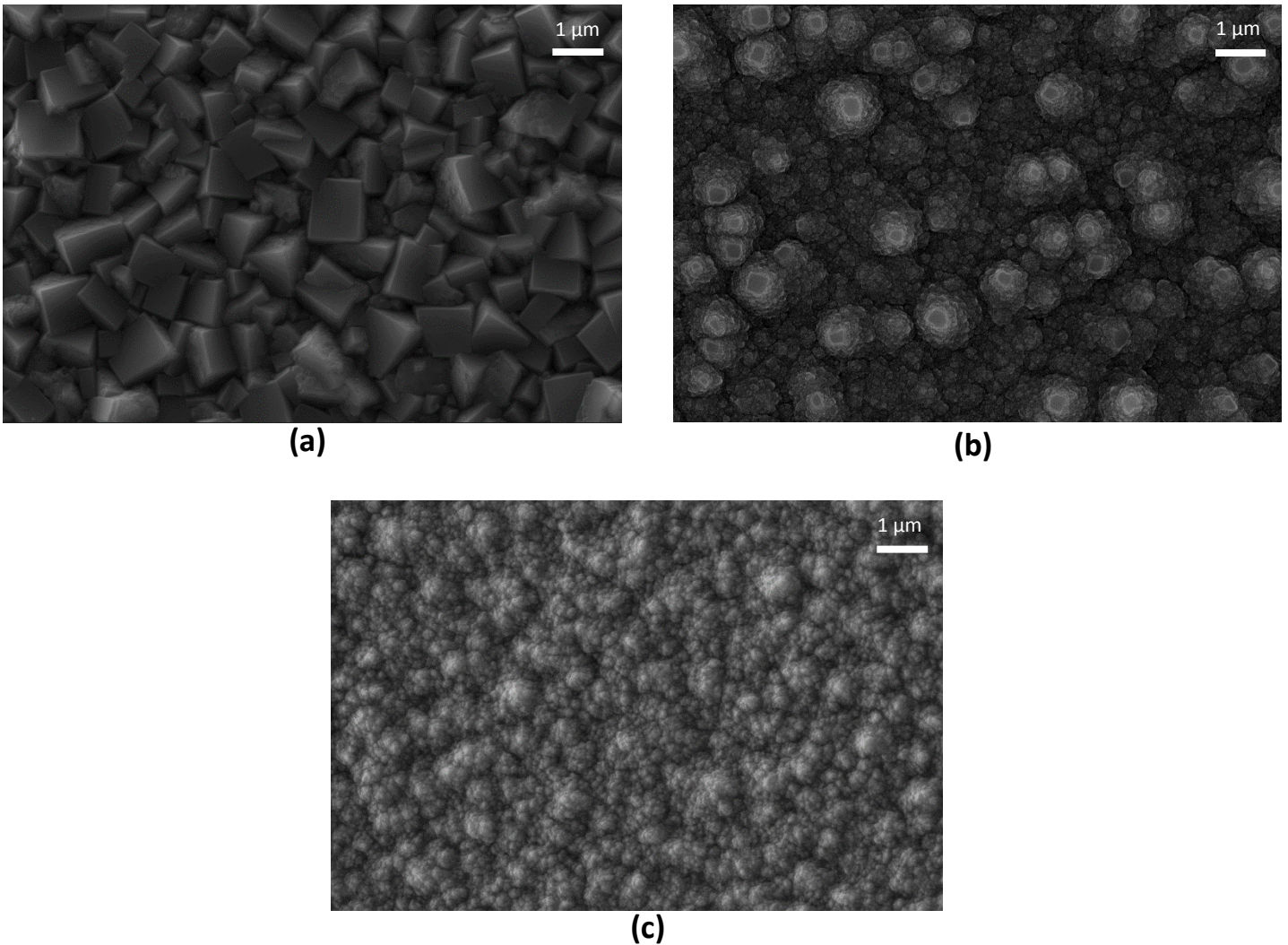


Figure 3.23: SEM images of N-doped diamond samples to determine if increasing the amount of CH_4 with respect to NH_3 would decrease the amount of nitrogen atoms in the diamond lattice. The N_2/H_2 and NH_3/H_2 were kept constant at 0.23% and 0.13% respectively, (a) $\text{CH}_4:\text{NH}_3$ ratio of 6:1 with CH_4/H_2 at 0.81%, (b) $\text{CH}_4:\text{NH}_3$ ratio of 10:1 with CH_4/H_2 at 1.29% and (c) $\text{CH}_4:\text{NH}_3$ ratio of 15:1 with CH_4/H_2 at 1.94%.

Resistance was also measured for these ratios (**Table 3.5**) and there is a clear decrease in resistance for higher concentrations of methane. NCD has more sp^2 regions which are more conductive than sp^3 diamond, consequently, reducing the resistance.

Table 3.5: Resistance measurements of N-doped diamond as the methane concentration was increased.

CH_4/H_2	Ratio of $\text{CH}_4:\text{NH}_3$	Resistance / $\text{M}\Omega$
0.81%	6:1	180-210
1.29%	10:1	38-43
1.94%	15:1	0.01-0.03

It was concluded that this was not a good method to determine if the ratio of N:C atoms in the diamond lattice had been successfully reduced. As the proportion of nitrogen atoms in the diamond

lattice decreases, the resistance should increase as there are less dopants in the diamond lattice. There may be less incorporation of nitrogen atoms in the lattice but this cannot be concluded since we are comparing MCD to NCD, therefore, the experiment is not viable [54].

3.5.3 Increasing the amount of Lithium Atoms

The next step in this study was to try to increase the amount of lithium atoms in the diamond lattice so the 1:4 Li:N ratio could be achieved. For the initial Li:N co-doping process, conditions used were the standard CH₄/H₂ at 0.81%, NH₃/H₂ gas at 0.13% and N₂/H₂ at 0.23% or 0.28% with 100 μL Li₃N (see section 3.5). Since the 0.23% N₂/H₂ looked the most promising, this condition was used to investigate the effect of increasing Li₃N exposure on the diamond film.

The Raman data (**Figure 3.24**) were analysed as the Li₃N volume was increased. This highlights that the graphite peak remained relatively constant for 100 μL and 150 μL Li₃N solution. However, it greatly increases as the volume is further increased to 200 μL. Surprisingly, on further addition to 250 μL Li₃N, the graphite peaks decreases again. Although it does not reduce to the peak height seen for 100 μL and 150 μL Li₃N solution. The reason for this may be that when 250 μL Li₃N was added, not all the solution diffused into the diamond bulk. Non-diffused Li₃N was observed on the film surface after it was removed from the reactor (**Figure 3.25**). This is also the reason why no higher volumes of Li₃N were studied.

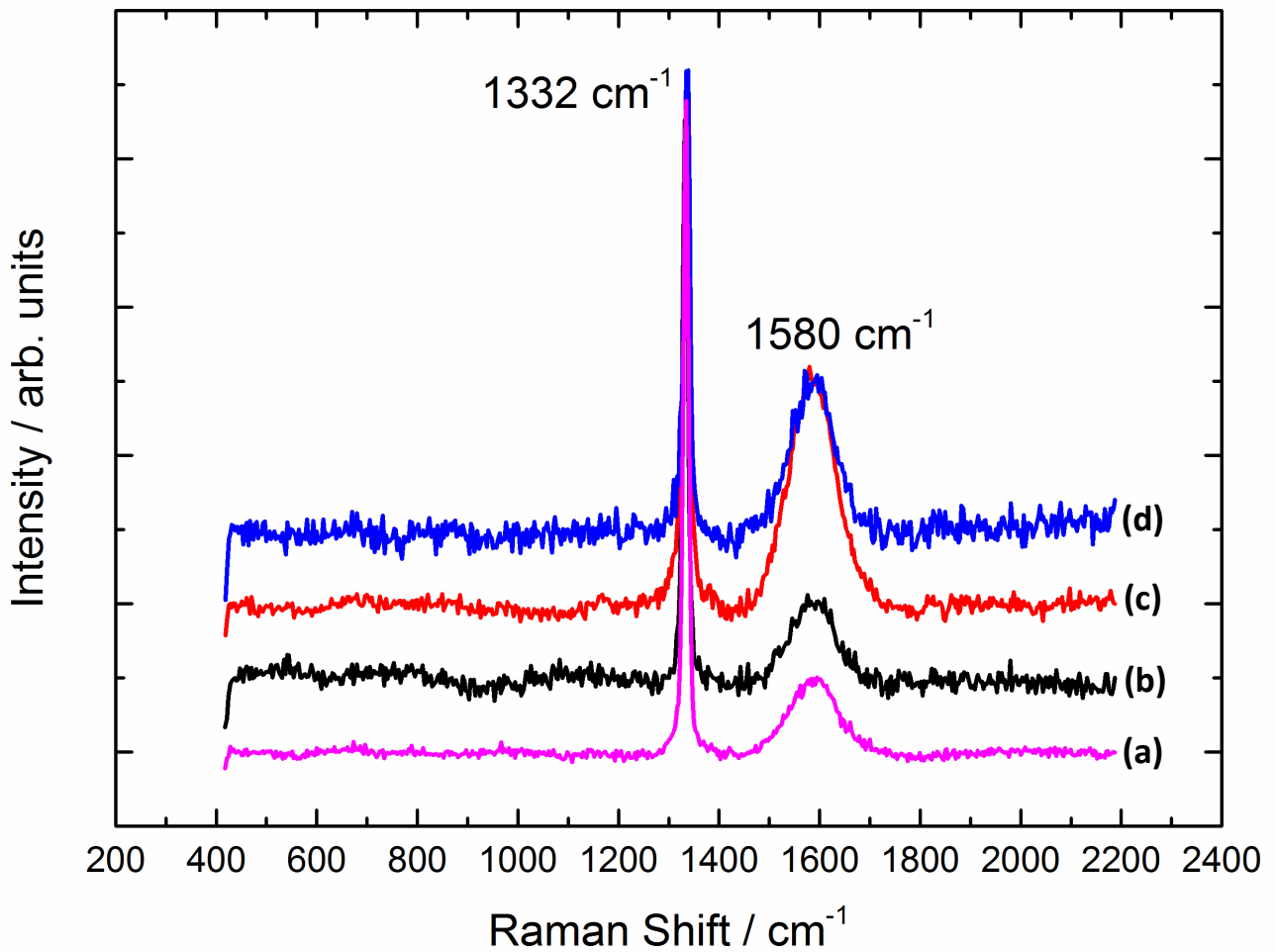


Figure 3.24: Raman spectra using UV, He:Cd 325 nm showing the diamond peak (1332 cm^{-1}) and the graphite peak (1580 cm^{-1}) demonstrating how the graphite peak changes with increasing volume of Li_3N solution. The CH_4/H_2 was at 0.81%, the NH_3/H_2 was 0.13% and the N_2/H_2 was 0.23%. All samples were grown on silicon substrates with (a) $100\ \mu\text{L}$ Li_3N solution, (b) $150\ \mu\text{L}$ Li_3N solution, (c) $200\ \mu\text{L}$ Li_3N solution and (d) $250\ \mu\text{L}$ Li_3N solution.

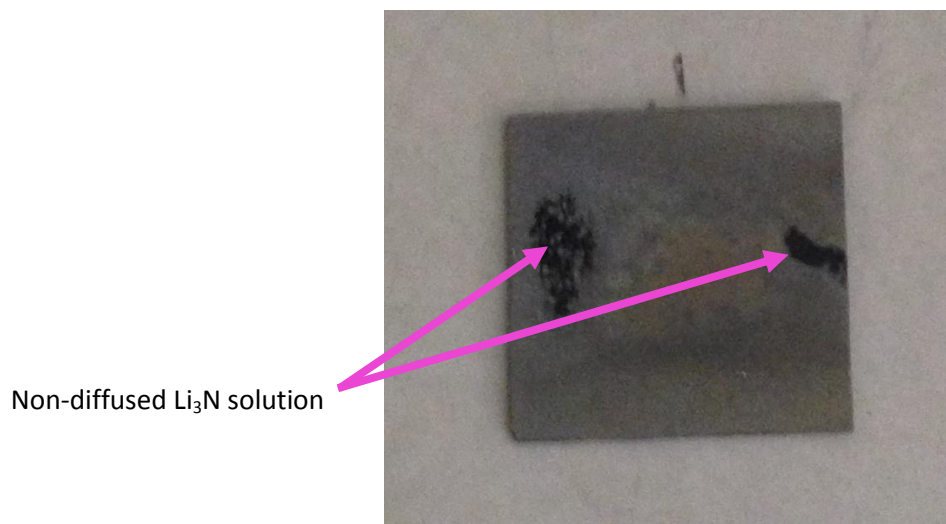


Figure 3.25: Photograph of non-diffused Li_3N solution that remained on the diamond film surface after $250\ \mu\text{L}$ was added.

The I_D/I_G values (**Figure 3.26**) are consistent with the Raman data, with both 200 μL and 250 μL Li_3N solution having values much lower than 100 μL and 150 μL . As the volume increases the graphite area becomes much more prominent and this has a negative effect on the film quality. The I_D/I_G values decrease from 9.21 with the introduction of 100 μL Li_3N solution to between 2 and 3 for 200 μL and 250 μL Li_3N solution.

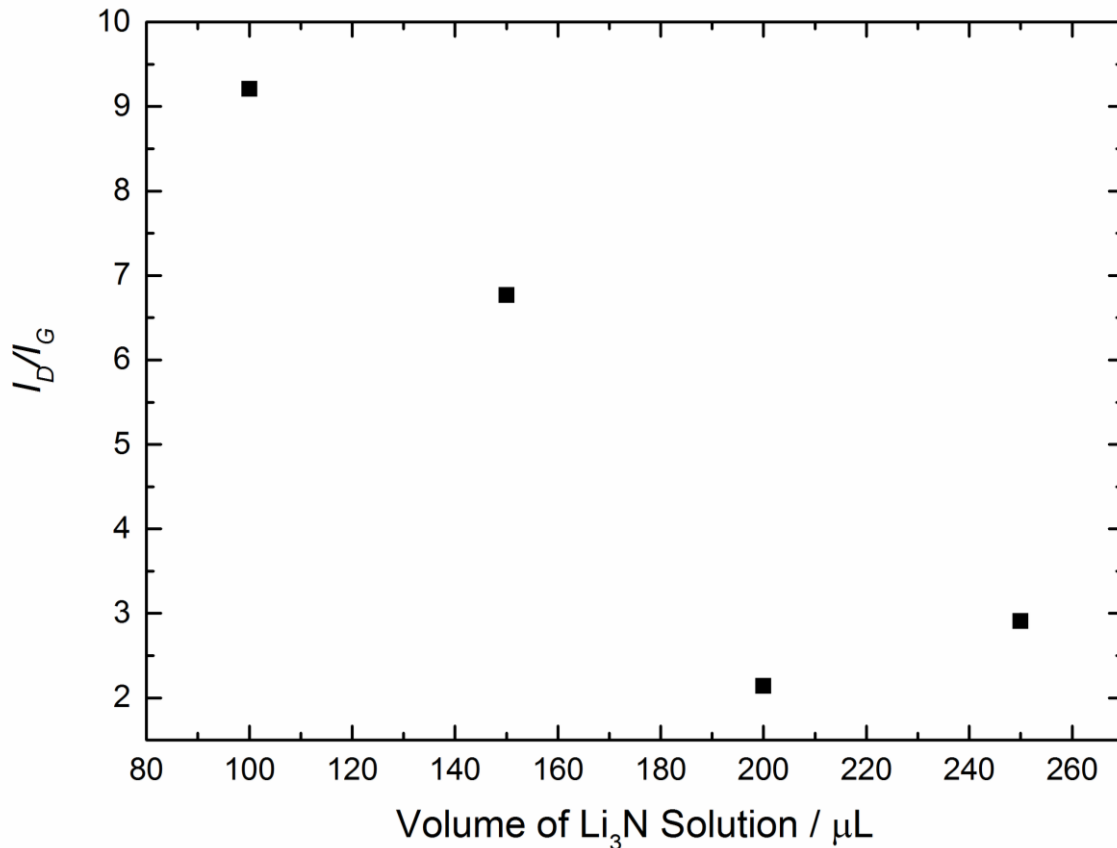


Figure 3.26: I_D/I_G data for Li:N diamond films as the volume of Li_3N solution increases.

It is possible that at 250 μL Li_3N solution, the solid solubility limit for lithium in diamond has been reached. This occurs at $\approx 5 \times 10^{19} \text{ cm}^{-3}$ [24]. To determine this, SIMS would need to be performed on this sample to determine the lithium concentration. Above this solubility limit, the Li_3N forms lithium carbide and therefore lithium atoms no longer incorporate into the diamond lattice. Raman spectroscopy was performed on the part of the diamond sample where Li_3N could be seen on the surface after diffusion. This was compared to the same sample where no Li_3N could be seen (**Figure 3.27**). This gives evidence that lithium carbide is on the surface of the film since there is no diamond peak where there is non-diffused Li_3N .

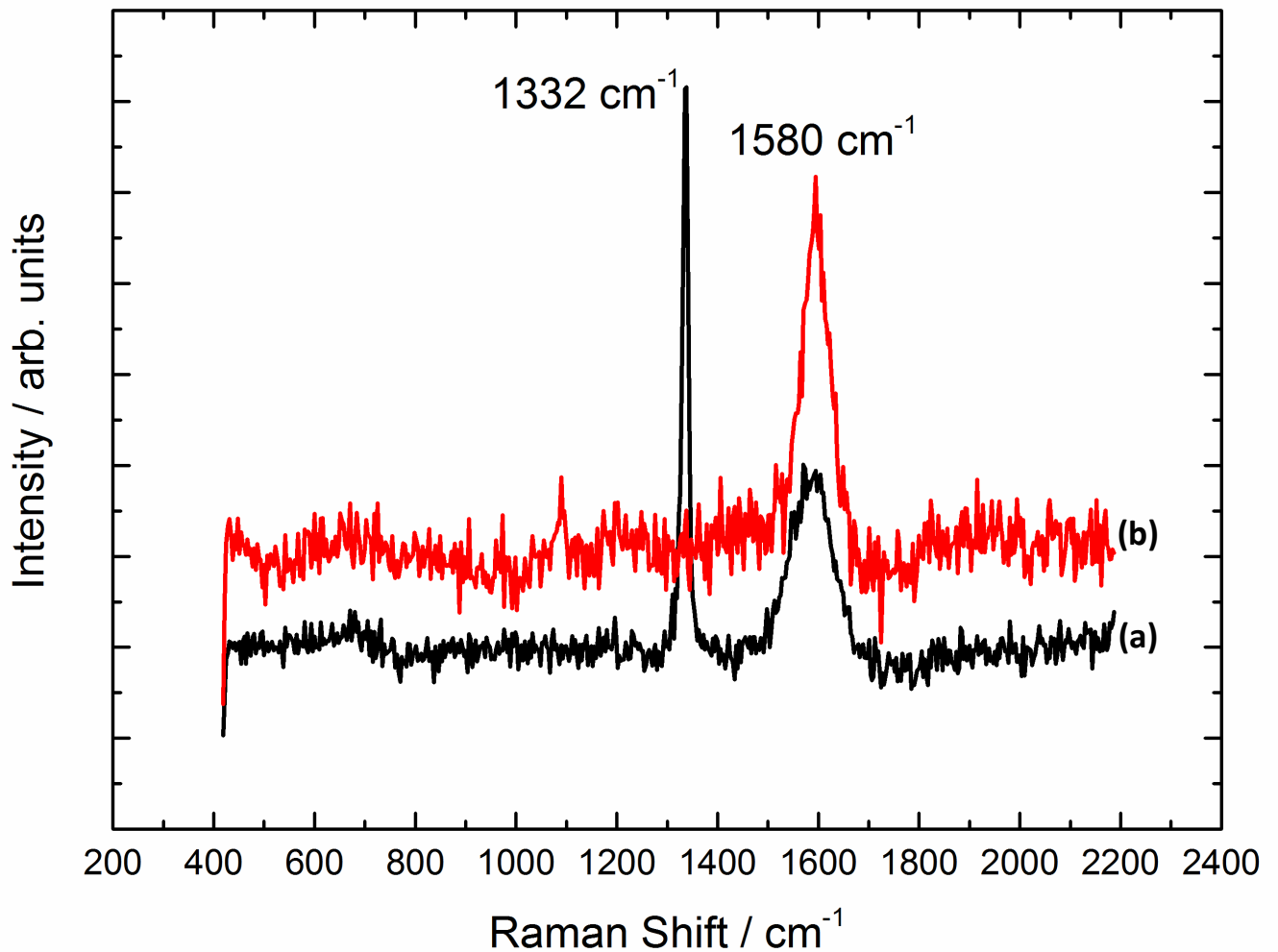
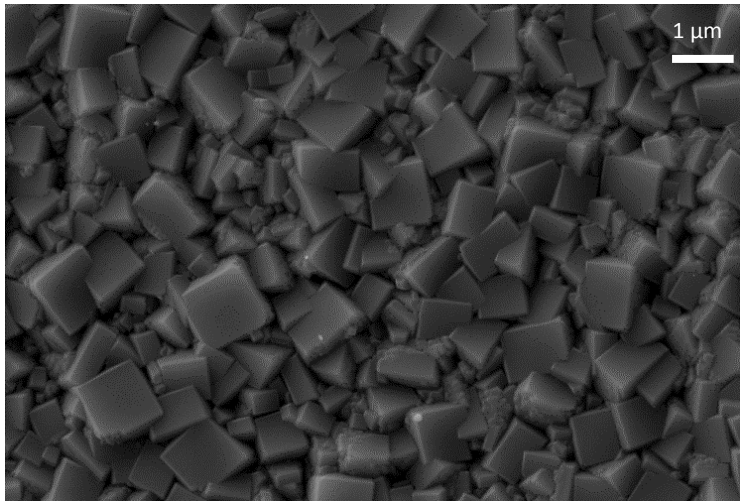
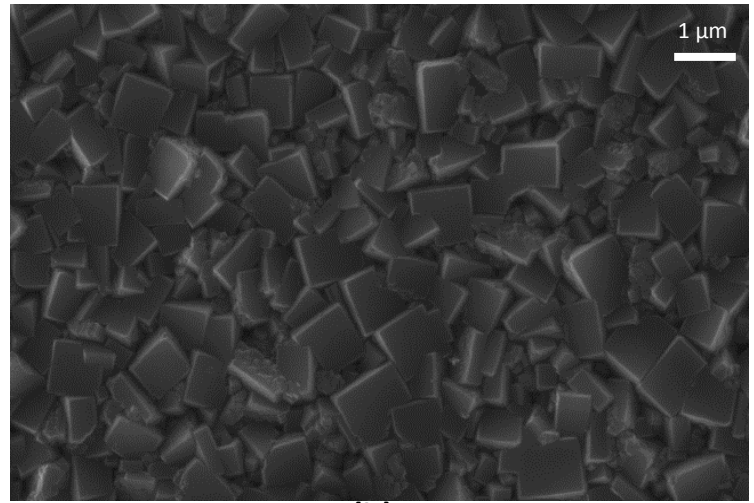


Figure 3.27: Raman spectra using UV, He:Cd 325 nm showing the diamond peak (1332 cm^{-1}) and the graphite peak (1580 cm^{-1}) comparing Li:N co-doped diamond samples with $250\text{ }\mu\text{L}$ Li_3N solution with and without Li_3N on the surface after diffusion. The CH_4/H_2 was constant at 0.81%, the N_2/H_2 was 0.23% and the NH_3/H_2 was 0.13% for the samples on silicon substrates with (a) no Li_3N on surface (b) Li_3N on the surface.

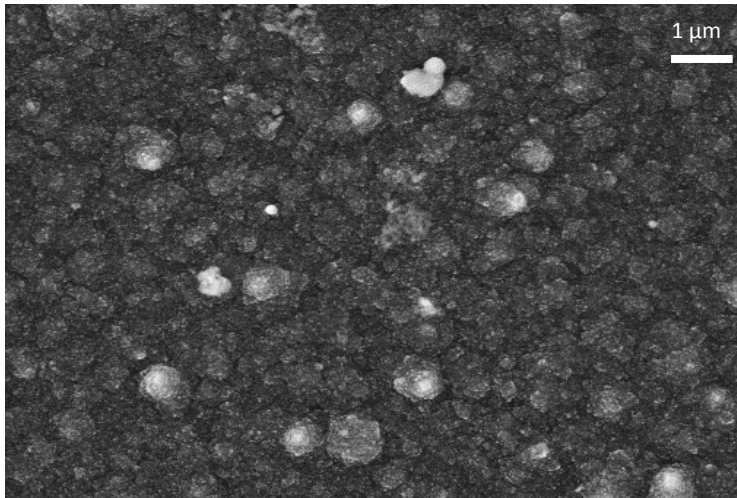
The SEM images (**Figure 3.28**) highlight that the film quality does drastically change as the volume of Li_3N solution is increased. For both $100\text{ }\mu\text{L}$ and $150\text{ }\mu\text{L}$ Li_3N the film quality demonstrates uniform $\{100\}$ square facets. At higher volumes of $200\text{ }\mu\text{L}$ and $250\text{ }\mu\text{L}$ Li_3N , the films appear to change from MCD to NCD. This is exhibited by the cauliflower-type structure seen in **Figure 3.27 (c) and (d)**. This also explains the prominent graphite peaks observed in the Raman data and the low I_D/I_G values, as NCD has a more sp^2 graphite than MCD.



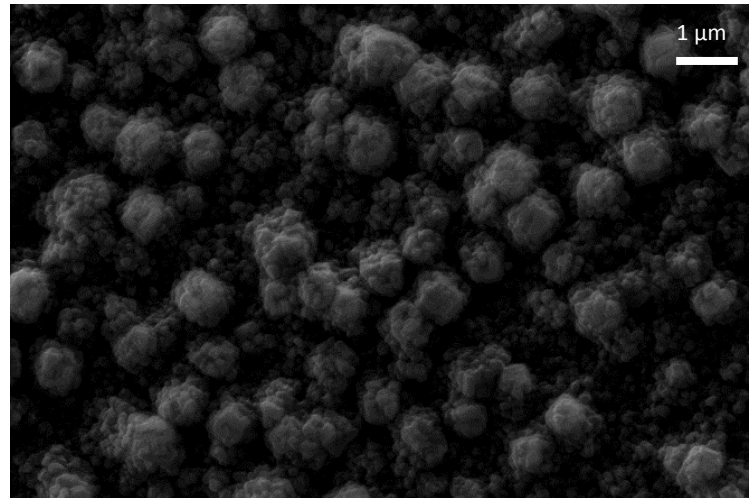
(a)



(b)



(c)



(d)

Figure 3.28: SEM images showing the morphology of Li:N co-doped diamond samples with increasing amounts of Li_3N solution on silicon substrates. All samples have 0.81% CH_4/H_2 , 0.23% N_2/H_2 and 0.13% NH_3/H_2 , (a) 100 μL Li_3N solution, (b) 150 μL Li_3N solution, (c) 200 μL Li_3N solution and (d) 250 μL Li_3N solution.

It was postulated that as the Li:N ratio reached 1:4, the resistance should decrease as the diamond film is becoming increasingly more semiconducting. Therefore, the resistance of the films needed to be measured. For the 1:4 Li:N sample to be achieved it was expected to obtain a resistance of $\leq 1 \text{ M}\Omega$.

The resistance measurements (**Table 3.6**) for the Li:N co-doped samples highlight that as the amount of Li_3N solution is increased, the resistance decreases, as was expected. The resistance is highest at 7-16 $\text{M}\Omega$ for 100 μL which then decreases to 5-6 $\text{M}\Omega$ at 150 μL and then further decreases to 1-3 $\text{M}\Omega$ at 200 μL . There is then an increase to 2-5 $\text{M}\Omega$ at 250 μL but this can be explained by the fact that full diffusion did not occur in this sample. However, these results for 200 μL and 250 μL Li_3N need to be assessed with care. As seen with the SEM images these samples are nanocrystalline. NCD has a larger amount of sp^2 graphite which has a lower resistance than sp^3 diamond and therefore may be affecting the resistance results.

Table 3.6: Table highlighting the resistance measurements as the amount Li₃N solution is increased.

Amount of Li ₃ N solution added / μL	Resistance/ $\text{M}\Omega$
100	7-16
150	5-6
200	1-3
250	2-5

These values for resistance are decreasing and going in the right direction to produce n-type diamond. However, when the Li:N co-doped diamond films were repeated with the same conditions, often the resistance results were not consistent. This could be due to the silver contacts; sometimes these could become scratched or may not have formed complete squares on the sample (see section 2.6.1). Nonetheless, sometimes even when the squares appeared perfect, consistent results were still not obtained. This cannot be explained, yet it should be noted that the majority of results produced a low resistance. Repeats would need to be performed to fully investigate how often these inconsistent results occurred. Perhaps, the lithium atom incorporation was not successful for all samples or resistance measurements are not a consistent and reliable way of assessing the results.

Since the 200 μL Li₃N sample produced the lowest resistance, the ratio of Li:N was then obtained using SIMS (**Figure 3.29**). The data shows that there is a consistent concentration of nitrogen atoms throughout the film. The lithium atom concentration is at the maximum at a depth of between 0-20 nm of the diamond film. The concentration then gradually drops for the remainder of the film from $\approx 3 \times 10^{19} \text{ cm}^{-3}$ at the maximum to $\approx 5 \times 10^{17} \text{ cm}^{-3}$ at the minimum. Ideally the lithium atom concentration would be constant throughout the film, though it was expected to have more lithium atoms on the surface of the film. Potentially new diffusion conditions could result in a more uniform lithium atom distribution. The slight decrease in lithium atoms observed in the first 10 nm of film is due to the undoped capping layer that was grown for 5 minutes. The depth profile was only run for the first 100 nm of sample, after this depth the trend remained the same for the remainder of the film. The line for carbon is for intensity which is produced as a baseline so the concentrations of nitrogen and lithium atoms can be calculated.

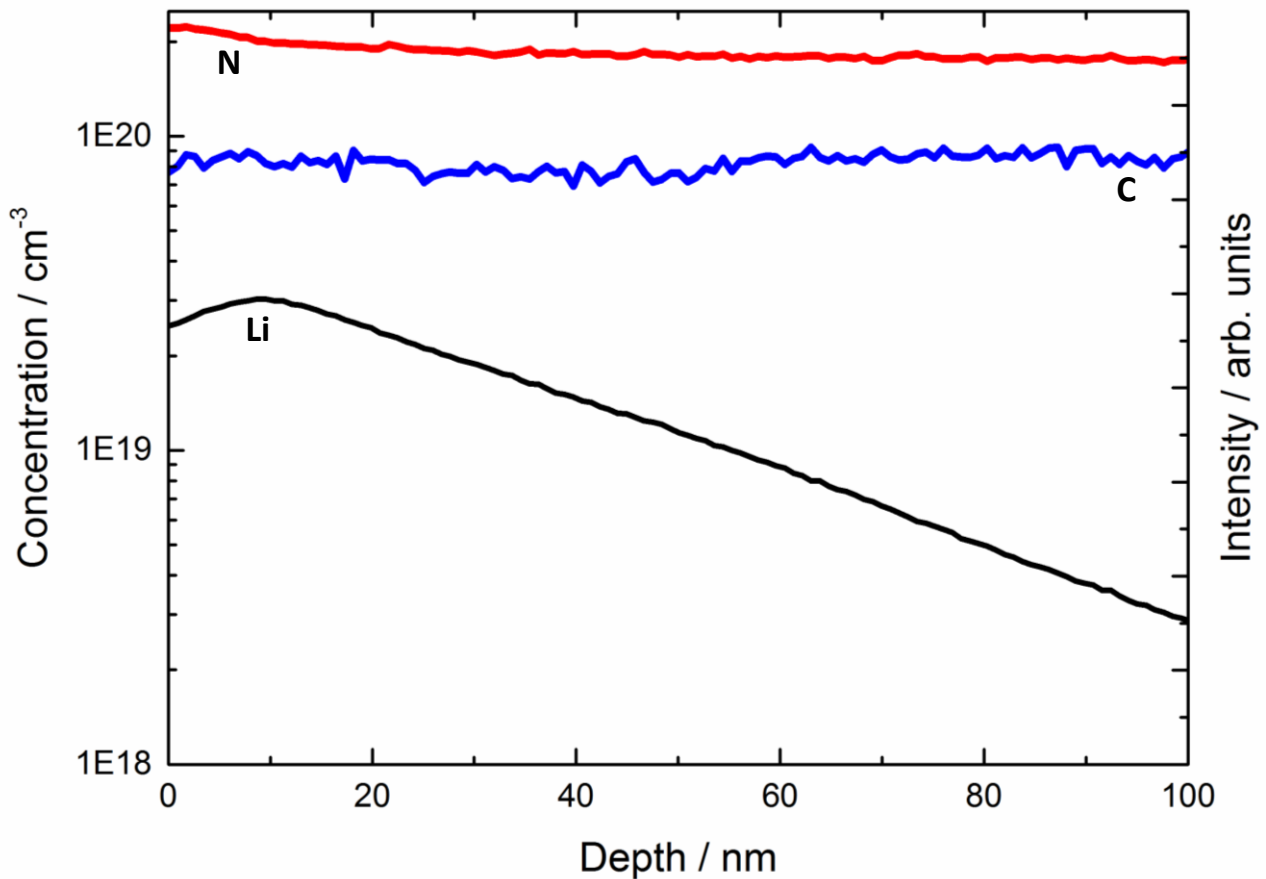


Figure 3.29: SIMS depth profile of the first 100 nm of a Li:N diamond film with an undoped capping layer grown for 5 minutes. The figure shows the concentrations of lithium and nitrogen atoms on the left axis and the intensity of carbon, used as baseline on the right axis.

To calculate the ratio of Li:N, the maximum concentration of lithium atoms was used, which as stated previously was $\approx 3 \times 10^{19} \text{ cm}^{-3}$. Since the nitrogen atom concentration was uniform throughout the film, an average was taken $\approx 2 \times 10^{20} \text{ cm}^{-3}$. This gives a ratio of 1:6.7 (**Equation 3.1**). Although this ratio is not quite the required 1:4 ratio it is close to this and therefore possibly with a few changes to experimental conditions a 1:4 ratio could be achieved.

$$ratio = \frac{\text{average concentration of N atoms}}{\text{maximum concentration of Li atoms}} \quad \text{Equation 3.1}$$

3.5.4 No Capping Layer after Lithium Diffusion

As was postulated in section 3.5.1, the resistance may decrease if an undoped capping layer was not used. In section 3.5.1 there is evidence that this does not work if an N-doped capping layer was used. However, it was suggested that no capping layer at all could decrease the resistance as then there is no insulating diamond on the surface of the film. This was studied using 200 μL Li_3N solution since this had produced the lowest resistance in the previous section (see section 3.5.3).

The Raman data (**Figure 3.30**) highlights that there was a major reduction in graphite peak at 1580 cm^{-1} when no capping layer was added after lithium diffusion. This demonstrates that there is a

higher film quality and it is most probably no longer nanocrystalline. SEM images would need to be studied to clarify this.

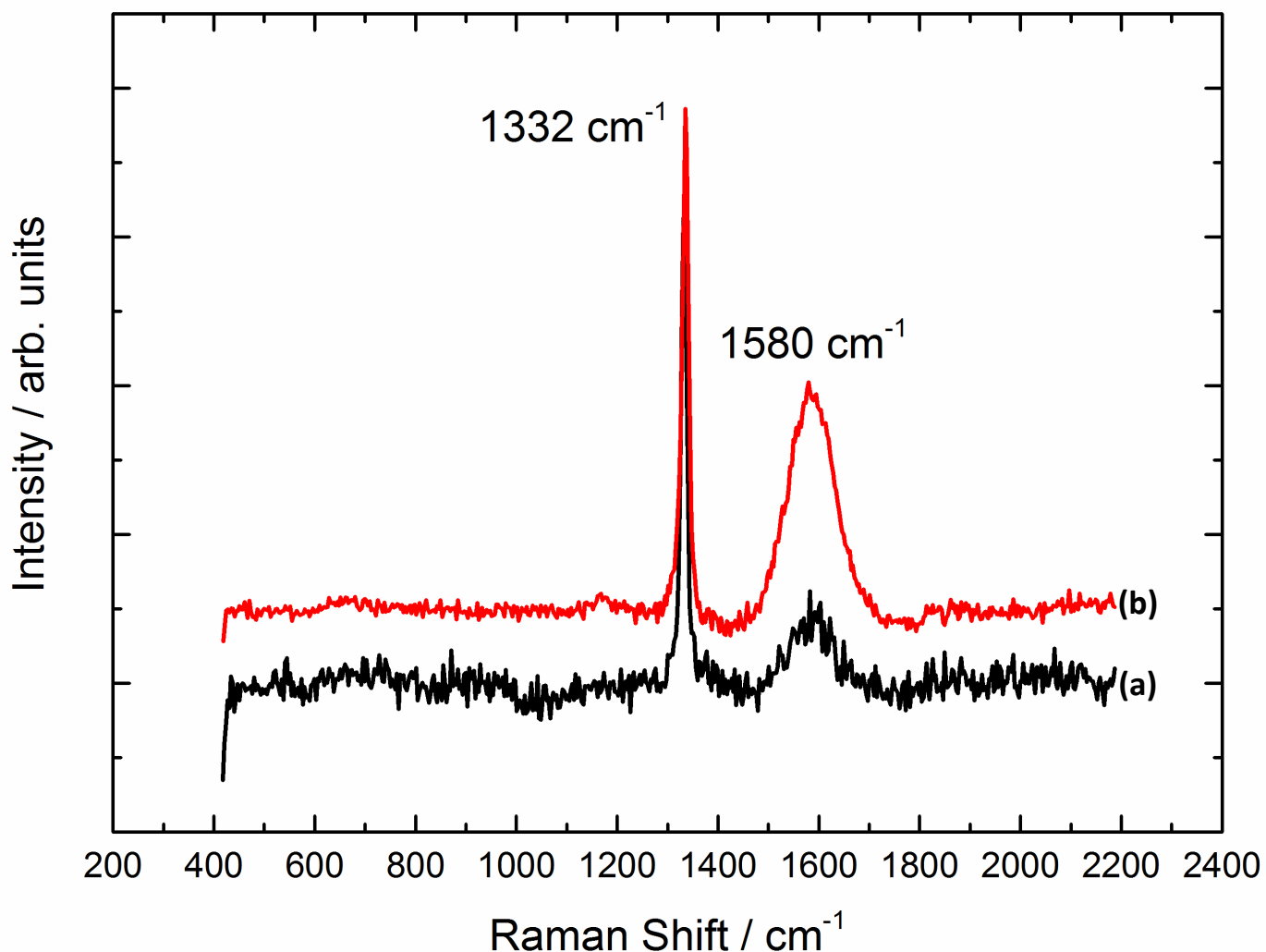


Figure 3.30: Raman spectra using UV, He:Cd 325 nm showing the diamond peak (1332 cm^{-1}) and the graphite peak (1580 cm^{-1}) comparing Li:N co-doped diamond samples with $200\text{ }\mu\text{L}$ Li_3N solution with and without a capping layer of CH_4 , (a) no capping layer (b) with a capping layer.

Since the Raman data looked promising, resistance was then measured for the samples with no capping layer and compared to those with a capping layer (**Table 3.7**). Resistance measurements show that no capping layer increases the resistance dramatically. One possible reason for this is that without a capping layer, there is no encapsulation of the lithium atoms. Therefore they are not incorporating into the diamond lattice as effectively. No further analysis (SIMS, SEM) was performed since if resistance did not decrease then the ratio of Li:N will not be lowered.

Table 3.7: Table highlighting the change in resistance of Li:N co-doped diamond films, with and without a capping layer after lithium diffusion.

Li:N co-doped sample	Resistance/ MΩ
With capping layer	1-3
No capping layer	110-120

3.5.5 Acid Washing

One of the many applications of n-type diamond is for use as an acid sensor [21,55]. To investigate if the Li:N co-doped diamond samples could be used as an acid sensor, acid washing was performed to study how the resistance of samples changed before and after acid washing. Ideally, the resistance would be unchanged, therefore giving evidence that the sample is resistant to the acid.

Although 0.23% N₂/H₂ was used for the majority of the Li:N co-doped samples that were grown, both 0.23% and 0.28% N₂/H₂ were acid washed to provide a wider variety of results to be analysed. A N-doped 0.23% N₂/H₂ sample with no lithium atom incorporation was also investigated for completion.

The results (**Table 3.8**) are inconclusive and do not determine whether or not Li:N co-doped diamond films are resistant to acid washing. There is no general trend that can be observed and this could be due to unreliable resistance results or perhaps due to the acid washing process itself. The resistance of the Li:N co-doped samples increases in some cases and this increase in resistance could be a result of how the acid affects the diamond surface.

Table 3.8: Table highlighting how the resistance changes with N-doped and Li:N co-doped diamond films before and after acid washing.

N ₂ /H ₂	Resistance / MΩ			
	Prior to Acid Wash	After acid Wash 1	After acid Wash 2	After acid Wash 3
N-doped film with 0.23% N ₂ /H ₂	154-156	95-114	-	-
Li:N co-doped film with 0.23 N ₂ /H ₂	7-16	168-174	101-125	-
Li:N co-doped film with 0.28 N ₂ /H ₂	127-135	473-487	127-157	>500

Possibly, when the diamond samples react with H₂SO₄, the surface, which was oxygen terminated, is now terminated with hydroxyls groups. Upon further silver contact addition, another oxygen termination should remove these hydroxyls from the surface and replace them with oxygen. However, a different outcome would occur if, during the acid wash, OH bonds are formed all the way across the surface, not just between the silver contacts. Consequently, when further silver contacts and oxygen termination occurs, there will still be OH groups underneath the new silver contacts that have been evaporated onto the sample. These would not undergo oxygen termination as they would be trapped underneath the contacts during the process. Alternatively, these could also be H bonds as opposed to OH bonds as there may be no oxygen underneath the original contact

for the proton to attach too. Therefore, a single hydrogen atom may attach to the diamond surface and become trapped underneath the silver contacts (**Figure 3.31**).

If this mechanism occurred, it would be postulated that a second acid wash would result in the same resistance recorded after the first acid wash. From the samples tested, the results decrease in resistance which cannot be explained, unless these OH bonds under the silver contacts are reducing the resistance. This would not be expected as oxygen is an insulating layer. Furthermore, there were many samples chosen and only a select few have been stated (**Table 3.8**). However, other results show an increase in resistance, therefore there is a lack of consistency within the results. A possible explanation is that the predicated mechanism is occurring, but since the surface is already terminated with O, OH or H bonds, an equilibrium is set up where the additional protons are added and removed from the surface. Therefore, this would result in random resistance readings depending on where the reaction was stopped in the equilibrium process.

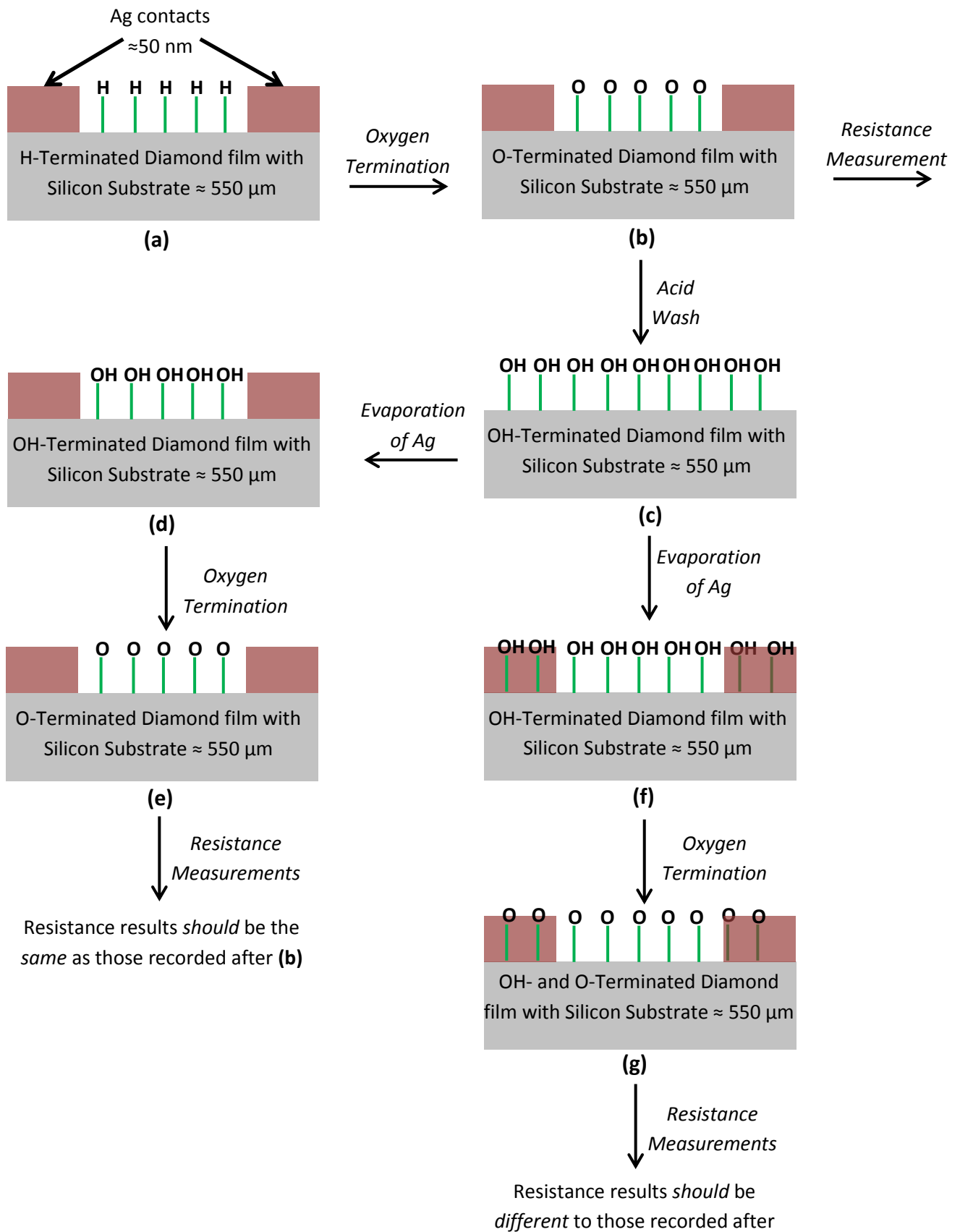


Figure 3.31: Schematic highlighting a possible reason for the different resistance measurements before and after acid washing, (a) shows the H-terminated diamond films with the Ag contacts, (b) the O-terminated surface when resistance measurements are taken, (c) after acid washing the OH-terminated surface, this may also be H-terminated, (d) after acid wash the repeat of Ag evaporation followed by (e) O-termination and resistance measurements. These *should* be the

same as after (b). Alternatively, (f) could occur where there are OH (or H) groups underneath the Ag contacts, (g) O-termination where the OHs underneath the Ag contacts remain unchanged. This will give *different* resistance results to after (b).

An alternative possibility is that since the acid being used is so strong, it is affecting more than just the surface of the diamond lattice and is having some effect on the bulk. Although it would be unlikely that this would be having an effect on the diamond lattice, since this is so strong, it could be reacting with the dopants in some manner.

Previous results of acid washing include surface cleaning of DLC with acid for removal of sp^2 carbon. This also results in negligible etching of the diamond. Multiple acids were used in this procedure, (i) chromic acid at a temperature of 455 K, (ii) a 1:1 solution of H_2O_2 and NH_3OH and (iii) HNO_3 , HF and CH_3COOH in a 1:1:1 ratio [56].

Furthermore, concentrated H_2SO_4 (90 vol%) and HNO_3 (10 vol%) have also been used to etch C60. C60 becomes unstable and etches to diamond and graphite phases. This process is at ambient temperature and was reacted for 12 hours [57].

To determine if etching of graphite had occurred in this study, Raman spectroscopy would need to be investigated. A reduction in the graphite peak at 1580 cm^{-1} would be observed before and after acid washing.

Although suggestions can be made as to what may be occurring, overall, it can be concluded that either the Li:N co-doped diamond films are not stable to acid, or some element of the experiment causes inconsistent results. Therefore, further thought into an additional experiment is required.

4.0 Conclusions

The aim of this study was to produce a Li:N co-doped diamond film with a ratio of 1:4. It was believed that this ratio could produce n-type semiconductivity.

N-doped diamond was fabricated using a HFCVD process, and the optimum quantities of NH_3 gas and N_2 gas were evaluated. It was important to produce a diamond film of good quality and morphology. The optimum value for NH_3/H_2 was 0.13% and the optimum N_2/H_2 value was 0.23%, although 0.28% was also promising. This was evaluated with Raman spectroscopy, SEM images and I_D/I_G values. The N-doped diamond was grown before the lithium atoms were incorporated to ensure no lithium atom aggregation.

Silicon and molybdenum substrates were analysed to determine which produced a more uniform diamond film. Molybdenum substrates, having a very low resistivity in comparison to diamond, lowered the resistance of the diamond films, so did not provide accurate results. The main method for determining if a low Li:N ratio had been achieved was based on resistance measurements. Therefore, an accurate reading was crucial. The silicon substrates had a resistivity that was closer to diamond's so they did not interfere with the resistance results. Therefore, silicon substrates were chosen for film growth. Furthermore, in some cases molybdenum substrates resulted in delamination of the diamond film, which is another disadvantage.

N-doped diamond and undoped diamond films were compared to see the effect of nitrogen atoms on the diamond lattice. It was concluded that undoped diamond has a lower graphite peak in Raman data and that it also had a lower resistance. This is because the undoped diamond performs as though it is a p-type diamond due to the dangling bonds at grain boundaries. SEM images highlighted random facets for undoped diamond whereas the N-doped diamond produced {100} square facets. This highlighted how the incorporation of nitrogen atoms changed the film morphology.

Lithium atoms were then incorporated into the N-doped diamond by diffusion using the hot filament reactor. These Li:N co-doped films appeared to have similar morphology to the N-doped samples but with much higher I_D/I_G values. This meant that the proportion of sp^3 carbon (diamond) to sp^2 carbon (graphite) was higher leading to a higher quality film morphology. Resistance values were also measured and these demonstrated that lithium atom incorporation greatly decreased the resistance of the films. However, the resistance remained too high to produce the required ratio of 1:4 Li:N.

To try to decrease the resistance, different lithium diffusion conditions were evaluated. After lithium diffusion, a capping layer was grown to encapsulate the lithium atoms. The capping layer previously used was undoped. This was changed to N-doped to try to reduce the resistance. However, this had the opposite effect and increased resistance. Therefore, this was not an effective method.

Decreasing the number of nitrogen atoms was also studied to try to decrease the resistance which should help in achieving the 1:4 ratio of Li:N required. To do this, the amount of methane with respect to ammonia was increased. However, this resulted in nanocrystalline diamond, which due to the increase in grain boundaries and graphite areas, results in more conductive films. Therefore, a

very low resistance was recorded but since this was a result of NCD (not MCD) these results were not viable.

Therefore, the next step was to try to increase the amount of lithium atom incorporation. This was accomplished by increasing the volume of Li_3N solution that was drop-cast onto the N-doped diamond films. This in turn decreased the resistance of the films. However, if the volume used was too high, it resulted in the formation of NCD films. Furthermore, the lithium atoms did not undergo the complete diffusion process into the diamond film as some remained on the surface after diffusion. The sample with the lowest resistance of $1.8 \text{ M}\Omega$ was analysed using SIMS to determine the Li:N ratio. This was achieved using $200 \mu\text{L}$ Li_3N solution and obtained a ratio of 1:6.7 of Li:N. Therefore the proportion of nitrogen atoms needed to be decreased further.

To try to decrease this ratio, the capping layer after lithium diffusion was changed. Previously, an N-doped capping layer had been accomplished instead of an undoped capping layer. This did not produce a lower resistance. Therefore it was postulated that no capping layer at all might have an effect. However, this again increased the resistance.

Finally, an acid washing experiment was performed to determine whether Li:N co-doped diamond could be used as an acid sensor. This was analysed by taking resistance measurements before and after the acid wash. These results were inconclusive and gave inconsistent resistance results. The reason for this inconsistency is not known. There could be many reasons such as, the acid was so strong and interfered with the dopants in the bulk, or hydroxyl bonds were being formed on the film surface. Alternatively, this could be due to the inconsistency that tends to occur with resistance measurements.

Overall a 1:4 ratio of Li:N was not obtained. However, previous work in this area has included a ratio of 1:18 Li:N being fabricated [24]. Therefore, since a ratio of 1:6.7 was achieved, it highlights that the ratio has been significantly decreased. Potentially with a few changes to experimental conditions a 1:4 Li:N ratio could be obtained.

5.0 Further Work

Further work involves trying to decrease the ratio from 1:6.7 to 1:4 of Li:N and to try to obtain more reliable resistance results.

5.1 Decreasing the Nitrogen Atoms

Currently a ratio of 1:6.7 has been obtained. To decrease this to 1:4, a number of methods could be attempted. Firstly the proportion of nitrogen could be decreased further. This could be done by lowering the amount of NH_3 gas, since this was responsible for nitrogen atom incorporation. However, the amount used for this study (0.13% NH_3/H_2) was already relatively low. The current MFC is not sensitive enough to accurately introduce lower concentrations of NH_3 gas into the diamond film. Therefore, a more sensitive MFC would need to be obtained to decrease the nitrogen atom incorporation in the lattice.

5.2 Different Diffusion Methods

It is difficult to increase the volume of Li_3N solution since at 250 μL , not all the Li_3N diffused into the lattice. Therefore, anything above this volume using the current diffusion methods was impractical. However, different diffusion methods may lead to better diffusion, hence higher volumes of Li_3N could be obtained. The lithium was diffused for 1 hour under a hydrogen atmosphere. If diffusion time was longer, the lithium atoms would have more time to diffuse into the bulk. This would only work if the solubility limit of lithium in diamond had not been exceeded. To be viable, the reason for the limited diffusion must be due to a time constraint. The lithium atoms would not have enough time to fully diffuse into the lattice.

5.3 Changing the Capping Layer

Using different capping layers has been slightly looked into in this study but more can be done here to see if the resistance can be decreased. The resistance was lowest when the undoped capping layer was used. It appeared, from the study that changing the capping layer tends to increase the resistance. However, if the capping layer was grown for longer, this would encapsulate more lithium atoms into the lattice. Therefore, this should decrease the resistance.

5.4 Further Analysis

It would also be beneficial to complete analysis for increasing volumes of Li_3N solution. SIMS should be performed on all samples from 100 μL to 250 μL . This was only achieved for the 200 μL sample as this gave the lowest resistance. However, all samples from 150 μL and above gave resistance values $< 5 \text{ M}\Omega$ and therefore should be analysed. The ratio of the 100 μL sample should also be analysed for comparison. Furthermore, the 150 μL sample had a highly crystalline film morphology and therefore could provide a lower ratio of Li:N.

5.5 Resistance Measurements

The resistance measurements were relatively inconstant, yet this is the main method for determining the n-type diamond properties of the film. Therefore this needs to be a reliable test. A conductivity meter cannot be used as the diamond films are not in solution form.

A more accurate resistance needs to be obtained. This can be achieved using the Van der Pauw method which is very common for measuring resistivity. This could be a feasible method as the diamond films are solid and flat with uniform thickness. Additionally, the film has easy application of four ohmic contacts for electrodes. All of which are required for Van der Pauw measurements. A current is applied along one edge of the film between two of the contacts. The voltage across the opposite edge is measured between the other two contacts. Resistance can be measured (**Equation 5.1**) using the current and voltage.

$$V = IR \qquad \text{Equation 5.1}$$

Hall Effect measurements can also be used by recording the Hall voltage. This can be used in combination with the Van der Pauw method to determine if p-type or n-type diamond had been fabricated.

5.6 Oxygen Termination

Before resistance measurements were studied, oxygen termination was carried out to remove the surface conductivity on the film. However, it has been suggested that the ozone plasma treatment does not provide 100% coverage of oxygen. Therefore surface conductivity may still be an issue. X-ray photoelectron spectroscopy (XPS) may provide information on the percentage coverage which would be useful.

6.0 Appendix

6.1 Calculation of Li₃N concentration

Molar Mass Li₃N: 34.8 g mol⁻¹

Mass of Li₃N: 85 mg

$$\text{moles} = \frac{\text{mass}}{\text{molar mass}} \quad \text{Equation 6.1}$$

Moles Li₃N: 2.44 × 10⁻³ mol

Volume of solvent: 5 mL

$$\text{concentration} = \frac{\text{moles}}{\text{volume}} \quad \text{Equation 6.2}$$

Concentration Li₃N: 0.49 mol.dm⁻³

6.2 SEM for Increasing NH₃ Concentration

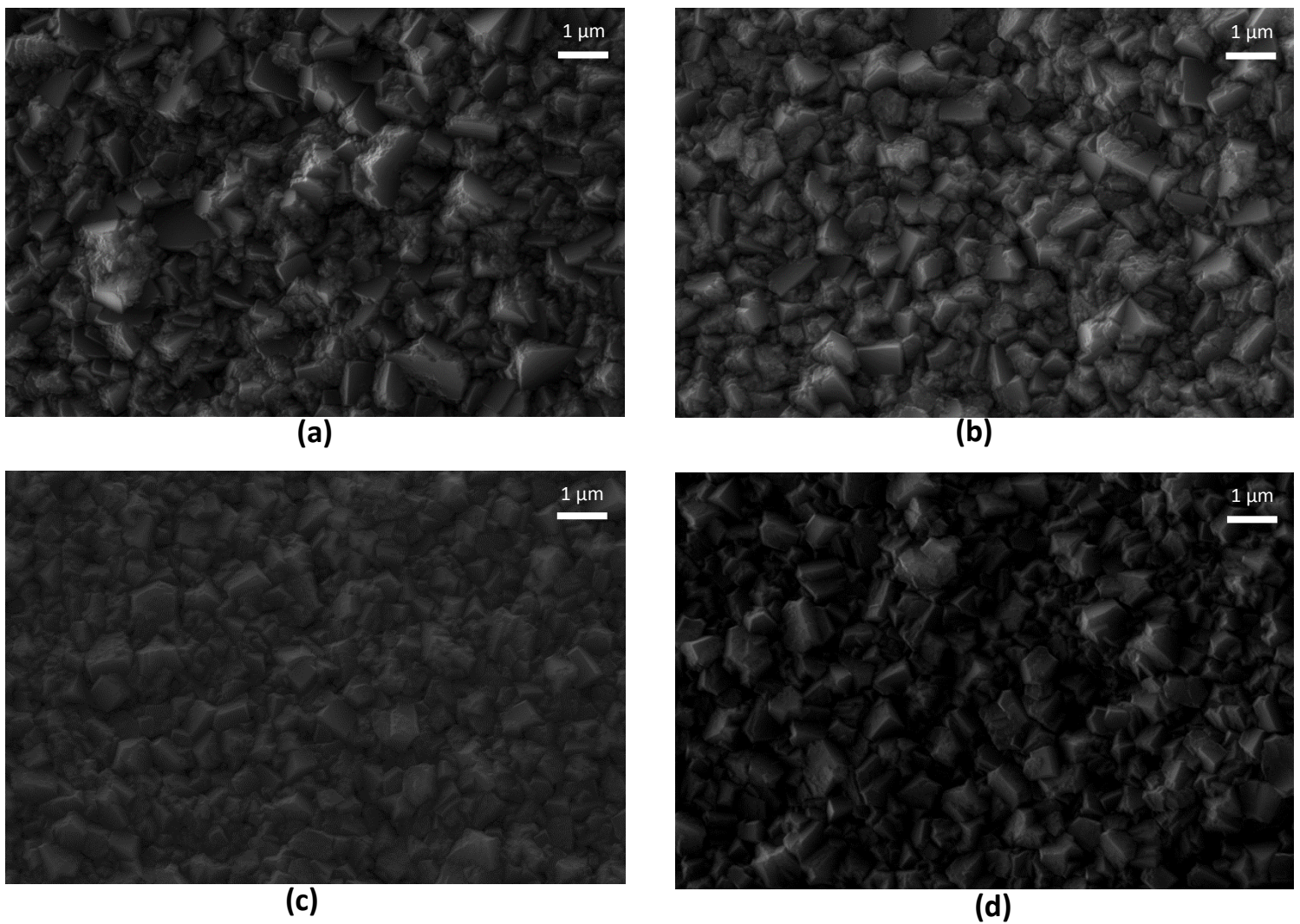


Figure 6.1 SEM images showing the morphology of N-doped diamond samples on molybdenum substrates. CH₄/ H₂ was constant at 0.81% and no N₂ gas was used. The amount of NH₃/H₂ was (a) 0.17 %, (b) 0.24%, (c) 0.31% and (d) 0.34%.

6.3 SEM for Undoped Diamond on a Molybdenum Substrate

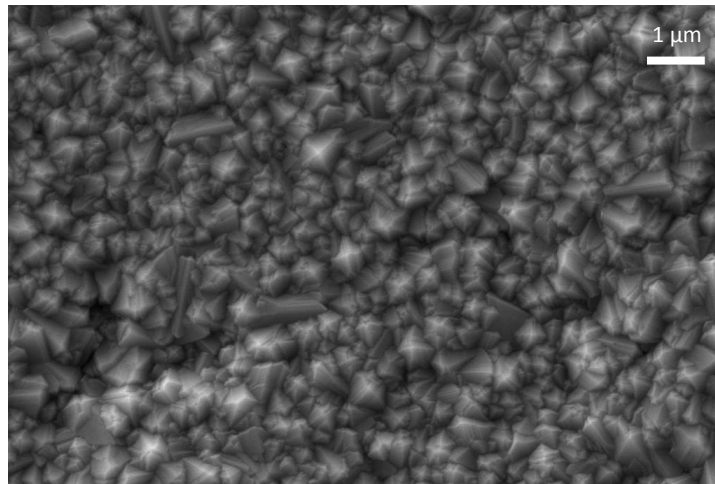


Figure 6.2 SEM images showing the morphology of an undoped diamond samples on a molybdenum substrates. CH_4/H_2 was constant at 0.81%.

6.4 Resistance Measurements for Li:N co-doped Diamond

Table 6.1: Resistance Measurements of Li:N co-doped Diamond.

Volume of $\text{Li}_3\text{N}/ \mu\text{L}$	Resistance/ $\text{M}\Omega$
100	125-145
150	313-314
200	46-50
250	130-180

6.5 Resistance Measurements with no Capping Layer

Table 6.2: Resistance Measurements of Li:N co-doped Diamond.

Capping Layer	Resistance/ $\text{M}\Omega$
No Capping Layer	315-320

6.6 Resistance Measurements before and after Acid Washing

Table 6.3: Resistance Measurements for N-doped and Li:N co-doped diamond before and after acid washing

N₂/H₂	Resistance / MΩ		
	Prior to Acid Wash	After acid Wash 1	After acid Wash 2
N-doped film with 0.23% N ₂ /H ₂	2-5	4-10	-
Li:N co-doped film with 0.23 N ₂ /H ₂	125-145	16-20 230-245 310-321	210-235 399-400 459-464

7.0 Bibliography

- [1] R. Kalish, *Carbon*. **37**, 1999, 781–785.
- [2] P.W. May, *Philos. Trans. R. Soc. A Math. Phys. Eng. Sci.* **358**, 2000, 473–495.
- [3] P.W. May, *Endeavour*. **19**, 1995, 101–106.
- [4] K.E. Spear, J.P. Dismukes, *Synthetic Diamond: emerging CVD science and technology*, 1994.
- [5] M.N.R. Ashfold, P.W. May, C.A. Rego, N.M. Everitt, *Chem. Soc. Rev.* **23**, 1992, 21–30.
- [6] K. Takahashi, A. Yoshikawa, A. Sandhu, *Wide Bandgap Semiconductors: Fundamental Properties and Modern Photonic and Electronic Devices*, 2007.
- [7] J. Robertson, *J. Vac. Sci. Technol. B Microelectron. Nanom. Struct.* **18**, 2000, 1785.
- [8] J.P. Goss, P.R. Briddon, *Phys. Rev. B.* **75**, 2007, 1–9.
- [9] K. Furuya, F. Munakata, K. Matsuo, Y. Akimune, J. Ye, A. Okada, *J. Therm. Anal. Calorim.* **69**, 2002, 873–879.
- [10] S. Jin, T.D. Moustakas, *Appl. Phys. Lett.* **65**, 1994, 403.
- [11] S.-S. Li, H.-A. Ma, X.-L. Li, T.-C. Su, G.-F. Huang, Y. Li, et al., *Chinese Phys. B.* **20**, 2011, 028103.
- [12] H.-J. Herzog, *J. Electrochem. Soc.* **131**, 1984, 2969.
- [13] B. Cordero, V. Gómez, A.E. Platero-Prats, M. Revés, J. Echeverría, E. Cremades, et al., *Dalton Trans.* 2008, 2832–2838.
- [14] Y. Li, X. Jia, H. Ma, J. Zhang, F. Wang, N. Chen, et al., *Cryst. Eng. Comm.* **16**, 2014, 7547–7551.
- [15] S. A. Kajihara, A. Antonelli, J. Bernholc, *Phys. Rev. Lett.* **66**, 1991, 2010–2013.
- [16] M.E. Zvanut, W.E. Carlos, J.A. Freitas, K.D. Jamison, R.P. Hellmer, *Appl. Phys. Lett.* **65**, 1994, 2287.
- [17] N. Casanova, A. Tajani, E. Gheeraert, E. Bustarret, J. A. Garrido, C.E. Nebel, et al., *Diam. Relat. Mater.* **11**, 2002, 328–331.
- [18] S. Koizumi, M. Kamo, Y. Sato, H. Ozaki, T. Inuzuka, *Appl. Phys. Lett.* **71**, 1997, 1065.
- [19] H. Kato, T. Makino, S. Yamasaki, H. Okushi, *J. Phys. D. Appl. Phys.* **40**, 2007, 6189–6200.
- [20] P. Politzer, J.S. Murray, P. Lane, *J. Comput. Chem.* **24**, 2003, 505–11.
- [21] A. Kraft, *Int. J. Electrochem. Sci.* **2**, 2007, 355–385.

- [22] E. Rohrer, C. Graeff, R. Janssen, C. Nebel, M. Stutzmann, H. Güttler, et al., *Phys. Rev. B.* **54**, 1996, 7874–7880.
- [23] S. Bohr, R. Haubner, B. Lux, *Appl. Phys. Lett.* **68**, 1996, 1075–1077.
- [24] M.Z. Othman, *Studies of n-type Doping and Surface Modification of CVD Diamond for use in Thermionic Applications*, 2014.
- [25] S. Jin, M. Fanciulli, T.D. Moustakas, L.H. Robins, *Diam. Relat. Mater.* **3**, 1994, 878–882.
- [26] Z. Yiming, F. Larsson, K. Larsson, *Theor. Chem. Acc.* **133**, 2013, 1432.
- [27] R.G. Farrer, *Solid State Commun.* **7**, 1969, 685–688.
- [28] B.B. Li, M.C. Tosin, A. C. Peterlevitz, V. Baranauskas, *Appl. Phys. Lett.* **73**, 1998, 812.
- [29] R. Job, M. Werner, A. Denisenko, A. Zaitsev, W.R. Fahrner, *Diam. Relat. Mater.* **5**, 1996, 757–760.
- [30] G. Popovici, T. Sung, S. Khasawinah, M. A. Prelas, R.G. Wilson, *J. Appl. Phys.* **77**, 1995, 5625.
- [31] E.B. Lombardi, A. Mainwood, *Diam. Relat. Mater.* **17**, 2008, 1340–1352.
- [32] P.W. May, M. Davey, K.N. Rosser, P.J. Heard, *Mater. Res. Soc. Symp. Proc.* **1039**, 2008, 1–5.
- [33] F.A. Cotton, G. Wilkinson, *Advanced Inorganic Chemistry: A Comprehensive Text*, 1980.
- [34] S.C. Eaton, A.B. Anderson, J.C. Angus, Y.E. Evstefeeva, Y. V. Pleskov, *Electrochem. Solid-State Lett.* **5**, 2002, G65.
- [35] S. Vaddiraju, S.C. Eaton, J. Chaney, M. Sunkara, *Electrochem. Solid-State Lett.* **7**, 2004, G331–G334.
- [36] W. Song, Y. Kim, D.S. Jung, S.I. Lee, W. Jung, O.-J. Kwon, et al., *Appl. Surf. Sci.* **284**, 2013, 53–58.
- [37] M.Z. Othman, P.W. May, N.A. Fox, P.J. Diam. Relat. Mater. **44**, 2014, 1–7.
- [38] J.E. Moussa, N. Marom, N. Sai, J.R. Chelikowsky, *Phys. Rev. Lett.* **108**, 2012, 226404.
- [39] C.X. Wang, C.X. Gao, T.C. Zhang, H.W. Liu, X. Li, Y.H. Han, et al., *Chin. Phys. Lett.* **19**, 2002, 1513–1515.
- [40] T. Tomikawa, Y. Nishibayashi, S. Shikata, *Diam. Relat. Mater.* **3**, 1994, 1389–1392.
- [41] H. Okushi, *Diam. Relat. Mater.* **10**, 2001, 281–288.
- [42] N. Fujimori, A. Doi, T. Inai, *Vacuum.* **36**, 1986, 99–102.
- [43] Y. Oshiki, H. Kaneko, J. F. Fujita, K. Hayashi, K. Meguro, A. Homma, et al., *Diam. Relat. Mater.* **15**, 2006, 1508–1512.

- [44] P. Patnaik, Handbook of Inorganic Chemicals, 2002.
- [45] P.K. Chu, L. Li, Mater. Chem. Phys. **96**, 2006, 253–277.
- [46] A. Mette, C. Schetter, D. Wissen, S. Lust, S. Glunz, G. Willeke, IEEE, **1**, 2006, 1056–1059.
- [47] A. Qureshi, W.P. Kang, J.L. Davidson, Y. Gurbuz, Diam. Relat. Mater. **18**, 2009, 1401–1420.
- [48] T. Liu, D. Raabe, Appl. Phys. Lett. **94**, 2009, 021119.
- [49] P. Becker, P. Seyfried, H. Siegert, Z. Phys. B - Condens. Matter. **48**, 1982, 17–21.
- [50] W.L.E. Wong, M. Gupta, Adv. Eng. Mater. **7**, 2005, 250–256.
- [51] R.A. Holmwood, R. Glang, J. Chem. Eng. Data. **10**, 1965, 162–163.
- [52] S. Bhattacharyya, O. Auciello, J. Birrell, J. A. Carlisle, L. A. Curtiss, A. N. Goyette, et al., Appl. Phys. Lett. **79**, 2001, 1441.
- [53] N.C. Wu, Y.B. Xia, S.H. Tan, L.J. Wang, J.M. Liu, Q.F. Su, Chin. Phys. Lett. **23**, 2006, 2595–2597.
- [54] P.W. May, Carbon Based Mater. Mater. Sci. Found. **65-66**, 2010, 147–175.
- [55] S. Wenmackers, P. Christiaens, W. Deferme, M. Daenen, K. Haenen, M. Nesládek, et al., Mater. Sci. Forum. **492-493**, 2005, 267–272.
- [56] J. Kim, C. Lee, J. Korean Phys. Soc. **42**, 2003, 956–960.
- [57] F. Zhang, F. Ahmed, G. Holzhuter, E. Burkel, Journal Cryst. Growth. **340**, 2012, 1–5.